Modelling and Grid impact of Slip Synchronous Generator (SSG) on weak distribution grids

by

Edwin Mangwende

Thesis presented in partial fulfilment of the requirements for the degree Master in Engineering at Stellenbosch University in the Department of Electrical and Electronic Engineering

Study leader: Prof. H.J Vermeulen

December 2019

Acknowledgements

I would like to acknowledge and appreciate Prof HJ Vermeulen for his valuable assistance, guidance and efforts throughout the course of this project, without which this study would not have been possible. In the same breath, I would like to thank Mr Nelius Bekker for all his assistance and extend my gratitude also to my mother, father, brothers and Clyde for their enormous amount of support they provided during my study.

Declaration

By submitting this thesis electronically, I declare that the entirety of the work contained therein is my own, original work, that I am the sole author thereof (save to the extent explicitly otherwise stated), that reproduction and publication thereof by Stellenbosch University will not infringe any third party rights and that I have not previously in its entirety or in part submitted it for obtaining any qualification.

Signature: …… December 2019

E. Mangwende

Abstract

The integration of renewable energy resources is becoming more appealing, specifically Wind Turbine Systems (WTS) due to the innovative ways in which they are designed. These innovative designs make them economic viable to be used in power generation applications. Small wind turbine systems are ideal to reduce the power losses associated with feeding remote distribution grids, as these systems can be installed close to the loads. These systems are known as distributed generation as they are connected to the distribution network level, rather than to the transmission level as is the case for traditional generation systems.

In this study the dynamic behaviour of a 15 kW, fixed speed fixed pitch downwind turbine that can form part of a distributed generation system, is investigated. The small wind turbine system uses a Slip Synchronous Permanent Magnet Generator (SS-PMG) also known as Slip Synchronous Generator (SSG). The generator is a direct driven and direct grid connected generator. This configuration is more efficient and reliable than traditional configurations, since the losses and cost associated with the gearbox and converter electronics, as well as the maintenance cost of these components, are eliminated.

To study the dynamic behaviour of the WTS, both the mechanical and electrical components that form the system are modelled in the Simulink and DigSILENT platforms. The mechanical model comprises of the wind model, aerodynamic model and the mechanical drive train of the system whilst the electrical model consists of the SSG model and grid model. The new concept generator is an SSG whose build-in DigSILENT model does not exist. To study the dynamic behaviour of the WTS in DigSILENT a model is developed by transformation the SSG to a Permanent Magnet Synchronous Generator (PMSG). The PMSG is then implemented using the existing synchronous generator model of DigSILENT with a fixed field excitation. The rest of the mechanical system is modelled using the DigSILENT Simulation Language (DSL).

Using the models developed from the dynamic equations, the transient stability of the system is analysed. A benchmark network for the weak power network with embedded WTS is represented as a Thevenin equivalent circuit. The network is analysed for single and three-phase faults. The systems interaction with the grid network is also analysed and whether the SS-PMSG is capable of Low Voltage Ride Through (LVRT) is investigated. Finally, the simulated results of both the Simulink and DigSILENT model are presented and compared.

Opsomming

Die integrasie van hernubare energiehulpbronne word meer aanloklik, veral Wind Turbine Stelsels (WTS) as gevolg van die innoverende maniere waarop hulle ontwerp word. Hierdie innoverende ontwerpe maak hulle ekonomies lewensvatbaar om in kragopwekking toepassings gebruik te word. Klein wind turbine stelsels is ideaal om die drywingsverliese wat verband hou met die verspreiding van afgeleë verspreidingsnetwerke te verminder, aangesien hierdie stelsels naby die laste geïnstalleer kan word. Hierdie stelsels staan bekend as verspreide generasie aangesien hulle gekoppel word op verspreidingsnetwerkvlak, eerder as die transmissievlak soos in die geval van tradisionele generasiestelsels

In hierdie studie word die dinamiese gedrag van 'n 15 kW, vaste-spoed vaste-invalshoek wind turbine, wat deel kan uitmaak van 'n verspreide generasie stelsel, ondersoek. Die klein wind turbine stelsel gebruik 'n Slip Sinchrone Permanent Magneet Generator (SS-PMG), ook bekend as Slip Sinchrone Generator (SSG). Die generator is 'n direkte-aangedrewe en direkte netwerk gekoppelde generator. Hierdie konfigurasie is meer doeltreffend en betroubaar as tradisionele konfigurasies, aangesien die verliese en koste verbonde aan die ratkas en omskakel elektronika, sowel as die onderhoudskoste van hierdie komponente, uitgeskakel word.

Om die dinamiese gedrag van die WTS te bestudeer, word beide die meganiese en elektriese komponente waaruit die stelsel bestaan gemodelleer in die Simulink en DigSILENT platforms. Die meganiese model bestaan uit die wind model, aërodinamiese model en die meganiese aandryfstelsel van die stelsel terwyl die elektriese model uit die SSG model en netwerk model bestaan. Die nuwe konsep generator is 'n SSG waarvoor 'n ingeboude DigSILENT-model nie bestaan nie. Om die dinamiese gedrag van die WTS in DigSILENT te bestudeer, word 'n model ontwikkel deur die SSG te transformeer na 'n Permanente Magnetiese Sinkroniese Generator (PMSG). Die PMSG word dan geïmplementeer met behulp van die bestaande sinkroniese generator model van DigSILENT met 'n vaste veldopwinding. Die res van die meganiese stelsel word gemodelleer met behulp van die “DigSILENT Simulation Language (DSL)”.

Deur gebruik te maak van die modelle wat ontwikkel is uit die dinamiese vergelykings, word die oorgangstabiliteit van die stelsel geanaliseer. 'n Maatstaf netwerk vir die swak kragnetwerk met geïntegreerde WTS word voorgestel as 'n Thevenin ekwivalente stroombaan. Die netwerk word geanaliseer vir enkel- en driefase foute. Die stelsel interaksie met die netwerk word ook geanaliseer en daar word ondersoek of die SS-PMSG Lae Spanning Deur Ry (LSDR) vermoë het. Ten slotte word die gesimuleerde resultate van beide die Simulink en DigSILENT-model aangebied en vergelyk.

Table of Contents

List of figures

List of Tables

Nomenclature

Abbreviation	Description
Eskom	Electricity Supply Commission
RE	Renewable Energy
DEA	Department of Environmental Affairs
UNFCCC	United Nations Framework Convention on Climate Change
IRP	Integrated Resource Plan for electricity
GHG	Greenhouse Gas
REFIT	Renewable Energy Feed-In-Tariffs
NERSA	National Energy Regulator of South Africa
REIPPP	Renewable Energy Independent Power Producer Programme
IPPPP	Independent Power Producer Procurement Program
PV	Photovoltaic
CSP	Concentrating solar power
IPP	Independent Power Producers
SSG	Slip Synchronous Generator
SWT	Small Wind Turbine
AC	Alternating Current
DC	Direct Current
IEC	International Electrotechnical Commission
NRCan	Natural Resources Canada
CanWEA	Canadian Wind Energy Association
REEEP	Renewable Energy & Energy Efficiency Partnership
BWE	Bundesverband Wind Energie
MCS	Micro-generation Certification Scheme
AWEA	American Wind Energy Association
WTG	Wind Turbine Generator
WECS	Wind Energy Conversion System

HAWT	Horizontal Axis Wind Turbines
VAWT	Vertical Axis Wind Turbines
FS-FP	Fixed-speed fixed-pitch
FS-VP	Fixed-speed variable-pitch
VS-FP	Variable-speed fixed pitch
VS-VP	Variable-speed variable-pitch
SCIG	Squirrel-Cage Induction Generator
WRIG	Wound Rotor Induction Generator
DFIG	Doubly Fed Induction Generator
DFAG	Doubly Fed Asynchronous Generator
VSC	Voltage-Source Converter
STATCOM	Static Synchronous Compensator
AVR	Automatic Voltage Regulator
SS-PMG	Slip Synchronous Permanent Magnet Generator
SSG	Slip Synchronous Generator
PMIG	Permanent Magnet Induction Generator
PMSG	Permanent Magnet Synchronous Generator
WECS	Wind Energy Conversion System
PM	Permanent Magnet
CSG	Convectional Synchronous Generator
RPP	renewable power plant
MV	Medium Voltage
LV	Low Voltage
HV	High Voltage
NSP	Network Service Providers
PCC	Point of Common Coupling
POC	Point of Connection
TS	Transmission System

DS	Distribution System
IPP	Independent Power Producers
PFCC	Power Factor Correction Capacitors
AVR	Automatic voltage regulator
WPP	Wind power plant
VRT	Voltage Ride-Through
LVRT	Low Voltage Ride-Through
HVRT	High Voltage Ride-Through
NERC	North American Electric Reliability Corporation
ISO	Independent System Operators
FACTS	Flexible Alternating Current Transmission System
CFCT	Critical Fault Clearing Time
EMT	Electromagnetic Transient Models
DSL	Dynamic Simulation Language
DigSILENT	Digital SImuLator for Electrical NeTwork
MATLAB	Matrix Laboratory
GUI	Graphical User Interface
PSS	power system stabilizer
RRF	Rotor-oriented dq-Reference Frame

Symbols

Parameter	Description	Unit
$v(t)$	Wind speed	ms^{-1}
$v_f(t)$	Low-frequency component wind speed	ms^{-1}
$v_m(t)$	Turbulence component wind speed	ms^{-1}
t_p	Time interval for instantaneous speed	sec
A	Swept area of wind turbine	m^2
$\Phi(\omega)$	Kaimal spectrum	
K_v	Kaimal constant	
ω	Rotor speed	rad/s
T_v	Kaimal constant	
P_{wt}	Kinetic wind power	W
$\dot{m}$	Mass flow rate	kgs^{-1}
V_w	Wind speed	ms^{-1}
p	Air density	kgm^{-2}
R	Blade radius	m
C_P	Power coefficient	p.u.
C_Q	Torque coefficient	p.u.
λ	Tip speed ratio	p.u.
$\theta_{pitch}.$	Pitch angle	degrees
T_t	Torque applied on the main shaft of the IG-rotor	Nm
T_r	IG electrical torque response	Nm
T_m	PM-rotor torque response,	Nm
T_s	SG electrical torque response	Nm
ω	Angular velocity of the turbine	rad/s
n	Rotational speed	rev/mi
J_t	Inertia of the turbine	$kg.m^2$

J_{tr}	Inertia of the turbine and IG	kg.m^2
J_m	Inertia of the IG-rotor and PM-rotor	kg.m^2
B_m	PM-rotor viscous friction coefficient	Nm/rad. s^{-1}
B_r	Slip-rotor viscous friction coefficient	Nm/rad. s^{-1}
B_{mo}	Slip-rotor static friction constant	Nm
C_i	Turbine's characteristic coefficients	p.u.
ω_t	Turbine's spin speed	rad/s
i_{qr}	IG q-axis current response	A
i_{dr}	IG d-axis current response	A
R_r	IG resistance	Ω
L_{qr}	IG q-axis inductance	H
L_{dr}	IG d-axis inductance	H
ω_{sle}	Electrical slip speed	rad/s
λ_{mr}	IG PM flux-linkage	Wb.t
i_{qs}	SG q-axis current response	A
i_{ds}	SG d-axis current response	A
R_s	SG resistance	Ω
L_{qs}	SG q-axis inductance	H
L_{ds}	SG d-axis inductance	H
ω_{me}	Electrical frequency at the stator terminals	rad/s
ω_m	PM rotor speed	rad/s
λ_{ms}	SG PM flux-linkage	Wb.t
v_s	Voltage source	V
E_s	Induced voltage source	V
K_{gen}	Generator constant	
K_1	IG generator constant	
E_2	IG per-phase induced voltage	V

f_1	Grid frequency	Hz
N_2	IG per-phase number of turn's	turns
ϕ_{PM}	PM flux	T
R_2	IG per-phase resistance	Ω
f_2	IG per-phase frequency	Hz
Φ_2	IG flux per pole	Wb
I_2	IG per-phase rotor current	A
E	Induced electromotive force	V
U_s	Stator voltage	V
U_h	Voltage representing the main field	V
I_s	Stator current	A
X_f	Field winding reactance	Ω
X_h	Main reactance	Ω
$X_{\sigma s}$	The stator leakage reactance	Ω
R_s	Stator reactance	Ω
Ψ_{PM}	Permanent magnet flux	Wb
δ	Load angle	rad
Ψ_E	DC excited flux	Wb
φ	Power factor	p.u.
I_f	Excitation current	A
ω_{gen}	Generator rotational speed.	rad/s
m	number of phases	
P_{gen}	Generator active power	W
T_e	Electromagnetic torque	Nm
Q_{gen}	Generator reactive power	VA
P	number of pole pairs	
Ω_{gen}	Mechanical generator speed	rad/s

U_{sd}	d-axis stator voltage	V
U_{sq}	q-axis stator voltage	V
i_{sd}	d-axis stator current	A
i_{sq}	q-axis stator current	A
ψ_{sd}	d-axis stator flux linkage	Wb
ψ_{sq}	q-axis stator flux linkage	Wb
L_d	d-axis inductance	H
L_q	q-axis inductance	H
X_d	d-axis synchronous reactance	Ω
X_q	q-axis synchronous reactance	Ω
X'_d	d-axis transient reactance	Ω
X'_q	q-axis transient reactance	Ω
X''_d	d-axis sub-transient reactance	Ω
X''_q	q-axis sub-transient reactance	Ω

Chapter 1: Project Motivation and Project Description

1.1 Introduction

The South Africa's electrification program, with inclusion of the successful integration of renewable energy into the diverse electricity generation mix is founded in the Constitution (1996) and Bill of rights [1]. This is mandated in a number of key government policy papers, starting with the White Paper on Energy Policy of 1998 [2, 3]. Critical on the government agenda at the time was the mass rollout of electricity to people who were previously excluded from accessing energy services. The national electricity utility, Electricity Supply Commission (Eskom), however had excess capacity at the time and the development of renewable energy (RE) technology options were limited to a few demonstration or pilot projects wholly funded by the international donor community [2]. The second policy document on renewable energy, namely the Renewable Energy White Paper (2003) policy, set a target of 10 000 GWh of energy to be produced from renewable energy sources by 2013 [4]. The concluding section of this document recommended strategies on how to achieve the goals, but the drafting of such a document was not immediately undertaken [2].

The National Climate Change Response Policy White Paper of 2011 by the Department of Environmental Affairs (DEA) represents the final policy paper that supported the country's renewable energy aspirations [5]. Cabinet, in 2008, adopted a peak, plateau and decline trajectory. This strategy was proposed to let the country's emissions to grow up to a peak of around 550Mt CO_2-eq between 2020 to 2025, flatten out for a decade, and decline from 2030-35 onwards, as shown in Figure 1-1. On a global scale the precedence was set with Kyoto protocol, an international agreement linked to the United Nations Framework Convention on Climate Change (UNFCCC), which commits its parties by setting internationally binding emission reduction targets [6].

In 2010, considering the plateau and decline scenarios shown in Figure 1-1 for carbon emissions, the Integrated Resource Plan for electricity (IRP, 2010) was established under the Electricity Regulation Act. The IRP was later redrafted in 2013 [7]. The IRP was established to weigh in decision making of national policy and to provide a planning framework to manage electricity demand for the period from 2010 to 2030. Table 1-1 summarises the future potential roll out of wind energy projects in the country considering the promulgated IRP 2010 and the updated draft IRP.

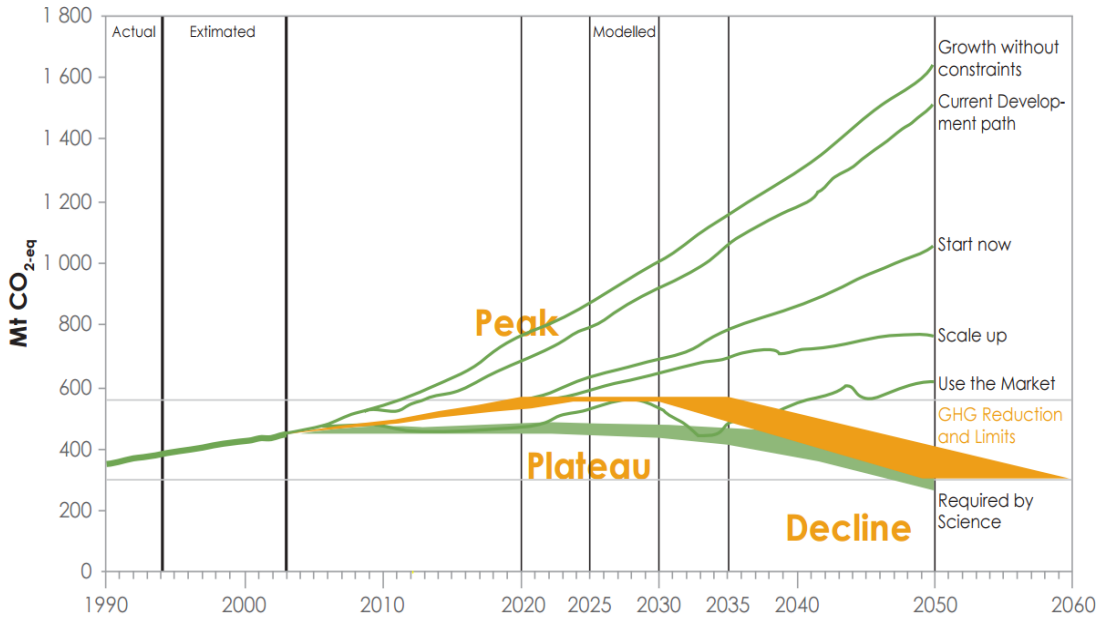

Figure 1-1: South Africa Greenhouse Gas (GHG) emission reductions and limits [8].

Table 1-1: Potential future wind capacity roll-out according to IRP 2010 and IRP 2013 [7].

Indicator	IRP 2011	IRP 2013
	MW	MW
2030 Wind Power Target	9 100 (Excluding Sere wind farm)	4 360
REIPPPP Awarded (Round 1, 2, 3)	1 984	1 984
Total Capacity Remaining	7 116	2 376

Renewable Energy Feed-In-Tariffs (REFITs) where introduced in 2008 to incentivise the roll out of renewable energy on a large-scale. This structure was informed by international experience, as it has been widely used to encourage and accommodate renewable energy [2]. In 2011 the National Energy Regulator of South Africa (NERSA), after adjustments of the tariff policy, abolished the REFIT programme and opened a competitive bidding process for renewable energy, termed the Renewable Energy Independent Power Producer Programme (REIPPP). The REIPPP covers technologies identified in the IRP 2010, namely onshore wind, solar Photovoltaic (PV), solar Concentrating solar

power (CSP), biomass, biogas, landfill gas, and small hydro. After successful initial implementation of the REIPPP, the year of 2016 saw an unfortunate impasse in the installation of renewable energy capacity. As result, about 37 renewable energy projects did come to financial close, this included 12 wind farm projects. The REIPPPP had 5 bid windows in which 6 327 MW from 92 independent power producers (IPPs) were awarded. When the first 4 rounds of bidding completed, 34 projects were allocated to wind IPPs with a capacity of 3 357 MW [9, 10]. The success of the REIPPP is highly dependent on private sector investment [11].

Small Wind Turbines (SWT) require much higher capital costs in comparison to large wind turbines in order to achieve lower capacity factors. The SWT can however, contribute to meet electricity demands in remote areas, also provide local economic and social benefits particularly when utilised for off-grid electrification [12]. The deployment and development of small wind turbines is expanding, with a variety of sizes and styles having been developed. The horizontal axis wind turbines dominate the market (74% share of the market) [13], but face challenges of low turbulent wind speeds as they are generally located close to settlements where trees, buildings and other infrastructure is in the vicinity. Reliable performance under these conditions can be achieved with vertical-axis technologies, which can also operate with very low noise levels production [12].

1.2 Project motivation

The local power grid experiences constraints due to a relatively small margin between peak demand and the available generating capacity [14]. The nominal installed generation capacity is about 45,645MW, of which Eskom contributes approximately 95%, while the remainder comes from independent power producers (IPPs) and imports [14]. Plans are underway to diversify the electricity generation mix through the Independent Power Producer Procurement Program (IPPPP) [10]. The installed capacity currently consists of 85% of thermal power plants, 10% hydroelectric plants, 4% nuclear power plant, and 1% non-hydro renewable energy [14]. The renewable energy industry is therefore small, with ample scope for expansion.

Many remote areas in the world are not connected to an electrical grid and, if connected, the load is connected through weak distribution grids. Small wind generators have potential for electrification of these remote areas, thereby mitigating the need for expensive transmission system infrastructure. Embedded systems or distributed systems, furthermore, reduce system losses [15], as the point of generation is connected close to the load. This also assists in maintaining system stability.

The world market for small wind technologies is growing. As of the end of 2015, the cumulative total of installed capacity worldwide has reached more than 948 MW, which represents an increase of 14%

compared to the 803 MW recorded in 2014. The industry of small wind technologies is, however, in its infancy stage. Three countries dominate in small wind power generation which are, namely China, USA and UK [13]. Figure 1-2 shows some the installed capacity of small wind technologies by country and Figure 1-3 shows the number of cumulative units installed as of end of 2015.

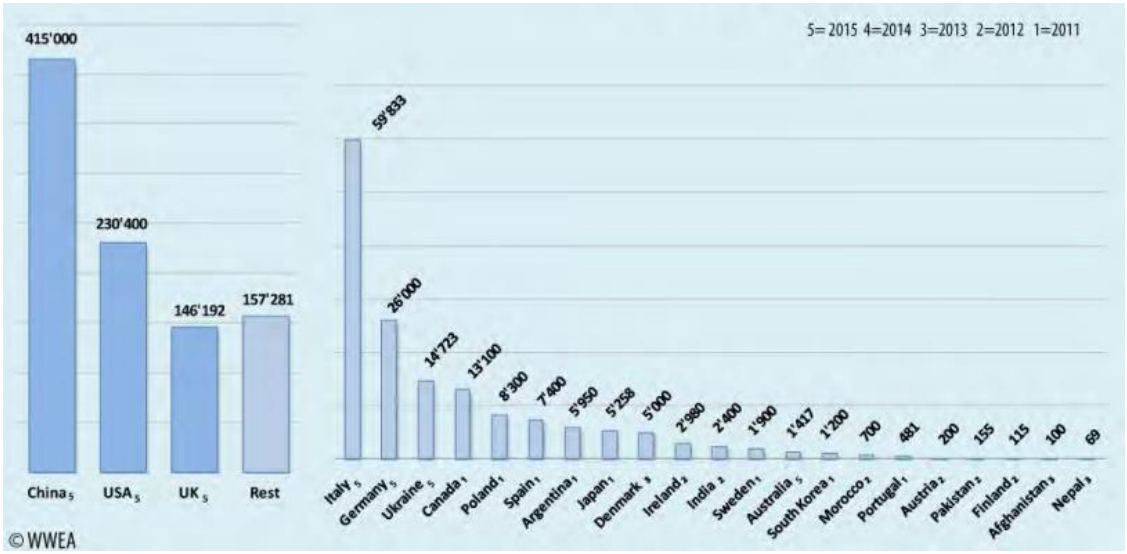

Figure 1-2: Installed small wind technology capacities by country [16]

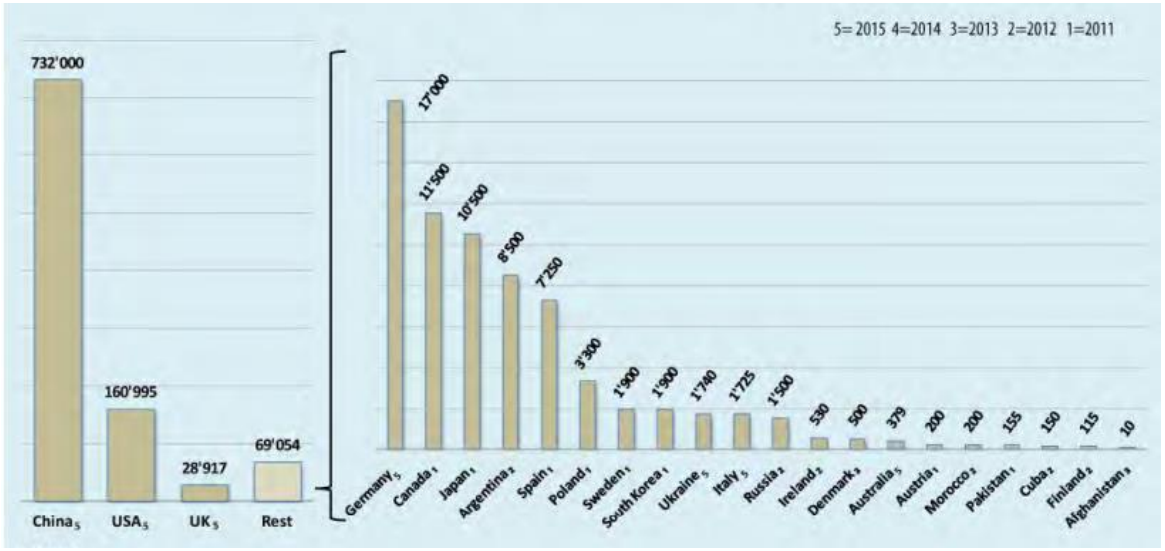

Figure 1-3: Installed number of small wind technology units by country [16]

The installed wind energy capacity in South Africa, after being stagnant since 2002 when the first 10 MW installation of wind power occurred, peaked to a cumulative capacity of 1471 MW by the end of 2016 [17]. Figure 1-4 shows the growth of installed wind generation capacity. This is expected to

expand due to the REIPPP, which presently has more than 3365 MW under different developmental stages.

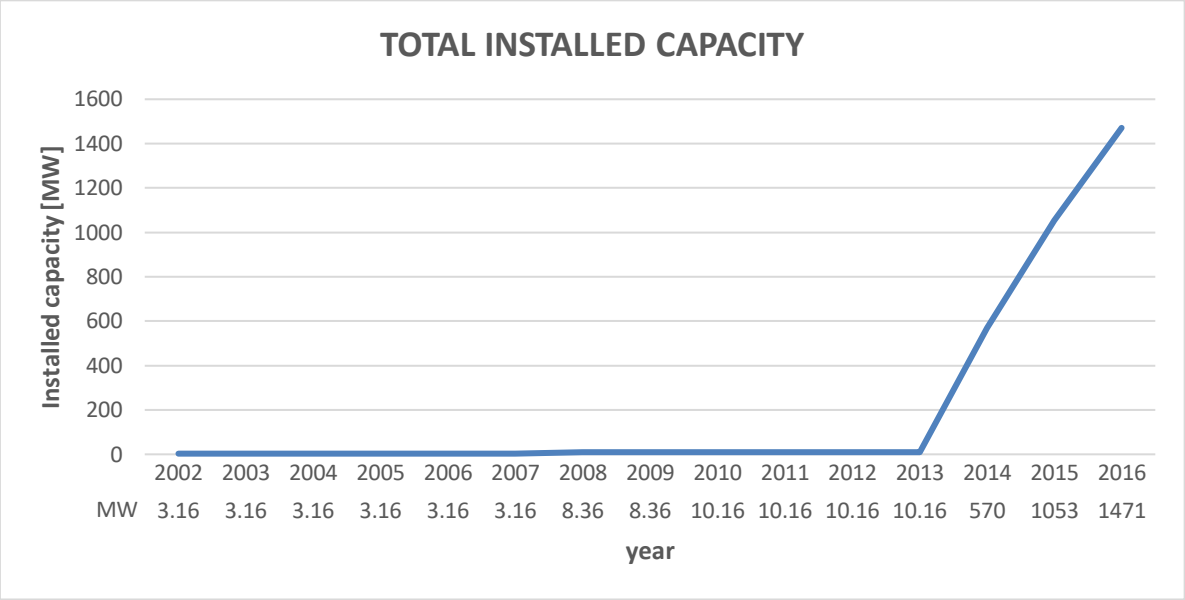

Figure 1-4: Total installed wind energy capacity of South Africa [17].

The Slip Synchronous Generator (SSG), currently being developed, represents one of the new concept small generators with potential for wind energy applications. It is both directly coupled to the turbine and the distribution grid network, hence reducing the downtime typically caused by gearbox and power electronic converter failures [18, 19, 20, 21]. This research project investigates the performance of the SSG machine for wind generation applications when tied to weak rural distribution grids.

1.3 Project description

1.3.1 Overview

The project investigates the performance of an embedded direct driven SSG in weak electrical grids and the grid interaction behaviour for transient stability analysis of the distribution network under fault conditions. This remainder of this section highlights the key research questions, research objectives and research tasks pertaining to the investigation. In order to investigate the steady-state and dynamic performance of the embedded SSG, a case study is carried out for a benchmarked grid network representing a weak grid network as a Thevenin equivalent circuit. The investigation considers the effects on network stability during single and three-phase faults.

1.3.2 Project objectives

The project involves implementation of a dynamic model of an SSG in both the MATLAB/Simulink and DigSILENT platform, then the simulation and analysis of the behaviour of the embedded wind generator when tied to weak electrical distribution grids. Transient network analysis is conducted to show how the system grid interaction is impacted when there is a transient fault on the grid network. The following research objectives have been identified for the project:

- The development and implementation of a dynamic model of the SSG in Matlab/Simulink.
- Analysing the effects of changing wind conditions on the behaviour of the SSG.
- The development and implementation of a dynamic model of the SSG in DigSILENT
- Comparing simulated dynamic model responses obtained with Matlab/Simulink to those obtained with DigSILENT.
- Conducting a case study of the SSG connected in a weak network with the view to investigate the effects on grid stability.
-

1.3.3 Research questions

The project objectives give rise to the following research questions:

- What analytical software is suitable to study the effects of embedded wind generation on weak remote distribution grids?
- Which software platform performs the best for modelling the system performance for normal, fault and switching conditions?
- How does the SSG perform in weak rural/remote grids with reference to the following?
  - System stability
  - Low Voltage Ride Through (LVRT) during grid faults

1.3.4 Research tasks

The research tasks implemented for the thesis are as follows:

- Perform a literature review of the technologies pertaining to small wind energy conservative system.
- Implement a dynamic model of the SSG in Matlab/Simulink and test the model implementation for dynamic scenarios.

- Implement a dynamic model of the SSG in DigSILENT and compare the performance of the model implementation with the results obtained with the model implemented in Matlab/Simulink
- Model a benchmark network topology for weak distributed systems.
- Perform case studies of the dynamic performance of the SSG for a typical rural network.

1.4 Overview of report

The remainder of the document is structured as follows:

- Chapter 2: Literature review:

This section explores the definition of a small wind turbine and considers the classification of wind turbine systems, especially with reference to their behaviour when connected to the grid. The network grid code for renewable energy in South Africa is outlined, especially in the context of embedded systems. Lastly, the nature and characteristics of weak networks are described and the available software tools for analysing the case studies are reviewed.

- Chapter 3: Model development and implementation:

This section focusses on the development of the mechanical model, control model and the fixed speed SSG wind turbine dynamic model on the Matlab/Simulink and DigSILENT platforms. The mechanical model consists of the wind resource, aerodynamic model and drive train with a fixed pitch stall control acting on the blade turbines. The theory of the SSG`s steady state and dynamic behaviour during normal, fault and switching conditions is introduced.

- Chapter 4: Simulated model performances:

Simulation results are presented for a case study of the SSG for a distribution network characterised by a weak electrical grid network in the DigSILENT and Matlab/Simulink platforms.

- Chapter 5: Case studies results:

Simulated results are presented for the dynamic performance of the SSG turbine system in the case study network.

- Chapter 6: Conclusions and recommendations

Final conclusions and recommendations for further work in this field are presented.

Chapter 2: Literature review

2.1 Overview

Wind energy systems which are now currently classified as big or in some instances large wind systems evolved from what is today referred to as small wind systems [13]. In the pioneering stages wind turbines mostly had capacities of less than 100 kW and were located predominantly in remote isolated areas [12].

There is still no definitive globally unified definition of small wind systems. Small wind systems were originally defined in the context of producing small amounts of power to mainly supply residential sector loads. However, this definition varies in the global context, as the associated power consumption patterns are unique in the different parts of the world [13].

Technically, a variety of definitions for Small Wind Turbines (SWTs) are available, as summarised in Table 2-1. One of these definitions, as covered by the IEC, defines a SWT in standard IEC 61400-2 as "having a rotor swept area of less than 200 m^2, which typically equates to a rated power of approximately 50 kW generating at a voltage level below 1000 V AC or 1500 V DC. In addition to this definition, several countries have proposed their own definitions of small wind systems [13]."

The various definitions of the upper capacity limit of small wind ranges between 15kW to 100 kW for the five largest small wind countries [13]. The modern definition of upper limit capacity leans towards 100 kW, mainly due to the definition prevalent in the North American and European markets. This is the definition adopted for the purposes of this investigation. For the purposes of standardisation, however, it is important that a common definition of small wind should be agreed upon in the longer term.

Table 2-1: International classifications of small wind systems [13].

	Authority/Association	Turbine Classification	Rated Capacity [W]	Remarks
International	International Electrotechnical Commission (IEC)	Small Wind Turbine	≈50	IEC 61400-2 defines SWTs as having a rotor swept area of less than 200 m^2, rated power of approximately 50 kW, voltage below 1'000 V AC or 1'500 V DC
Canada	Natural Resources Canada (NRCan)Canadian Wind Energy Association (CanWEA)	Mini Wind Turbine	0.3-1	Adopted in the Survey of the Small Wind by Marbek Resource Consultants
		Small Wind Turbine	1-30	
China	Renewable Energy & Energy Efficiency Partnership (REEEP)	Small Wind Turbine	<100	Adopted in the recent National Policy, Strategy and Roadmap Study for China Small Wind Power Industry Development
Germany	Bundesverband WindEnergie (BWE)	Small Wind Turbine	<75	Adopted in the recent BWE-Marktübersicht spezial – Kleinwindanlagen
United Kingdom	Renewable UK	Micro Wind	0 – 0.15	0,5-5 m Height / Up to 1'000 kWh Annual Energy Production
		Small Wind	1.5 – 15	2-50 m Height / Up to 50'000 kWh Annual Energy Production
		Small-medium Wind	15 – 100	50-250 m Height / Up to 200'000 kWh Annual Energy Production
	Microgeneration Certification Scheme (MCS)	Micro & Small Wind Turbine	<50	Only turbines smaller than 50 kW qualify for the MCS feed-in tariff programme in UK
USA	American Wind Energy Association (AWEA)	Small Wind Turbine	<100	Adopted in the most recent AWEA Small Wind Report 2010 and the AWEA Small Wind Turbine Global Market Study

2.2 Wind maps

Wind speed is an exogenous input signal applied to a Wind Energy Conversion System (WECS) that determines its behaviour. The stochastic variation of wind speed is highly dependent on the given site and on atmospheric conditions. Figure 2-1 shows a map of the mean wind speed for South Africa. It represents possible appealing geographical areas where wind power generation farms have a potential to be installed. It's more appealing to install the wind turbine system close to or at coastal regions as they are characterised by strong wind speeds.

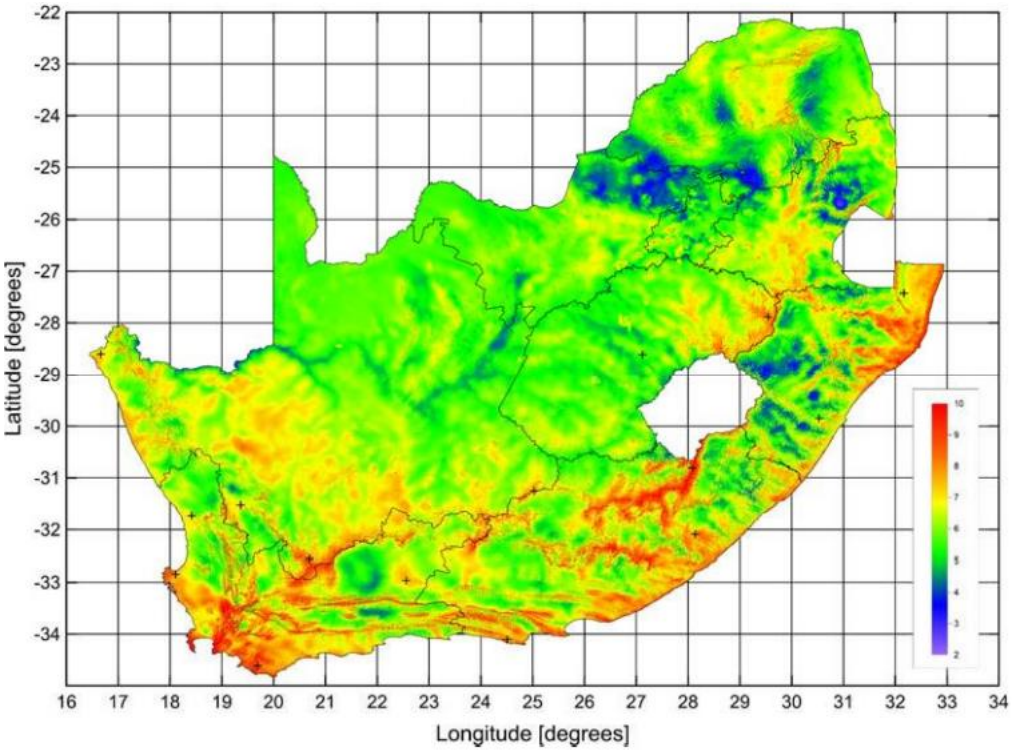

Figure 2-1: South Africa mean wind speed [ms^{-1}] at a height of 100 m [22].

2.3 Wind turbine classification

2.3.1 Overview

A wind turbine system converts the kinetic energy of a moving mass of air into mechanical energy. This is achieved by using aerodynamic rotor blades combined with various methodologies for mechanical power control. This is followed by the electro-mechanical energy conversion using a generator, which is tied to the electrical grid for power transmission [15].

Wind turbines can be installed onshore or offshore. Before the early 2000's, wind power was predominantly harnessed by onshore wind farms. The onshore wind system is generally preferred as it represents the cheaper option that requires less infrastructure and less advanced and specialized technology compared to the offshore option. The drawback in optimization of onshore wind turbines is the stochastic nature of wind speeds over land. Wind turbines are characterised by inefficiencies, since they can be only optimized for a specific wind speed, while wind speed and wind direction exhibit large variability. Many of the problems that hinder onshore wind systems are greatly alleviated in offshore farms. Wind speeds over the ocean are typically more consistent and much higher compared to onshore wind speeds. Offshore wind turbines can therefore be optimized to operate at high efficiencies. There is a public dislike for onshore wind turbines marring landscapes, which makes offshore wind appealing. Most of the large cities, furthermore, tend to be located near shorelines, thus avoiding the expense of transmitting power over long distances associated with offshore wind farms. Offshore wind farms are, however, considerably more expensive to design, build, install and maintain.

Onshore technologies can be either connected on the upwind or downwind direction. Upwind turbines, which are the most popular design, have the rotor facing the wind thereby making the design able to avoid the wind shade introduced by the tower. However, the wind shade in front of the tower cannot be eliminated, even if the tower is round and smooth. The upwind machine needs a yaw mechanism to keep the blades facing the wind and the blades need to rather inflexible and positioned at some distance from the tower [23]. Downwind turbines have the blades on the lee side of the tower. They may be designed without a yaw mechanism, if the rotor and nacelle have a design that can make the nacelle follow the wind passively. In this design the rotor may be made more flexible and the structural dynamics of the machine may thus be lighter than compared to an upwind machine. The drawback is that it may give rise to more fatigue loading on the turbine compared to an upwind design. This results from fluctuation in wind power due to the rotor passing through the wind shade of the tower [23].

2.3.2 Horizontal- and vertical- axis wind turbines

Wind turbines are classified into two generic types, namely Horizontal Axis Wind Turbines (HAWT) and Vertical Axis Wind Turbines (VAWT), based on the orientation of their spin axis. A horizontal axis machine has its blades rotating on an axis parallel to the ground. A vertical axis machine has its blades rotating on an axis perpendicular to the ground. Figure 2-2 illustrates the blade orientations of horizontal-axis and vertical-axis wind turbines.

There are advantages and disadvantages for each of these designs. However, compared with the horizontal axis type, very few vertical axis machines are available commercially [24]. The advantages of the HAWT system include high turbine efficiency, high power density, low-cut-in wind speeds and low cost per unit power output. The main advantage of the VAWT system is that it can accept wind from any direction, so that yaw control is not necessary. The drawbacks of the VAWT system are that the turbine system needs an external energy source to rotate the blade during start-up and that the maximum practical height that the turbine can reach is limited because the axis of the wind turbine is supported only on one end at the ground.

Wind turbines can be categorised further by their mechanical power and speed control mechanisms. The turbine blades draw and convert the motion of air to torque, and the torque is regulated to optimise energy capture whilst preventing damage in the process [25].

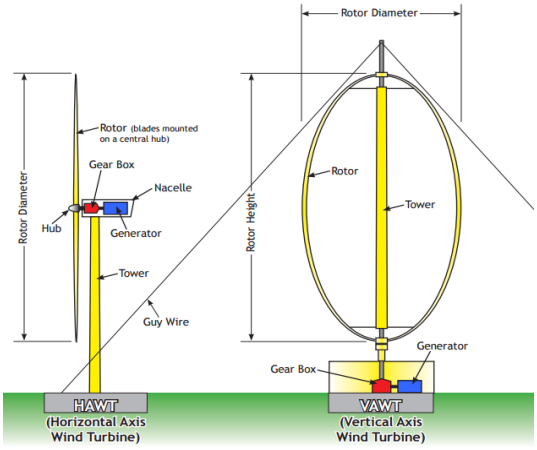

Figure 2-2: Blade orientations of horizontal-axis and vertical-axis wind turbines [24].

2.3.3 Speed control of wind turbines

The power output of the wind turbine system can be either optimised or limited through the use of different control methods. These control principles include pitch angle and yaw control, which are illustrated in Figure 2-3. Pitch angle control adjusts the blades to alter the wind turbine speed, thereby controlling the generator speed. The objective of this control is to optimise the blade angle in order to control the output power for wind speeds more than the rated value. Yaw control continuously alters the orientation of the entire wind turbine to ensure that the turbine is consistently facing into the wind to maximise the effective swept area. This increases the amount of energy captured and thus yields a high output power as a result. The drawback is that, due to the intermittent nature of wind, wind

direction can change rapidly, and the turbine may misalign with the wind direction, thereby causing a loss of power.

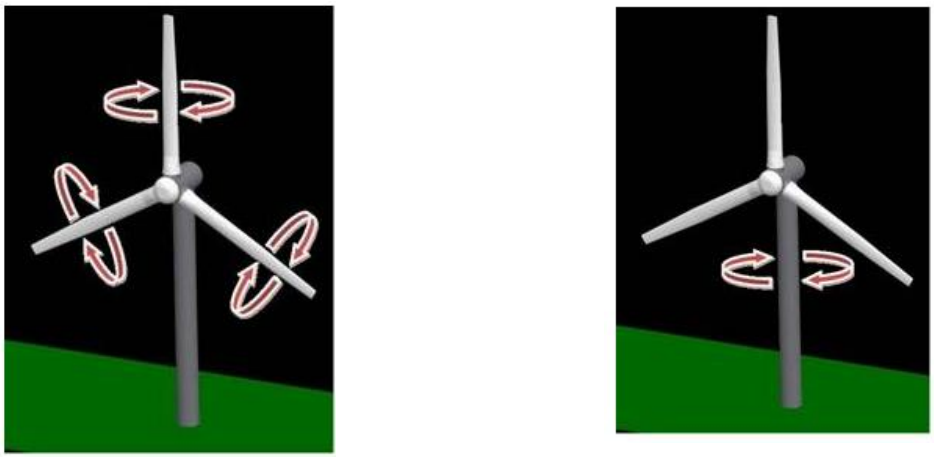

(a) (b)

Figure 2-3: Definition of (a) pitch angle and (b) yaw rotation [26]

The most common speed and pitch control strategies can be classified as follows:

- Fixed-speed fixed-pitch (FS-FP):

Fixed-speed fixed-pitch stall control regulation involves reducing the turbine's torque by altering the pitch of the turbine blades such that the air foil generates less aerodynamic force at high wind speed, until stalling. It is a simple, inexpensive and robust mechanical system. The generator is directly coupled to the power grid, and as a result the generator speed is synchronous to the power line frequency.

- Fixed-speed variable-pitch (FS-VP):

Fixed-speed variable-pitch control enables the wind turbine system to generate output power at fixed speed. Active stall regulation uses both the blade and stall pitch control methods to limit the power, as illustrated in Figure 2-4 . Below the rated speed, the FS-VP turbine has an optimum efficiency around region II. When the rated wind speed is exceeded, the pitch angle is altered constantly.

- Variable-speed fixed pitch (VS-FP):

Variable-speed fixed pitch control utilises passive stalling to achieve a fixed pitch and has the generator indirectly tied to the grid to enable the generator`s rotor and drive train to rotate independently from the grid network frequency.

- Variable-speed variable-pitch (VS-VP):

Variable-speed variable-pitch control is used to maximise the energy capture and to be able to increase the power when the turbine wind system is operating below the rated wind speed as illustrated in Figure 2-4 . When the wind speed exceeds the rated wind speed, the variable-speed and variable-pitch control allows efficient power regulation at rated power.

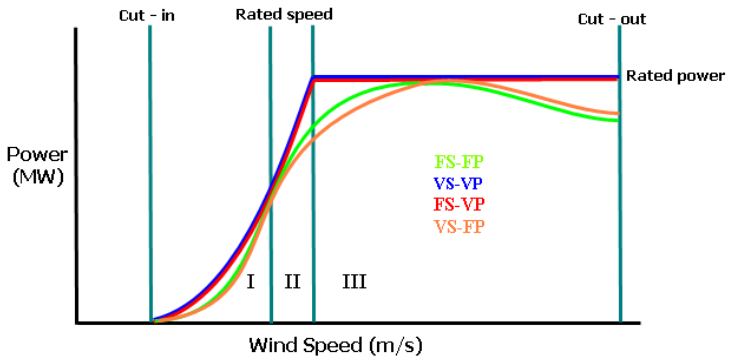

Figure 2-4: Wind turbine output power characteristics and wind speed regions [26]

2.3.4 Fixed and Variable speed wind turbines

A typical wind turbine system is comprised of an aerodynamic rotor that drives a low-speed shaft coupled to high-speed shaft via a gearbox, with the output shaft driving a generator. The fixed speed wind turbine system has its asynchronous generator generating power at a fixed rotational speed at different wind speed ranges. This type of wind turbine is directly coupled to the grid network through a transformer and the operating range of rotational speed of the generator is limited, not to exceed 1% to 2% of the nominal value.

The rotational speed of the variable speed wind turbine generator is variable, and the generator has the ability to generate power at different rotational speeds. The generator is not limited to only asynchronous generators, as some typical types include synchronous and permanent magnet type generators. The turbine is indirectly connected to the grid through power converters.

Wind turbines systems are further categorised according to the associated generator topology, including the following: fixed speed (Type 1); limited variable speed (Type 2); or variable speed with either partial (Type 3) or full power electronic conversion (Type 4); or a synchronous machine directly tied to the grid and with a mechanical torque converter between the rotor's low-speed shaft and the generator's high-speed shaft to maintain the generator speed at the electrical synchronous speed (Type 5) [15].

2.3.4.1 Type 1 wind turbine generator topology

The Type 1 Wind Turbine Generator (WTG) topology, shown in Figure 2-5 , incorporates a Squirrel-Cage Induction Generator (SCIG) that is connected directly to the step-up transformer. This is the most widely used and conventional wind turbine scheme. The topology is a stall or active stall controlled system with an aerodynamic rotor that couples via a gearbox to the SCIG. The turbine speed is determined by the grid network frequency. It is sometimes referred to as 'Danish concept', because it was developed and widely used in Danish wind turbines. Figure 2-6 illustrates the power flow characteristics at the SCIG terminals. While there is a bit of variability in output power with the slip of the machine, Type 1 turbines usually operate at or very close to a rated speed. The main disadvantage of induction machine is that it draws a lot of reactive power for excitation. Large currents are draw when the machine is started online. To improve these effects the turbine typically is coupled through a soft starter and is operated with discrete steps of capacitor banks [27].

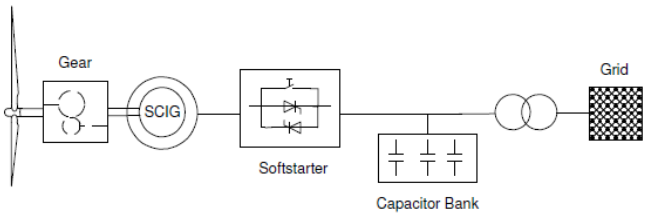

Figure 2-5: Type I wind turbine generator topology [27, 28]

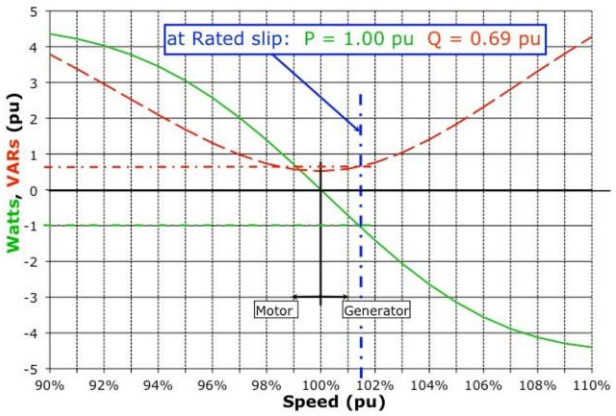

Figure 2-6: Variation of real and reactive power for the Type I WTG topology [15].

2.3.4.2 Type 2 wind turbine generator topology

The Type 2 WTG topology, shown in Figure 2-7 , incorporates a Wound Rotor Induction Generator (WRIG) with connections which are similar to the Type 1 turbine system with regards to its stator circuit. It does, however, incorporate an external variable rotor resistance. This arrangement is accomplished with a set of resistors and power electronics external to the rotor with currents flowing between the resistors and rotor via slip rings [27]. With a resistance in the rotor circuit, the active power curve can in be extended to the higher slip and higher speed ranges as shown in Figure 2-8. This in implies that the turbine would have to spin faster to create the same output power. To facilitate an efficient capture of energy the machine must have the ability to control the speed This usually implemented by the blade pitching mechanism. Typical speed variations of up to 10% are possible, which gives allowances for some degree of freedom in energy capture and self-protective torque control [15].

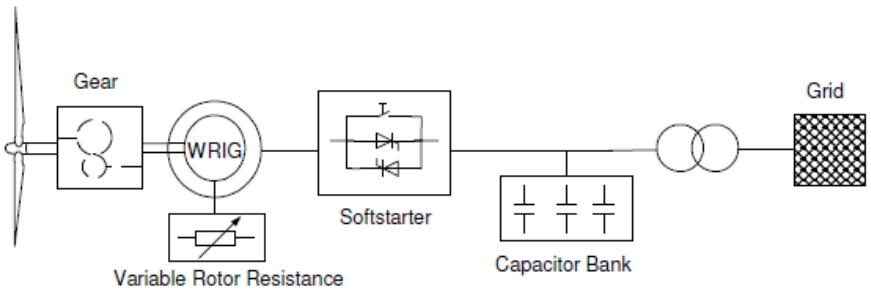

Figure 2-7: Type II wind turbine generator topology [27, 28]

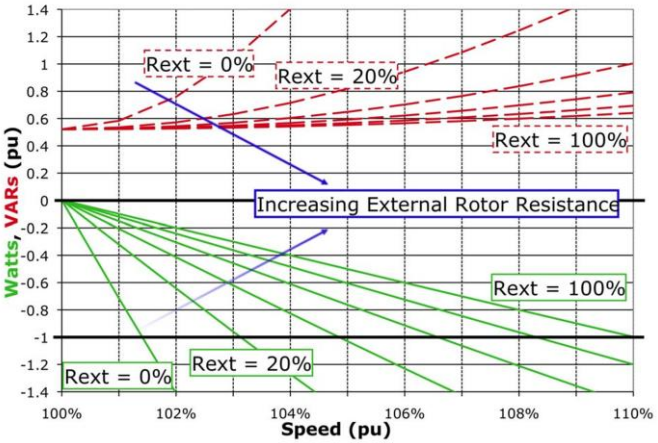

Figure 2-8: Variation of real and reactive power for the Type 2 WTG topology [15].

2.3.4.3 Type 3 wind turbine generator topology

The Type 3 WTG topology, shown in Figure 2-9, incorporates a Doubly Fed Induction Generator (DFIG), also known as Doubly Fed Asynchronous Generator (DFAG). This is a modification of the Type 2 topology design where a variable frequency ac excitation system is utilised rather than simply using an external resistance in the rotor circuit. The rotor excitation is supplied through slip rings using a current regulated voltage-source converter (VSC) that can instantaneously adjust the magnitude and phase of the rotor currents. The active power is feed to the grid to the grid through a converter connected back-to-back to a rotor-side converter as shown [29].

A great deal of control of the output power can be achieved through the set of converters, which are mostly rated at only 30% of the rating of the machine. This control ability is possible since a small amount power injected into the rotor circuit can affect a large control of power in the stator circuit. The DFIG real power can be delivered to the grid from the generator's stator circuit, and also delivered to the grid through the grid-connected inverter when the generator speed is above synchronous speed. When the generator speed is below synchronous speed, real power flows from the grid, via both converters, and from rotor to stator. These two modes, which is enable by the four-quadrant nature of the two electronic converters, makes it possible for a wider speed range of up to 50% both above and below synchronous speed, although narrower ranges are more common in practice.

The greatest advantage of the DFIG is that, just like convectional synchronous generators, it offers the benefits of separate real and reactive power control while being able to run asynchronously. Using the concepts of vector or field-oriented control of induction machine control schemes, the torque

producing components of the rotor flux can be made to respond fast enough so that the machine remains under relative control, even during significant grid disturbances. While more expensive than the Type 1 or 2 machines, the Type 3 is becoming popular due to its advantages [27].

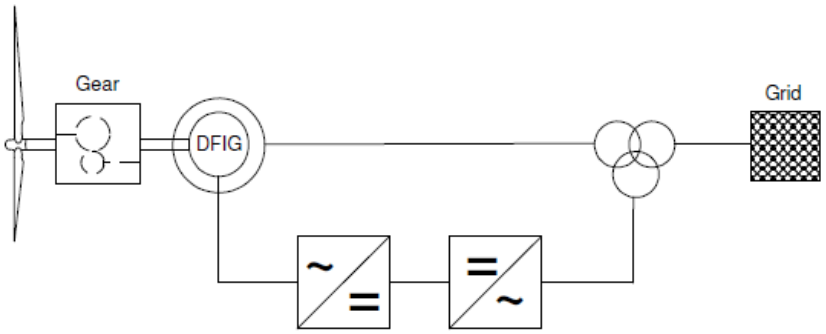

Figure 2-9: Type III wind turbine generator topology [30, 31].

2.3.4.4 Type 4 wind turbine generator topology

The Type 4 turbine wind turbine generator topology, shown in Figure 2-10 enables a great deal of flexibility in design and operation as the output of the rotating machine is connected to the grid through an electrical interface of a full-scale back-to-back frequency converter [27]. The turbine can rotate at its optimal aerodynamic speed, resulting in a variable output power from the machine. The generator can optionally be an asynchronous or synchronous generator. Figure 2-11 shows a modification of this topology [31]. The gearbox may be eliminated, usually when implementing a synchronous generator instead of an induction generator, such that the machine rotates at the slow turbine speed and generates an electrical frequency well below that of the grid frequency. This is no problem for a Type 4 turbine, as the inverters convert the power, and offer the possibility of reactive power supply to the grid, much like a Static Synchronous Compensator (STATCOM). The synchronous generator is electrically excited through a Direct Current (DC) system or by means of a permanent magnet.

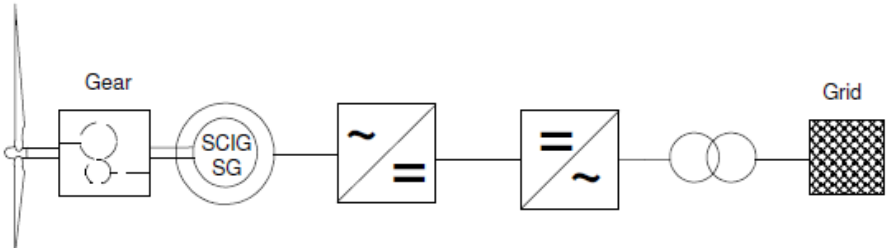

Figure 2-10: Type IV wind turbine generator topology [31, 28, 27]

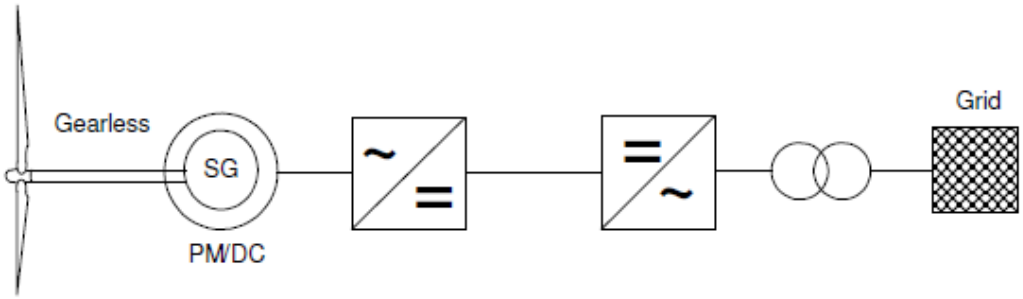

Figure 2-11: Variation of the Type IV wind turbine generator topology [28, 31, 27]

Table 2-2 shows a brief summary of the WTG topology classifications. It represents an alternative classification of wind turbine systems with the type ranging from type A to D rather than as represented in the above sections which ranges from type 1 to 4.

Table 2-2: Classification of wind turbine generators with reference to stall control, speed control and pitch control [31]

Blade angle control	stall/active stall control		pitch control			
Speed control	fixed speed		variable speed			
Grid connection	direct grid connection		direct grid connection	partial scale converter	full scale converter	
Drive train	gear	gear	gear	gear	gear	gearless
Generator	SCIG	SCIG with pole changeable stator winding	WRIG with variable rotor resistance	DFIG	DCSG/PMSG SCIG	Multipole DCSG/PMSG
Speed range	n_{rated} (~2% slip)	n_1 ; n_2 (~2% slip)	1 - 1.1*n_{syn} (~10% slip)	0.7 - 1.3*n_{syn} (~ ±30% slip)	0...1*n_{rated}	0...1*n_{rated}
	TYPE A		TYPE B	TYPE C	TYPE D	

2.3.4.5 Type 5 WTG topology

The Type 5 turbine wind turbine generator topology, shown in Figure 2-12, makes use of a typical variable-speed wind turbine with its drive train connected to a torque/speed converter coupled to a synchronous generator [15].The variable speed is controlled by the torque/speed converter to a fixed speed determined by the grid frequency. The machine is connected to the network through a synchronizing circuit breaker. The synchronous generator can be implemented for any desired speed ranges and voltage levels. This approach requires speed and torque control of the torque/speed

converter along with the typical Automatic Voltage Regulator (AVR), synchronizing system, and generator protection system along with a grid-connected synchronous generator.

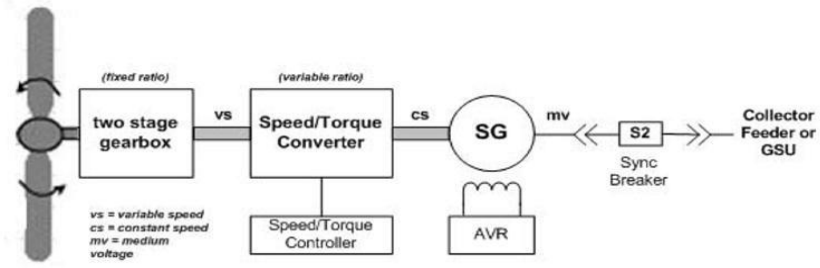

Figure 2-12: Type V wind turbine generator topology [15].

2.3.4.6 Generator concepts under development

The newest trend of wind turbine technology focuses on direct driven and direct grid coupled wind turbines, which employs a gearless drive train and without any power electronic converter [32] . One such type is the Slip Synchronous Permanent Magnet Generator (SS-PMG) topology also known as Slip Synchronous Generator (SSG), shown in Figure 2-13.

It can be described as a hybrid WTG design, which incorporates both the beneficial aspects of Permanent Magnet Induction Generator (PMIG) and Permanent Magnet Synchronous Generator (PMSG) [33, 20] . This evolutionary Wind Energy Conversion System (WECS) implements neither a gearbox nor a frequency converter as shown in Figure 2-13. The SSG is driven directly by a fixed speed wind turbine and is coupled directly to the grid through a grid synchronisation controller [33].

The SSG utilise a two-permanent magnet (PM) generators mechanically linked by a common PM rotor. The turbine and slip-rotor are mechanically linked and rotate in unison. The PM-rotor can rotate freely, without any mechanical connection to the other components. The slip-rotor can be implemented as either a short-circuited wound rotor or as a cage rotor. Together with the corresponding half of the PM-rotor, it constitutes a short-circuited PMSG, which develops substantial torque as soon as there is relative motion between the two rotors [20].

The second half of the PM-rotor couples with the stator to form a grid-connected PMSG. This side of the machine is driven indirectly by the torque from the wind turbine, which is transmitted through the first slip-rotor stage. The advantage of this connection is that it introduces damping and allows for some rotational speed difference between the turbine and the PM-rotor. There are effectively three

masses, namely the turbine and slip-rotor, the PM-rotor and the grid-connected stator. Although the connection between the PM-rotor and the stator is lightly damped, it is possible to avoid oscillations in this connection by making it substantially stiffer than the connection between the slip-rotor and the PM-rotor [33, 20]. If the slip-rotor to PM-rotor connection is less stiff, any disturbances will cause an oscillation to develop between these two masses (in this case the PM-rotor and stator effectively form a single mass). Any such oscillations will be attenuated quickly because the slip-rotor to PM-rotor connection is sufficiently damped. As a result, the SS-PMG will be able to remain connected to the grid in a stable manner, despite torque disturbances from wind gusts and tower shadow effects [33].

An additional advantage of the SSG design is that the turbine speed can vary by approximately 5 %, even while the PM-rotor speed is effectively fixed at synchronous speed. This means that the energy present in a wind gust can be captured as an increase in the rotational kinetic energy of the turbine and slip-rotor. This energy can then be delivered in a more gradual manner to the grid, without imposing harsh mechanical loads on the turbine or injecting a current spike on to the network. Like the torque filtering described above, this behaviour is inherent to the SSG and requires no control intervention to take place.

The characteristics of the SSG show a strong resemblance to those of a grid connected IG. The SSG is, however, superior to an Induction Generator (IG) in terms of its grid support capabilities. Since it is a direct-to-grid synchronous generator, the SSG contributes positively towards network inertia and provides natural grid voltage support by supplying reactive power whenever the network voltage drops.

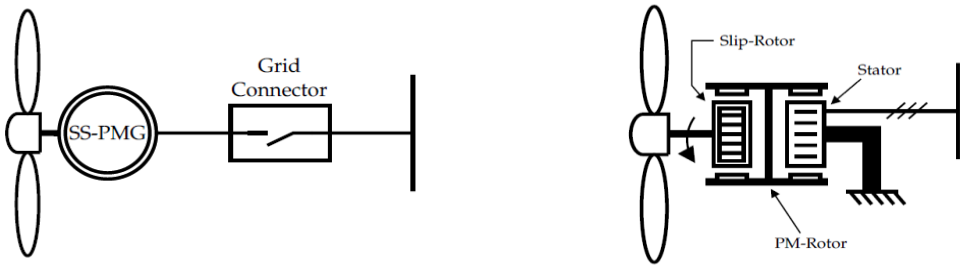

(a) (b)

Figure 2-13: Slip Synchronous Permanent Magnet Generator wind turbine generator topology (a) connected to the grid and (b) Cross-section of the conceptual SS-PMG layout [33]

.

In a permanent magnet induction generator, a relative of the SS-PMG, can be connected to the grid in two ways [34]. In the first case, the PMIG is switched on to the grid from standstill, which results in

high rotor and stator currents. Synchronism is achieved, but with a settling time of more than 40 s. In the second case, the PMIG is brought to synchronous speed and then connected to the grid with no attempt to match phase angles. This reduces transient currents, especially in the rotor, and achieves a much faster settling time. The PMIG can be treated like an IG rather than an SG in terms of grid connection. This corresponds with the objective of its design and is possible because the PM-induced flux linking its stator is relatively weak. In comparison, the SS-PMG has significantly stronger PM-induced flux linkages and is designed to exhibit SG-like behaviour on its grid side. As a result, the grid connection techniques applied for the permanent magnet induction generator are not appropriate for the SS-PMG [34].

To synchronise the SS-PMG with the grid, the same conditions applied to Convectional Synchronous Generators (CSGs) and DFIGs need to be met in the sense that the generator voltage, frequency, and phase angle must all agree, within certain limits, with the respective grid quantities. As in the case of the DFIG, the wind can be used to accelerate the turbine generator from rest. Since synchronisation cannot take place as quickly as with the DFIG, a speed controller is required to limit acceleration and bring the SS-PMG to synchronous speed in a controlled manner. At the same time, the synchronisation conditions need to be monitored continuously so that the SS-PMG can be connected to the grid as soon as all conditions are met [33].

2.4 Impact of wind turbine generators on power system stability

Modern wind farms are dominated by large wind turbines, which are of the order of several 100MW, that are integrated with the transmission network, hence causing a significant impact on the power system. This is mainly due by the following reasons [35, 36]

- The overall power system control due to the contribution of conventional power plants is decreasing due to unbundling, decentralisation and the replacement of the convectional power plants by renewable resources, as in our case wind turbines.
- For both offshore and onshore wind turbine systems, the capacity of installed turbine units is large and therefore their impact on the power system becomes significant.
- Wind power is often installed at remote places characterised by long radial power lines and weak grids usually far away from the main consumption centres.
- Wind turbine systems depends sorely on wind power, which is a fluctuating power source mainly depending on the prevailing wind and must be balanced.

- Large fluctuations in the system generation and consumption causes large current fluctuations and node voltage variations, which must be balanced

For this so called large wind turbine systems, the power system stability is critical and needs to be investigated. Power system stability mainly addresses the following:

- Voltage control through reactive power compensation
- Frequency control through active power dispatch

For constant voltage operation on the grid, the reactive power production and consumption must be balanced at each point in the system. This task was traditionally reserved for centralised power plants placed in vicinity to the grid nodes for which reactive power compensation was necessary. A problem arises when voltage control is assigned to wind turbines located at remote areas in distance to the consumption centres. Some wind turbine systems require reactive power that is dependent on the wind speed. For short term voltage stability, the wind turbine ability to supply reactive power is also essential, mainly due to voltage dips as a result of grid faults.

The intermittent nature of wind power makes it difficult for frequency regulation and active power dispatch, because the available power production is uncertain. Another regard is that wind turbine systems where given leeway to disconnect in the cases of grid faults. In the areas where there are high wind reserves this would cause significant loss of supply that impacts negatively on system stability and leading to wide area blackouts. Transmission system operators thus need the wind turbines to be able to ride through temporary faults for continuity of supply [37]. In some cases, the wind power from turbine systems are extended from primary to secondary control. In such scenarios a proposed solution is usually to curtail wind power and to release the power reserves when needed. With the increasing impact of the wind power on the grid network, there need be defined grid codes, specifying control tasks for the wind turbines in order to assure safe and stable operation of the power system. An overview of the present grid code requirements in South Africa is presented in the following subsection [38]

2.5 Network grid codes

2.5.1 Overview

A high penetration of renewable energies affects the stability of the grid, depending on whether the nature and capacity of the generating plants is supported by the grid. On this basis, the National Energy Regulator of South Africa (NERSA) approved in November 2012 the new grid code for connecting renewable power plants (RPPs) to the transmission system (TS) or the distribution system

(DS) in South Africa [38, 39]. In South Africa, renewable energy technologies are typically interfaced to the grid either at the transmission level or distribution level, depending on the capacity of generation. Both types of interconnections introduce challenges to the grid that influences the power system operation point, the load flow of real and reactive power, nodal voltages and power losses. The aim of the grid connection code is to ensure keep the power quality in accordance to the limits formulated in applicable standards adhering to safety and reliability of network operations [38]

2.5.2 Challenges faced by electricity distributors with increasing growth of RPPs

With the increase of embedded RPPs the nature of the medium voltage (MV) and low voltage (LV) systems is changing from a being passive radial network to an active network with bidirectional power flows. This creates multiple sources that may energise faults, thereby hindering the network protection, system operation and safety. The majority of embedded RPP being added possess inverter-interfaced generators, which have very specific technical characteristics considerably different to the convectional thermal generating plants [40, 41]. There are many potential challenges when large amounts of RPPs are connected to a distribution network, including the following [42]:

- Protection co-ordination: Risk of under-reach for impedance protection. The selectivity between series overcurrent or impedance protection may be lost, which may be alleviated by considering RPP when calculating settings.
- Voltage regulation: For weak systems the control of voltage may be difficult, especially since wind generation is intermittent in nature. This usually leads to overvoltage or under voltage following connection or loss of RPP.
- Islanding: During abnormal conditions or on operation of the protection for islanded power networks there may be concerns in the safety and power quality.
- Power factor: Low power factor may arise due to very light loads been feed by an excessive supply which in turn may cause spurious protection trips if it is not considered in the protection relay settings at the substation.

The following sections cover some of the technical aspects that renewable technology generating systems must identify to develop appropriately and plan adequately. The main objective of the grid connection code is to outline the minimum technical and grid connection requirements for RPPs to be connected grid network. The grid connection code applies to number of RPP technologies, including photovoltaic, concentrated solar power, small hydro, landfill gas, biomass, biogas and wind. The

requirements of the RPP grid connection code are organised according to defined categories as illustrated in following Table 2-3:

Table 2-3: RPP categories [39].

Sub-categories	Rated power range	Voltage connection
A1	0 < A1 ≤ 13,8 kVA	LV
A2	13,8 kVA < A2 < 100 kVA	LV
A3	100 kVA ≤ A3 < 1 MVA	LV
B	1 MVA ≤ B < 20 MVA	MV&LV
C	≥ 20 MVA	HV

2.5.3 The South African RPP grid code

The South African renewable power plant code came into effect on November 2012 [38]. The code services to incorporate renewable technologies into the network and serve as an operational guideline for the Network Service Providers (NSP). The safe operating network voltage and frequency operating ranges and the corresponding trip times are highlighted, which give an indication of the normal operating conditions. For abnormal conditions, the required active and reactive power control ranges regarding the need for mitigating voltage suppression and power surges are outlined. The voltage and frequency operating ranges determine the limits within which the RPPs must not disconnect from the grid and must sustain operation. The active and reactive power control requirements determine control capabilities under various fault and system situations.

2.5.3.1 Tolerance of frequency and voltage deviations

The RPP shall be able to withstand frequency and voltage deviations at the Point of Common Coupling (PCC) under normal and abnormal operating conditions, while reducing the active power as little as possible [38].

2.5.3.2 Normal operating conditions

RPPs should remain continuously connected to the Transmission System (TS) or Distribution System (DS) at maximum stipulated active power output under normal system conditions. The RPP shall be able to operate continuously at normal rated output at frequencies in range from 49 Hz to 51 Hz remain connected to the power system at frequencies within a range shown Figure 2-14.

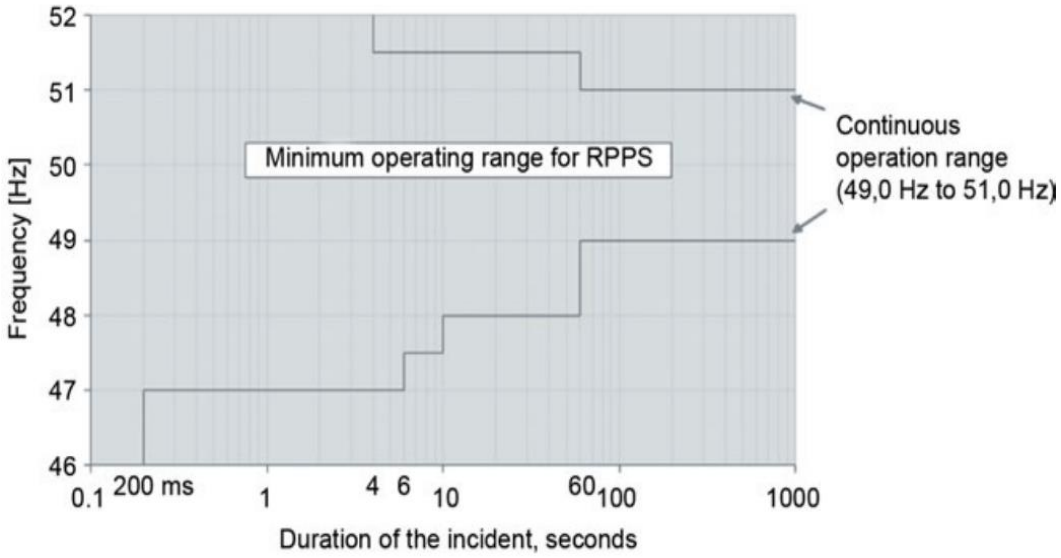

Figure 2-14: Minimum frequency operating range of a RPP during frequency disturbance [39].

The normal voltage at the PCC is dependent on the category the RPP. For category A, it should be capable to operate continuously within the voltage range of -15% to +10% around the nominal voltage at the PCC. Category B and C should be able to operate continuously within the voltage angle as shown in Table 2-4, measured at the PCC.

Table 2-4: Voltage limits for different Independent Power Producers (IPP) categories [39]

Sub-categories	Voltage Limits
A1, A2, A3	±15% to ±10%
B	±10%
C	±10%

2.5.3.3 Abnormal operating conditions

In the event of an abnormality, the RPPs of categories A1 and A2 shall remain connected to the grid for network voltage dips on any or all phases, measured at the HV terminals of the grid connected transformer, without disconnecting or exhibiting any reduction in its output, as shown in Figure 2-15 and Figure 2-16. The maximum disconnection times for the renewable system when operating in category A1 and A2 is shown in

Table 2-5.

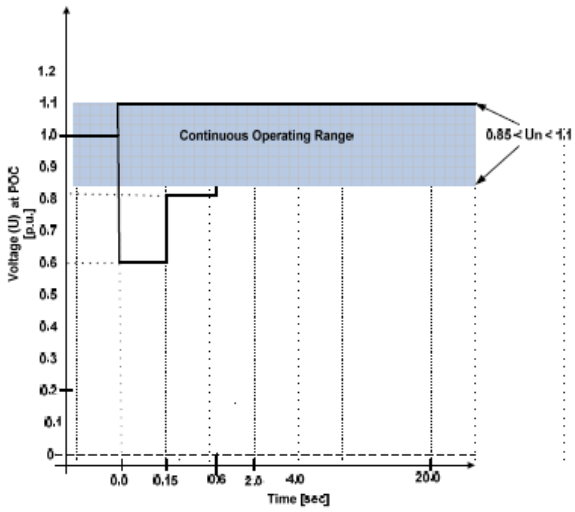

Figure 2-15: Voltage ride through capability for RPPs of category A1 and A2 [39].

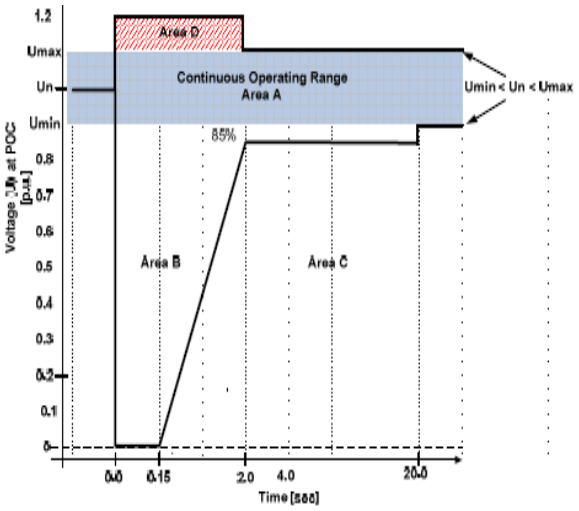

Figure 2-16: Voltage ride through capability for RPPs of category A3, B and C [39].

It is required that the RPPs of category A3, B and C, shall remain transiently stable and connected to the system for any type of symmetrical and asymmetrical short circuit fault. They should fulfil at the PPC the voltage conditions shown in the Figure 2-15 and Figure 2-16. The area D is for the category C RRPs only. Furthermore, the RPP must be capable of continuous operation down to 90% of rated voltage at the PCC. The RPPs must provide mandatory voltage support during voltage dips and supply or absorb reactive current without disconnecting unless if the fault evolves to area C where disconnection is allowed.

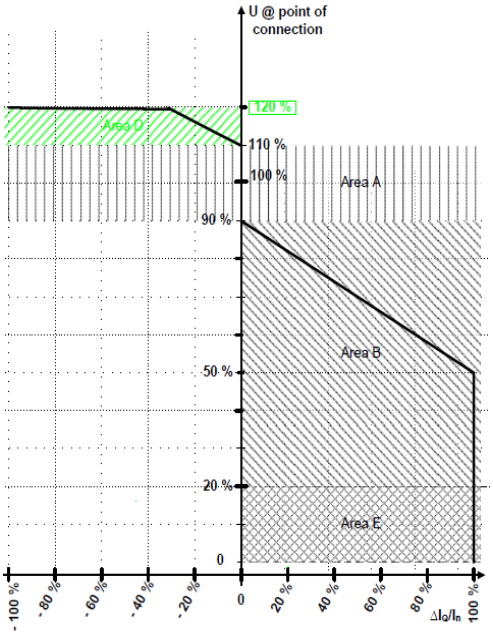

Figure 2-17: Requirements for Reactive Power Support, IQ, during voltage drops or peaks at the Point of Connection (*POC)* [39]

Table 2-5: Disconnection times as a function of voltage variation [38]

Voltage range [at the POC]	Maximum trip time [Second]
V < 50 %	0.2s
50 % ≤ V < 85 %	2 s
85 % ≤ V ≤ 110 %	Continuous operation
110 % < V < 120 %	2 s
120 % ≤ V	0,16 s

2.5.3.4 Frequency response

The RRP should be able to operate continuously between frequencies ranging around the nominal frequency of 50Hz and for different periods of time for lower or higher frequencies up to a minimum or maximum limit. Operation outside these limits would damage the generating plants. The loss of generation leads to further frequency deviation and a black-out may occur.

2.5.3.5 Reactive power capability

Reactive power requirements for interconnection are specified at the PPC for the RRP. Power plants with inverter-based generators rely on the inverters to provide part or all the necessary reactive power at the PPC.

For RPP category A, A1 and A2 must operate at unit power factor, while category A3 must operate in accordance with a specified power factor characteristic curve, with reactive power ranging from 20% to 100% of rated power for power factors ranging between 0,95 lagging and 0,95 leading.

For categories B and, the RRP must be able to supply rated active power for power factors between 0,975 lagging and 0,975 leading for category B and between 0,95 lagging and 0,95 leading for category C, when operating above 20% of rated power [38]. This is illustrated in Fig. 21.

When operating above 20% of rated active power, categories B and C must have the capability of varying reactive power at the PPC within the ranges defined in Figure 2-18 .For active power outputs below 20% of rated value, the reactive power capability of the RPP may decrease due to low wind or solar resource, which may result in some generators in the plant to be disconnected from the grid. For active power levels below 5% of rated MW output, which is at point C in Figure 2-18, there is no reactive power capability requirement. In this range, it is required that the RPP operates within the tolerance range specified by point A and point B.

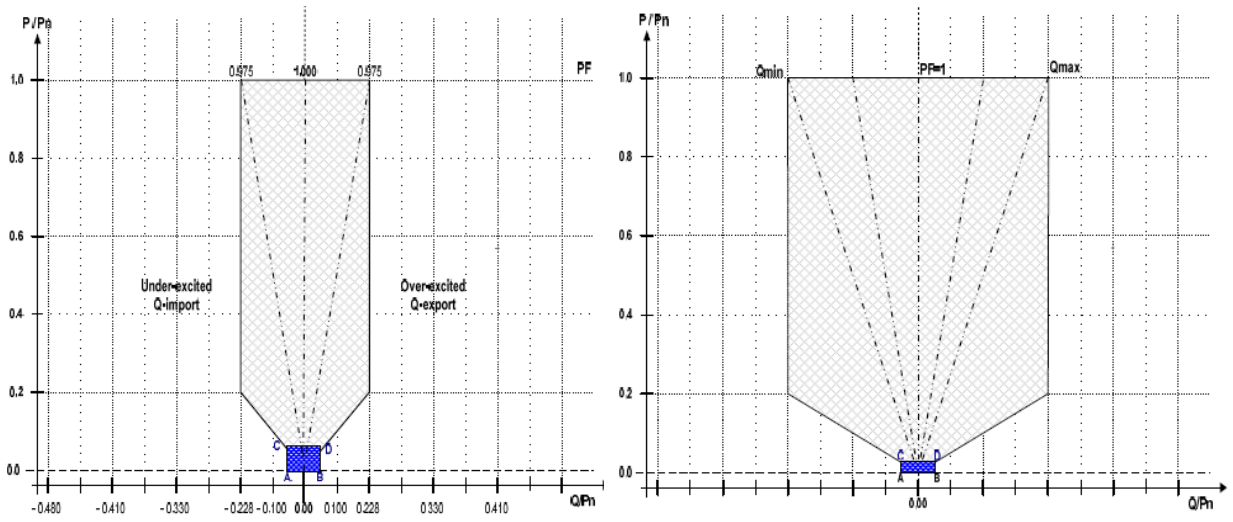

Figure 2-18: Reactive power requirements for RPPs of category B (left) and C (right) [39].

In addition, RPPs of category B and C must be designed with the capability to operate in a voltage, power factor or reactive power control modes. The actual operating mode as well as the operating point shall be agreed upon.

2.5.3.6 Power quality

The power quality and voltage regulation impact of the wind power system is monitored at the PPC. The power quality disturbances include voltage fluctuations, high-frequency currents and voltages and also unbalanced currents and voltages [38]. Voltage and current distortion levels emitted by the RPP at the POC are not to exceed the apportioned limits. The maximum allowable voltage change at the PPC after a switching operation by the RPP shall not be greater than 2%. Depending on the local state of the grid, the RPP shall be equipped with supplementary active power control functions. The constraint functions are used to avoid imbalances in the power system or overloading of the TS and DS in connection with the reconfiguration of the TS and DS in critical or unstable situations, as illustrated in Fig. 22.

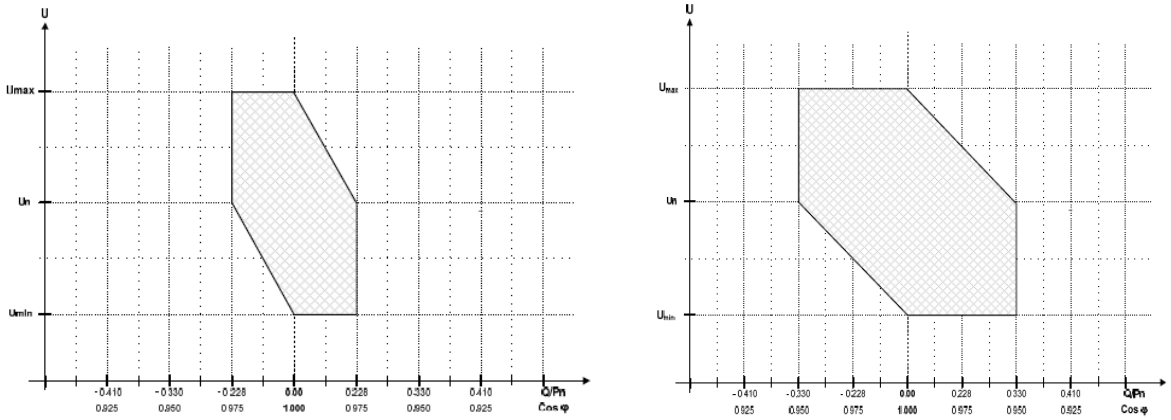

Figure 2-19: Requirements for voltage control range for RPPs of categories B and C [39].

2.6 Voltage, reactive power, and power factor control capabilities

2.6.1 Voltage control capabilities

The WTG system voltage control capabilities mainly depend on the wind turbine type under consideration. For the Type 1 and Type 2 WTGs, they do not typically offer any voltage control. As a result, these WTGs use Power Factor Correction Capacitors (PFCCs) to be able to maintain their power factor or reactive power output on the low-voltage terminals of the machine to a reference set point.

For the Types 3 through Type 5 WTGs they can be able control voltage. These WTGs can vary the reactive power at a given active power and terminal voltage which makes it possible for voltage control [43]. The voltage control for, Type 3 WTG is made possible by changing the direct component of the rotor current, Type 4 WTG voltage control can be done by varying the imaginary quadrature (reactive) component of current at the grid-side converter.

For the WTGs to be able to control voltage, the rating of the grid-side converter must higher than the MW rating of the machine. For the asynchronous generator implemented in the Type 5 WTG system, an automatic voltage regulator (AVR) is needed. The recent AVRs devices can be programmed to control reactive power, power factor and voltage [15].When a power transformer is of concern the voltage control capabilities of the WTG is used to control the voltage at the collector bus or on the HV side of the main power transformer.

2.6.2 Reactive power capabilities

Most grid codes require the wind power plant (WPP) to possess reactive power capability at the PCC defined over a specified power factor range, for example from 0.96 leading (inductive) to 0.956 lagging (capacitive).

As mentioned in section 2.6.1 , the Type 1 and Type 2 WTGs implements the PFCCs to maintain the power factor of the machine to a set reference point. The PFCCs is usually sized to maintain a slightly leading (inductive) power factor of around 0.98 at rated power output, which is referred as the no-load compensation. When there is full-load compensation, the PFCC is sized to have a unity power factor or, for some cases, a slightly lagging (capacitive) power factor at the machine's rated power output. The PFCCs typically consists of multiple stages of capacitors switched with a low-voltage alternating current (AC) contactor [44].

For the Type 3 WTGs it has a reactive power capability range which corresponds to a power factor of 0.95 lagging to 0.90 leading. The options for the DFIG also usually include an extended reactive power capability from 0.90 lagging to 0.90 leading. Other Type 3 WTGs can also manage to deliver reactive power even when there is no mechanical operation of the wind turbine, while no real power is generated [45, 46]

As stated in section 2.6.1, Type 4 WTGs are able to vary the grid side converter current, which makes it possible for the control of the power factor over a wide range. The reactive power limit curves for various terminal voltage levels are usually provided by the manufacturer. Similarly to the Type 3 WTGs, some Type 4 machines can able to deliver reactive power even when no active power is been generated [45]

For the Type 5 WTGs the synchronous generator has a dynamic reactive power capability which closely resembles that of Type 3 and 4 machines. Varying with type of machine design, the power factor operating range is usually varying from 0.8 leading to 0.8 lagging range at rated output of the generator. The typical operating range is usually 0.9 leading and lagging. For low power outputs

below rated power, the reactive power output is only limited by Stability issues, rotor or stator heating and local voltage conditions and it is unlikely to depend on the use of PFCCs. Similarly to the Type 3 and 4 WTGs, it is also possible to operate the machine as a synchronous condenser, requiring minimal active power output with adjustable reactive power output levels [15].

2.6.3 Voltage ride-through

Due to the different implementation of grid code standards the Voltage Ride-Through (VRT) capabilities of WTGs vary widely. In the United States, Low Voltage Ride-Through (LVRT) requirements are specified in [47], which requires for wind power plants to ride-through a three-phase fault on the HV side of the substation transformer for up to 9 cycles, depending on the primary fault clearing time of the fault interrupting circuit breakers at the location. There is no High Voltage Ride-Through (HVRT) requirement in the standardisation, but the North American Electric Reliability Corporation (NERC) and some Independent System Operators (ISO) are in the process of imposing such requirement.

For some European countries, the WPPs are required to operate at during disturbances at high voltage level up to 110% of the nominal voltage at the PCC [48]. The Type 1 WTGs usually have a limited VRT capability and may need to be furnished by a central reactive power compensation system to meet wind power plant VRT capability [49].

IN the case for a Type 5 WTG, it`s VRT resembles that of convectional synchronous generator. For the generator excitation system AVR capabilities and the mechanical design of the generator, that is the machine constants and time constants, will determine the performance of a synchronous generator during transient conditions. For the utility VRT requirements, the settings and operation of the turbine control system, excitation system and protection systems have to be coordinated depending on where the network situated [15].

2.6.4 WTG behaviour during grid short circuits

When the WTGs is under a transient disturbance, it`s response to the fault on the grid is mainly influenced by the type of WTG. Considering the Type 1 and Type 2 WTGs, they usually behave similarly to response of large induction machines used in industrial applications. The dynamic responses of the Types 3, 4, and 5 WTGs are dependent on the WTG controls. For short circuit analysis, the Type 1 WTG is represented as a voltage source in series with the direct axis sub-transient inductance [50, 51]. Usually the Type 1 WTG contribute short circuit current up to the value of its locked rotor current, typically of the order of 5 to 6 p.u.

For Type 2 WTGs, with the rotor resistance WRIG, if during the fault the external resistance control result in the generator rotor short-circuiting, this will result in a dynamic response similar to Type1. However, if the control action at or just shortly after fault inception were to result in insertion of the full external resistance, the equivalent voltage source behind Thevenin impedance representation for the WTG should be modified to include this significant resistance value in series with the equivalent turbine inductance [50].

Other wind turbine topologies employ some type of power electronic control. Consequently, the behaviour during short-circuit conditions cannot be ascertained directly from the physical structure of the electrical generator. Algorithms which control the power electronic switches can have significant influence on the short-circuit currents contributed by the turbine, and the details of these controllers are generally held closely by the turbine manufacturers. For Type 3 WTGs (DFIG), if during the fault, the rotor power controller remains active, the machine stator currents would be limited between 1.1 to 2.5 p.u. of the machine rated current [52, 53].

Under conditions where protective functions act as a crowbar on the rotor circuit, the short circuit behaviour defaults to 5 to 6 p.u. in the case of a fault applied directly to the WTG terminals [54] . for the wind turbines employing full-rated power converters as the interface to the grid (Type 4), currents during transient disturbances will be limited to slightly above rated current. This limitation is affected by the power converter control and is generally necessary to protect the power semiconductor switches.

Like in most circumstances the Type 5 WTGs exhibit typical synchronous generator behaviour even during grid faults. The generator contribution to the grid faults can be calculated from the machine constants, given by the generator manufacturer. Fault current contribution for line to ground faults will depend on the generator star point is grounded. The typical generator fault currents are at least 4 times rated current for close-in bolted three-phase faults. For the single-line to ground faults the fault current contribution ranges from near zero amps (from an ungrounded neutral) to magnitudes greater than the three-phase bolted level, depending on the zero-sequence impedance of solidly grounded generators [15].

2.7 Weak networks

2.7.1 Overview

Regardless of capacity and nature, most of the electrical networks will have inherent weaknesses. To limit any potential loss of supply the weak network must be managed. Even a network considered

robust can have some part of its sections that, depending on the network characteristics, is prone to weaknesses on various sections of the network at some particular instances [55]. A ‘weak’ network has been defined and investigated in various publications, but agreement on a concrete conjecture on how best to measure a weak network is inconsistent. In this research a network is considered weak when power system experiences transient events or disturbances and such dynamic events bring about sufficient change to the stability of the network to cause system disruptions and/or blackouts.

Since most power system networks possess different physical attributes and unique operational requirements, attempts to perform quantitative analysis of transient dynamic events can prove to be very difficult. The weakness of a network can be characterised in terms of various power system parameters, including the network frequency, rotor angle of the generating equipment, real and reactive power capacity, voltage fluctuations and other minor parameters, which, when not controlled within a certain operating range results in system instability. For rotating machines, the frequency and rotor angle are the preferred parameters.

For distribution grid networks in remote places where long feeders are operated usually at MV are prone to be characterised a weak. The grids mainly are to cater for small loads, when the load limit is exceeded the voltage level will be below the allowed minimum and or the thermal capacity of grid will have been exceeded [56].

2.7.2 Generation weaknesses

Every power system architecture will employ power generation sources to supply real and reactive power. During normal operating conditions, the supply must meet the required dynamic load demand. For abnormal conditions, the power stations must be equipped with protection systems that detects anomalies and absorbs some level of transient events, for both short and long-term load changes. For an interconnected network, the control area must have available spinning reserve of about 15% for stability concerns [38]. Most network interruptions are due to insufficient or loss of generation capacity availability. The changing load demand must be meet when the power system is under normal operating conditions, fault conditions and on occasions when the network is under planned maintenance. This forms the basis for the power network classification from weak to robust [55].

In real time, the generating units should have sufficient inertia to counter the transient events that are prevalent within weak networks. For rotational generators, high-speed machines generally have high capabilities to manage transients. Low-speed machines, which are common in remote installations, are less capability to handle transient events, which results in a weak network that is unable to meet the load fluctuations [42]

For wind turbine systems connected to weak networks, it is important to understand the role of inertia in the network. In the traditional approach, the inertia constant, H, is usually assumed as negligible. In recent studies the value of H is estimated for weak networks [42].

2.7.3 Transmission and distribution weaknesses

Robust transmission and distribution networks use a fully redundant architecture to ensure continuity of supply. As with generating stations, transmission and distribution bulk supply points have constraints in capacity. With strong networks, when there is loss of a transmission line, the system remains stable because of the excess capacity of other parallel lines or by utilising line compensation equipment in form of Flexible Alternating Current Transmission System (FACTS) technologies. Depending on the nature of the contingency criterion designed for the network, there are limits to the disturbances that the network can tolerate [42].

Remote locations where power is required, in most cases, are at long distances from major high-voltage bulk supply points. When a cost benefit analysis is conducted, the expected maximum demand will determine the type of network to invest in to deliver power. When the demand increases, the line capacity become constrained when long radial single circuit distribution feeders are in use, which is typical of weak networks [56]. Major concerns arise for this case when the transmission or distribution line trips on a fault, especially a sustained fault, thus leading to loss of supply which can give rise to instability in the main network. When not cleared in time, this could lead to blackouts and further instability of the network. In addition, when auto-reclosing schemes are in use, major interruptions can be experienced at remote locations with local generation during fault conditions [42]. When a wind turbine system is employed in this case, it can assist with low-voltage ride-through capability, but only for limited events and duration. If the wind generation is installed at the far end of a weak network, it will limit the load on the transmission lines but will result in serious transients on the line if supply is lost when a tripping event occurs.

With remote distribution networks, it is very difficult to limit interruptions due to transient events, as redundancy is not utilised in such arrangements. For such scenarios the critical fault clearing time (CFCT) will be critical. In order to limit interruptions to major sections of the network it will be essential to ensure that distribution lines will not cause the loss of large loads that could cause instability [57].

2.8 Modelling issues

When a wind turbine system is experiencing high amount of wind energy power system stability is of major concern. The appropriate power system simulation tools should be implemented for the accurate

representation of the wind turbine system as to be able to analyse the impact of the wind power on the grid [58]. The level of detail of the model implemented in the simulation tool is dependent on the chosen time frame of the simulation. The simulation time frame is determined by the purpose of the simulation. Where the contribution of balancing power is investigated, a longer time frame is implemented than for conducting transient stability analysis. The work conducted in this investigation focuses on stall control of a fixed speed wind turbine system directly tied to the network under fluctuating wind speed conditions, as well as considering the voltage grid support capability during faults. This calls for shorter time frame in the range of milliseconds to minutes. The Figure 2-20 summarises different control tasks and their alignment to the respective time frames.

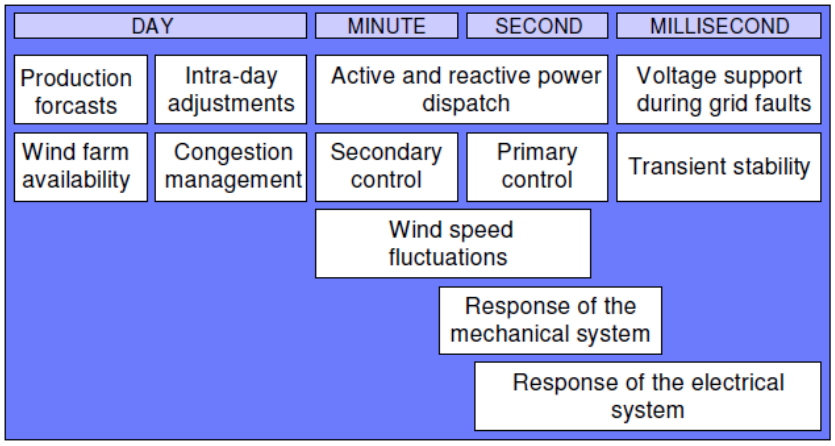

Figure 2-20: Alignment of control tasks to time frames [59, 60].

The time frames of interest can be summarised as follows:

- Days:

For power system operation and power flow studies the investigation of the availability of wind power and the production forecast is essential. This deals with aspects which concerns with long term operation of wind turbines such as in wind power contribution to intra-day adjustments and congestion aligned to a time frame of days. However, for the purposes of this thesis this time frame is beyond the scope of the targeted case studies.

- Minutes and seconds:

Wind speed fluctuations ranges from seconds to minutes. Wind turbine control for rapidly changing wind conditions and the dynamic characteristic of their controllers are covered in this time fame. The research targeted in this investigation focuses on the wind turbine`s capability to provide active and

reactive power during fluctuations in wind speeds. That implicates that this time frame is relevant for the case studies conducted in this thesis.

- Milliseconds:

A very short time frame is considered for the analysis of grid faults, voltage capability of wind turbines and the transient stability of the system. This implies that modelling of the wind turbine performance according this time frame is required. The response of the wind turbine`s electrical system to transient analysis during grid faults usually requires a short time frame in the ranges of milliseconds to seconds after the fault. The mechanical system has a higher response time, since the mechanical components have larger time constants when compared to electrical components

2.9 Simulation tools

The simulation models of the wind turbine system used in this project are developed in the dedicated power system analyses tool DIgital SImuLator for Electrical NeTwork (DigSILENT) and Matlab/Simulink. These simulation tools can support simulations with full electromagnetic transient models (EMT), providing instantaneous values of voltages and currents in the grid, combined with the ability to build dynamic models for movers.

2.9.1 DigSILENT

To build models for wind turbine systems, DigSILENT has a library dedicated for use in electrical power systems, but it consists typically of basic generic components. To implement the wind turbine system a user defined DigSILENT model is built using the programming language Dynamic Simulation Language (DSL), which is a combination of graphics and open source code.

DigSILENT has found application in the wind turbine industry [61, 35], as it combines models for electromagnetic transient simulations of instantaneous values with models for electromechanical simulations of RMS values. This makes the models useful for studies of grid faults (transient), power quality and control issues (longer-term) [61].

The RMS simulations are more appropriate for long simulation periods without transients, which is ideal for most studies of power quality and control issues. On the other hand, detailed models of instantaneous EMT values are required for reliable simulations of behaviour during grid faults. DIgSILENT provides both a comprehensive library of models for electrical components of power systems and a dynamic simulation language DSL. There are thus two types of models in DIgSILENT:

- Built-in models of electrical component models already existing in the DIgSILENT library, including models for generators, motors, controllers, power electronics, dynamic loads and various passive components.
- User defined models, which are created by the user.

DigSILENT is a powerful proprietary power system simulator, with the ability to either simulate with a fixed time step or a variable time step. It does, however, have drawbacks in building user defined generator models, other than the generic models already designed in its library.

2.9.2 Matlab/Simulink

The Matrix Laboratory (MATLAB) is a high-performance language for technical computing purposes. It uses a user-friendly environment that integrates computation, visualization, and programming with results to all computations expressed in familiar mathematical notation [62]. Its uses include the following: math and computation; algorithm development; data acquisition; modelling, simulation, and prototyping; data analysis, exploration, and visualization; scientific and engineering graphics; and application development, including graphical user interface building. The MATLAB system consists of the following five main parts [62]:

- **Development environment**: Which are set of tools and facilities that help to access all the MATLAB functions and files. Most of the tools are graphical user interfaces. The development environment includes the MATLAB desktop and Command Window, a command history, an editor and debugger, and browsers for viewing help, the workspace, files, and the search path [63].
- **MATLAB Mathematical function library**: This is a vast collection of computational algorithms ranging from elementary functions like sum, sine, cosine, and complex arithmetic, to more sophisticated functions like matrix inverse, matrix eigenvalues, Bessel functions, and fast Fourier transforms [63].
- **MATLAB Language**: This is a high-level matrix/array language with control flow statements, functions, data structures, input/output, and object-oriented programming features. It allows both "programming in the small" to rapidly create quick and dirty throw-away programs, and "programming in the large" to create complete large and complex application programs [63].
- **Graphics**: MATLAB has extensive facilities for displaying vectors and matrices as graphs, as well as annotating and printing these graphs. It includes high-level functions for two-dimensional and three-dimensional data visualization, image processing, animation, and presentation graphics. It also includes low-level functions that allow the user to fully customize the appearance of

graphics as well as to build complete graphical user interfaces on your MATLAB applications [63].

- **MATLAB Application Program Interface (API)**. This is a library that allows writing of C and Fortran programs that interact with MATLAB. It includes facilities for calling routines from MATLAB (dynamic linking), calling MATLAB as a computational engine, and for reading and writing MAT-files [63].

In the last few years, Simulink has become the most widely used software package in academia and industry for modelling and simulating dynamic systems [62]. Simulink is a graphical software package for modelling, simulating, and analysing dynamic systems and it is based on Matlab. It supports linear and nonlinear systems, modelled in continuous time, sampled time, or a hybrid of the two. Systems can also be multi-rate, which in tells that they have different parts that are sampled or updated at different rates.

Simulink provides a Graphical User Interface (GUI) for building models as block diagrams, using click-and-drag mouse operations. With this interface, the desired dynamic systems can be easily built. Simulink includes a comprehensive Simscape Power System block library which contains sinks, sources, linear and nonlinear components, and connectors. Using S-Functions, it is also possible to customize and create user-defined blocks.

Models are hierarchical, so the models can be built using both top-down and bottom-up approaches. The system can be viewed at a high level, and by double-clicking blocks the view can go down through the levels to see increasing levels of model detail. This approach provides insight into how a model is organized and how its parts interact. After defining a model, it can be simulated, using a choice of integration methods, either from the Simulink menus or by entering commands in the MATLAB Command Window. The menus are particularly convenient for interactive work, while the command-line approach is very useful for running a batch of simulations.

Using scopes and other display blocks, the simulation results can be analysed while the simulation is running. In addition, the parameters can be changed during the simulation for "what if" exploration. The simulation results can be put in the MATLAB workspace for post processing and visualization.

Model analysis tools include linearization and trimming tools, which can be accessed from the MATLAB command line, plus the many tools in MATLAB and its application toolboxes. Since MATLAB and Simulink are integrated, the models can be simulated, analysed, and revisited in either environment at any point.

Simulink software is tightly integrated with the MATLAB environment. It requires MATLAB to run, depending on it to define and evaluate model and block parameters. Simulink can also utilize many MATLAB features. For example, Simulink can use the MATLAB environment for the following:

- Define model inputs.
- Store model outputs for analysis and visualization.
- Perform functions within a model, through integrated calls to MATLAB operators and functions.

Chapter 3: Mathematical modelling and model implementations in Simulink and DigSILENT

3.1 Overview

The Slip Synchronous Generator (SSG) wind turbine system was introduced to ease the need for a heavy gearbox and expensive power electronic converter in the wind power system [32]. The machine uses the principles of a permanent magnet induction generator (PMIG) and has advantages regarding cost, reliability and construction complexity [20]. This chapter highlights the working principle of the SSG and gives a detail mathematical model description used to model and simulate the generator on the Matlab/Simulink and DigSILENT platforms. The wind turbine system employed for the purposes of this thesis is outlined in Figure 3-1.

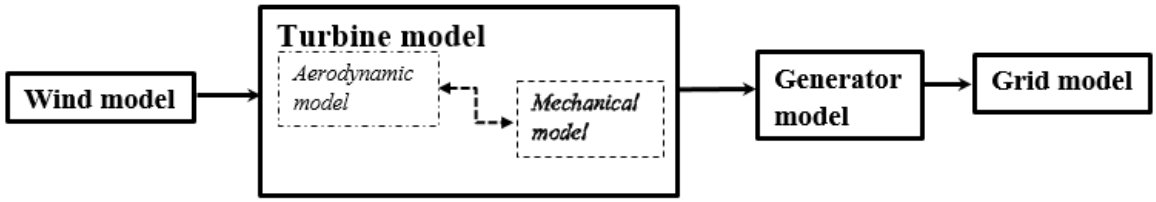

Figure 3-1: SSG wind power system.

1.1.2 Wind model

A wind turbine or its collective wind farm connected to the grid affects the power quality supplied by the grid as a result of the fluctuating character of the output power. The fluctuations are due to the variations of the wind speed and direction and has an effect on the control characteristics of the wind farm. Hence, in order to obtain a realistic simulation of the power fluctuations during the wind turbine system operation the wind is modelled.

The wind model was developed by Gavriluta *et al* based on the Kaimal spectra [64]. The wind model is a combination of two effects, which are the deterministic effects and stochastic effects. The deterministic section of the wind model is given by the mean wind speed and tower shadow variations. The stochastic part of the wind model covers the park scale coherence between the wind turbines in a wind farm as well as the effects of the rotational turbulence as seen by the wind turbine blades.

Only the horizontal component of the wind speed is considered in the model, since this is the component which has the most influence on the aerodynamic performance of the wind turbine. Rotational turbulence and tower shadow cause fluctuations in the turbine output power, for a 3-bladed

turbine the fluctuations occur at three time the rotational frequency and are the main root cause of flicker in the turbine output power for continuous operation of the wind turbine system. Flicker is avoided on the SSG due to its construction. The tower shadow effects are therefore neglected in modelling the wind model as discussed in literature [33].

The wind speed is estimated from the average value of the fixed-point wind speed over the entire span of the rotor, taking into consideration the tower shadow and the rotational turbulences. The wind speed profile is divided into two components, namely a low frequency component associated with long term variations and a turbulence component associated with fast, high frequency variations. From the two components mentioned above wind speed can be modelled by the following equation [64]:

$$v(t) = v_m(t) + v_f(t) \tag{3.1}$$

where $v_m(t)$ denotes the low-frequency component and $v_f(t)$ denotes the turbulence component.

These components where identified in Van der Hoven's large band (six decades) model, presented in Figure 3-2 [65]. The spectral gap of around 0.5mHz suggests that the turbulence component can be modelled as a zero-average random process.

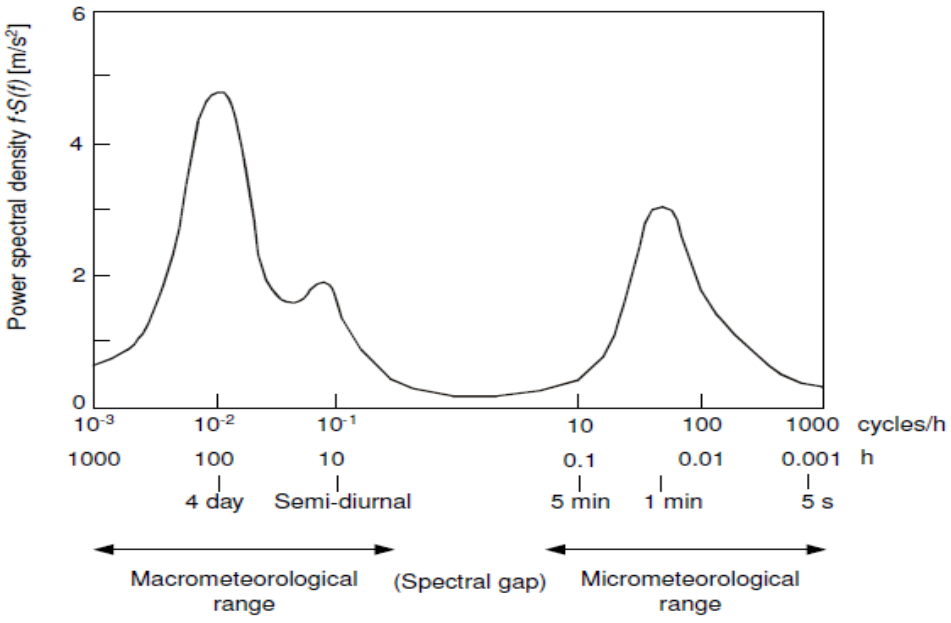

Figure 3-2: The Van der Hoven spectrum model of wind speed [65]

The model generates the wind speed for each simulation time step using the average wind speed and the instantaneous position of the rotor. The average wind speed can be either user defined or actual

average values from measurement masts. The tower shadow fluctuations produced from the passing of the wind turbine`s three blades past the tower is modelled from the rotor position.

3.1.1.1 Modelling of the wind speed

The mean speed or quasi-steady wind speed is associated with the low frequency component of the wind speed, which is attributed to the geostrophic winds. The mean wind speed is derived from the average of the instantaneous speed over an interval t_p, as shown in the following equation [66]

$$V_m = \frac{1}{t_p} \int_{t_0 - t_p/2}^{t_0 + t_p/2} v_m(t)\, dt \tag{3.2}$$

The fast changing components of wind resulting from turbulence and the local effects are modelled by approximating the wind spectrum at high frequencies with the Kaimal or the Von Karman spectrum, using the either of the following models [66]:

Kaimal Spectrum: $$\Phi(\omega) = \frac{K_v}{(1+\omega.T_v)^{5/3}} \tag{3.3}$$

Von Karman Spectrum: $$\Phi(\omega) = \frac{K_v}{(1+(\omega.T_v)^2)^{5/6}} \tag{3.4}$$

where K_v and T_v denotes the constants which dependent on the mean speed and site parameters such as the turbulence scale and turbulence intensity.

The mean wind speed and the turbulence represent the wind speed at a fixed point for time scales which might range from seconds to years. For realistic modelling, a wind turbine will be affected by additional turbulences originating from the tower shadow and wind shear. The distribution of wind is also altered by the presence of the turbine tower and, according to the Prandtl logarithmic law, rotating blades will experience different wind speeds depending on which direction they are facing. The model implementation used in this study uses the Kaimal spectrum for modelling the turbulence, and admittance filters for covering the effects of wind speed averaging and rotational sampling effects [67].

The wind model is comprised of a cascade of Kaimal, zero order and third order filters [68, 67]. For modelling the wind model, a generic block is shown in Figure 3-3 with input and output variables denoted in Table 3-1 and the respective parameters as defined in Table 3-2.

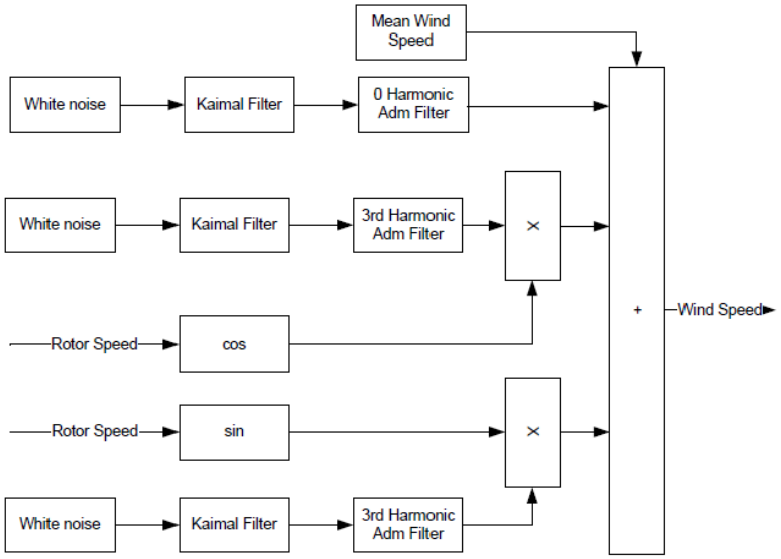

Figure 3-3: Harmonics filter method. Block Diagram [64].

Table 3-1: Input and output variable definitions of the wind model

Variable	Description	Unit	Variable	Description	Unit
N_w	White noise	-	V_m	Mean wind speed	m/s^2
W_t	Rotor speed	rad/sec	V_w	Wind speed	m/s^2

Table 3-2: Parameter definitions of the wind model

Parameter	Description	Unit	Parameter	Description	Unit
S_t	Sample time	sec	L	Length scale	m
R	Blade radius	m	σ	Turbine intensity	%

3.1.2 Turbine model

The turbine model consists of the aerodynamic model and mechanical model of the wind turbine.

3.1.2.1 Aerodynamic model

The concept behind wind power generation involves transforming the kinetic energy of the wind to electrical power. Considering the wind flow to be known, the kinetic wind power P_w [W] can be expressed as follows [69]

$$P_{wt} = \frac{1}{2}\dot{m}V_w^2 = \frac{1}{2}\rho A V_w^3 \tag{3.5}$$

where $\dot{m}$ denotes the mass flow rate [kg/s], V_w denotes the wind speed [m/s], p denotes the air density [kg/m^3] and A denotes the turbine swept area [m^2].

It is not possible to extract all the wind energy. The wind turbine rotor power is therefore based on the power coefficient C_P or the torque coefficient C_Q. The power coefficient is used to determine the aerodynamic power P_{wt} using the following equation [68];

$$P_{wt} = 0.5\pi\rho R^3 V_w^3 C_P \tag{3.6}$$

where R denotes the blade radius [m] and C_P denote the power coefficient. Alternatively, the aerodynamic torque T_{wt} can be determined from the torque coefficient using the following equation [68]:

$$T_{wt} = 0.5\pi\rho R^3 V_w^2 C_Q \tag{3.7}$$

The torque coefficient can be expressed as

$$C_Q = \frac{C_P}{\lambda} \tag{3.8}$$

where λ denotes the tip speed ratio.

For passive-stall, i.e. constant speed, wind turbines the power coefficient is function of tip speed ratio only, and for active stall and variable pitch/speed wind turbines it is function of both the tip speed ratio λ and the pitch angle θ_{pitch}.The power coefficient C_P is defined as the ratio between the mechanical power extracted by the converter and the power of the undisturbed air stream. The coefficient's value can be found in tables for some specific turbines or determined using the following analytic function [70]:

$$C_P(\lambda, \theta_{pitch}) = C_1 \left(C_2 \frac{1}{\Lambda} - C_3 \theta_{pitch} - C_4 \, {\theta_{pitch}}^{C_5} - C_6 \right) e^{-C_7 \frac{1}{\Lambda}} \tag{3.9}$$

with

$$\lambda = \frac{\omega_t R}{V_w} \tag{3.10}$$

and

$$\frac{1}{\Lambda} = \frac{1}{\lambda + C_8 \theta_{pitch}} - \frac{C_9}{1 + \theta_{pitch}^3} \tag{3.11}$$

where C_i denotes the turbine's characteristic coefficients give in Table 3-3, ω_t denotes the turbine's spin speed [rad/s], R denotes the radius of the turbine determined by the length of the blades [m] and V_w denotes the wind speed [m/s].

Table 3-3: Turbine characteristic coefficients [71].

Constants	C_1	C_2	C_3	C_4	C_5	C_6	C_7	C_8	C_9
Constant speed	0.44	125	0	0	0	6.94	16.5	0	-0.002
Variable speed	0.73	151	0.58	0.002	2.14	13.2	18.4	0.02	-0.003
Heier turbine	0.5	116	0.0	0	0	5	21	0.08	0.035

The angular velocity of the turbine can be calculated from the following equation:

$$\omega = \frac{2\pi n}{60} \tag{3.12}$$

where n denotes the rotational speed [rev/min].

3.1.2.2 Mechanical model

The mechanical or drive train model provides the coupling mechanism between the aerodynamic model and the electrical model as shown in Figure 3-1. Since the inception of wind systems, the main component of the mechanical model was the gearbox. As mentioned in chapter 2, wind technology is progressively changing by incorporating power electronics for the generator interface to the grid, using converter topologies (either in full or partial mode). Recently, for small wind turbines, there is an inclination towards direct drive generator systems, thus removing the need for a gearbox.

The mechanical model will be modelled using a gearless system. For this case the mechanical model only models the inertias in the system, as the damping and stiffness coefficients of the shaft are negligible. The dynamics of the turbine, slip rotor, and PM-rotor is expressed as follows [21, 33]:

$$T_t = T_r + J_{tr}\frac{dw_t}{dt} + B_r w_t + B_{r0} \tag{3.13}$$

$$T_m = T_r - T_s = J_m\frac{dw_m}{dt} + B_m w_m + B_{m0} \tag{3.14}$$

where T_t denotes the torque applied on the main shaft of the IG-rotor, J_{tr} denotes the inertia of the turbine and of the IG-rotor and J_m denotes the inertia of the PM-rotor. The B-terms serves to include all no-load rotational losses. Frictional losses are ignored in the model implemented for the purposes of this investigation.

The mechanical linkage between the turbine and the slip-rotor is much stiffer compared to the electromagnetic coupling between the slip-rotor and the PM-rotor. The turbine and slip-rotor are therefore combined as a single component in the mechanical domain. The overall resultant torque equations for the mechanical model can then be expressed as follows [72]:

$$T_t = T_r + J_{tr}\frac{dw_t}{dt} \tag{3.15}$$

$$T_m = T_r - T_s = J_m\frac{dw_m}{dt} \tag{3.16}$$

where

$$J_{tr} = J_r + J_t \tag{3.17}$$

3.1.3 Slip synchronous generator model

3.1.3.1 Permanent magnet induction generator working principle

Figure 3-4 shows the physical topology of the Permanent Magnet Induction Generator (PMIG). The operational principle of the PMIG, is the same as for that for convectional induction generator (IG). The only difference is that the flux is generated by permanent magnets mounted on a free rotating rotor instead of being excited from the generator's armature winding terminals.

The relevant equivalent circuits are shown in Figure 3-5. The use of permanent magnets to provide excitation is represented by the additional voltage source in the PMIG equivalent circuit which usually results in improved power factor since less reactive power will be needed or drawn from the supply.

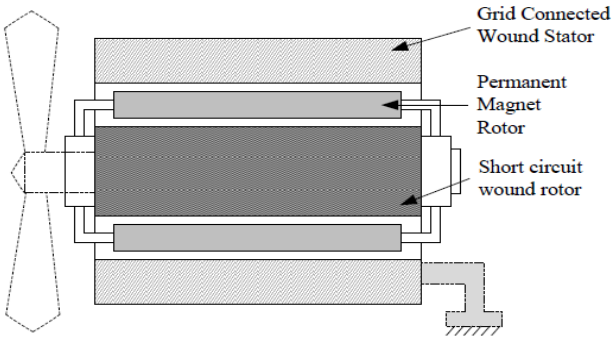

Figure 3-4: Physical topology of the permanent magnet induction generator [34]

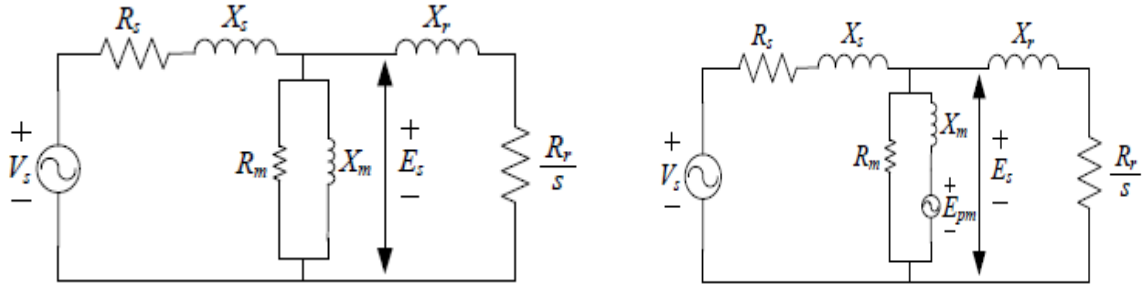

Figure 3-5 Equivalent circuits of the induction generator and permanent magnet induction generator [34]

The PMIG is has advantages for large diameter, high pole generators, because the IG rotor cage can be connected directly to the prime mover hence, there is no use for a gearbox. A PMIG, using an IG with slip, can be utilised with a soft grid connection without the need for a power electronic converter. This gives rise to lower cost and higher reliability. The major disadvantage of the PMIG topology is of the high construction complexity, which lead to the development of the Slip Synchronous Generator (SSG).

3.1.3.2 Overview of the Slip Synchronous Generator (SSG) topology

The SSG essentially consists of two Permanent Magnet (PM) generators tied together with a free rotating PM-rotor, as shown in Figure 3-6. One of the machines is a Permanent Magnet Synchronous Generator (PMSG) that has its stator connected to the grid and the other is a Permanent Magnet Induction Generator (PMIG) that has its short-circuited rotor directly coupled to the prime mover, as

shown in the equivalent circuit in Figure 3-7. The PMSG -rotor rotates at synchronous speed and the PMIG rotor rotates at slip speed relative to the synchronously rotating PMSG rotor [20].

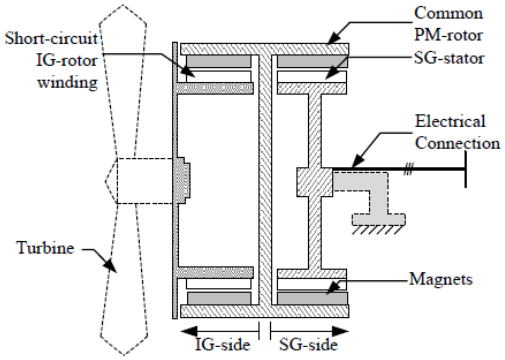

Figure 3-6: Physical topology of the slip synchronous induction generator [34].

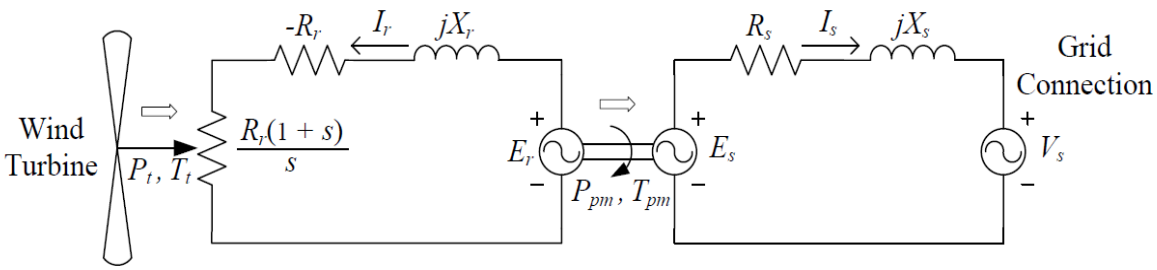

Figure 3-7: Equivalent circuit of the SSG [34].

The dynamic model of the SSG is based on the Parks model referenced in the rotor-synchronous ***dq*** reference frame. The two sides of the SSG are represented by two magnetically independent circuits. The equivalent circuits of the slip-rotor and stator are shown in Figure 3-8 with the slip-rotor short-circuited and the stator open circuited.

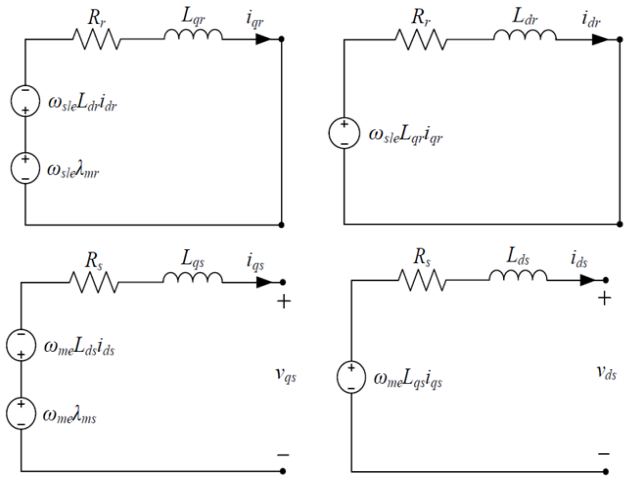

Figure 3-8:Equivalent dq electrical circuits for the SSG slip-rotor and stator [34, 20]

3.1.3.3 Mathematical model

The equivalent circuits shown in Figure 3-8 gives rise to the following differential equations which describes the system dynamics of the slip-rotor and stator [20]

$$0 = -i_{qr}R_r - L_{qr}\frac{di_{qr}}{dt} - \omega_{sle}L_{dr}i_{dr} + \omega_{sle}\lambda_{mr}, \tag{3.18}$$

$$0 = -i_{dr}R_r - L_{dr}\frac{di_{dr}}{dt} + \omega_{sle}L_{qr}i_{dr}, \tag{3.19}$$

$$v_{qs} = -i_{qs}R_s - L_{qs}\frac{di_{qs}}{dt} - \omega_{me}L_{ds}i_{ds} + \omega_{me}\lambda_{ms}, \tag{3.20}$$

and

$$v_{ds} = -i_{ds}R_s - L_{ds}\frac{di_{ds}}{dt} + \omega_{me}L_{qs}i_{qs} \tag{3.21}$$

where ω_m denotes the PM rotor speed, p denotes the number of poles, ω_{sle} denotes the electrical slip speed and ω_{me} denotes the electrical frequency at the stator terminals. Subscripts "r" and "s" in (3.18) to (3.20) refer to the IG rotor and SG stator respectively. The flux linkage due to the permanent magnets for the IG and SG are denoted by λ_{mr} and λ_{ms} respectively. The electrical slip speed and the electrical frequency at the stator terminals are given by the relationships [20, 72]:

$$\omega_{\text{sle}}=(\omega_t - \omega_m)\frac{p}{2} \tag{3.22}$$

And [72]:

$$\omega_{\text{me}}= \omega_m \frac{p}{2}. \tag{3.23}$$

The electromagnetic counter-torque developed by the slip-rotor and the stator is given by the following equations [72, 20]:

$$T_s = \frac{3}{4}p[(L_{qs} - L_{ds})i_{ds}i_{qs} + \lambda_{\text{ms}}\text{i}_{\text{qs}}] \tag{3.24}$$

$$T_r = \frac{3}{4}p[(L_{qr} - L_{dr})i_{dr}i_{qr} + \lambda_{mr}i_{qr}] \tag{3.25}$$

where T_s and T_r denotes the torque generated in the SG and IG respectively, assuming constant ***dq*** inductances and PM-flux linkages. This assumption results in some loss of accuracy, but this serves to simplify the numerical simulations whilst retaining the important dynamic characteristic of the SSG. The parameters used are those calculated for operation at rated conditions. The complete listings of all the parameters used are given in Appendix A.

3.2 Model implementations in Matlab/Simulink

The wind turbine system models can be subdivided into mechanical and electrical component models. The mechanical components consist of the wind model and the turbine model, whereas the turbine model consists of the aerodynamic and mechanical model. The electrical components consist of the generator model and the grid model.

3.2.1 Wind model

The wind model developed at RISØ National Laboratory is adopted for the purposes of the investigation [68]. This model is based on the Kaimal spectra. The main component of this model is the normally distributed white noise generator, which is a built-in block in the Matlab/Simulink library. The wind model structures implemented in Simulink are shown in Figure 3-9. The model has the turbine angular speed as input and wind speed as output. The turbulence induced by the tower shadow and wind shear are modelled in the rotor model.

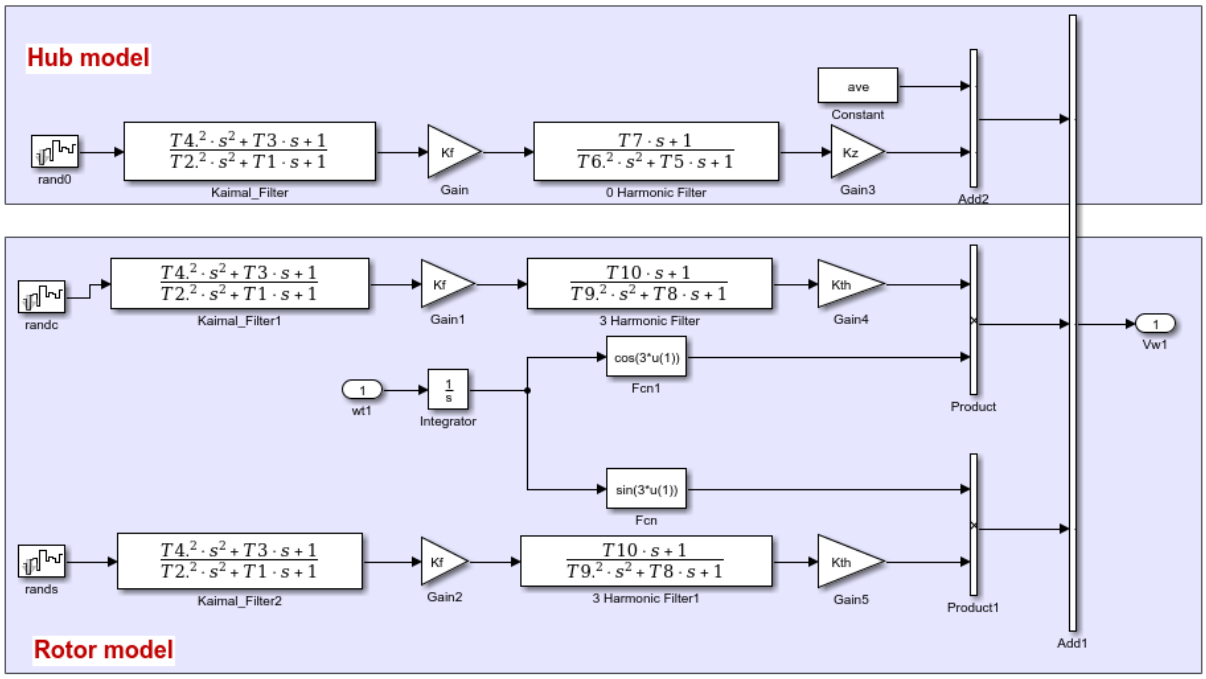

Figure 3-9: Wind model structures implemented in Simulink.

3.2.2 Aerodynamic model

The aerodynamic model represents the interface between the mechanical model and the wind model. It models how wind energy is harnessed into mechanical energy. The energy produced is fed to the electrical model either directly or through the mechanical interface. The aerodynamic model implemented in Simulink for the fixed speed wind turbine rotor is shown in Figure 3-10. The parameters used in the block diagram of the aerodynamic model include the blade radius, air density and the cut-in and cut-out speeds of the turbine. These are given in Appendix A.

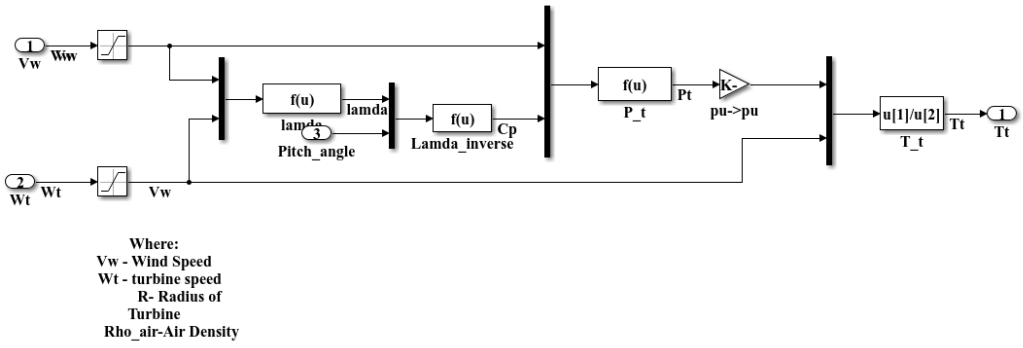

Figure 3-10: Aerodynamic model implemented in Simulink.

3.2.3 Mechanical model

The drive train is modelled using a gearless system. The drive train is approximated by a two-mass model that represents the turbine inertia of the wind turbine system, as the damping and stiffness coefficients of the shaft are negligible. The mechanical model implemented in Simulink for the gearless drive train system is shown in Figure 3-11 with the PMIG involved as the source for damping the external disturbances. The PMIG implemented in Simulink is shown in Figure 3-14. The parameters used in the block diagram of the mechanical model include the number of poles for the multi-pole SSG and the turbine moment of inertia of the one-mass model drive train. These are given in Appendix A.

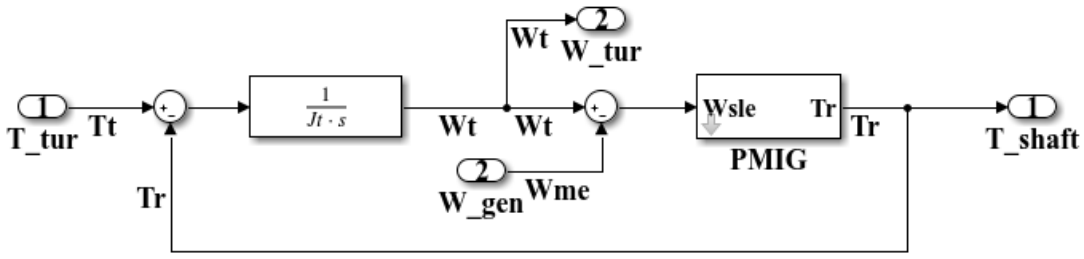

Figure 3-11: Mechanical model implemented in Simulink.

3.2.4 Generator model

The SSG comprises of a PMSG which is coupled to the mechanical model through a magnetic rotor link. The high-level hierarchy of the SSG model is shown in Figure 3-12. The model implemented in Simulink for the PM-rotor is shown in Figure 3-13, while the model implemented for the PMSG is shown in Figure 3-15. Figure 3-6 to Figure 3-8 show the Simulink tabs for the parameter sets used in the model implementations of the SSG wind turbine system (WTS). It includes parameters for the building blocks that constitute the generator, as illustrated in the tabs denoted as the PMSG and PM-rotor.

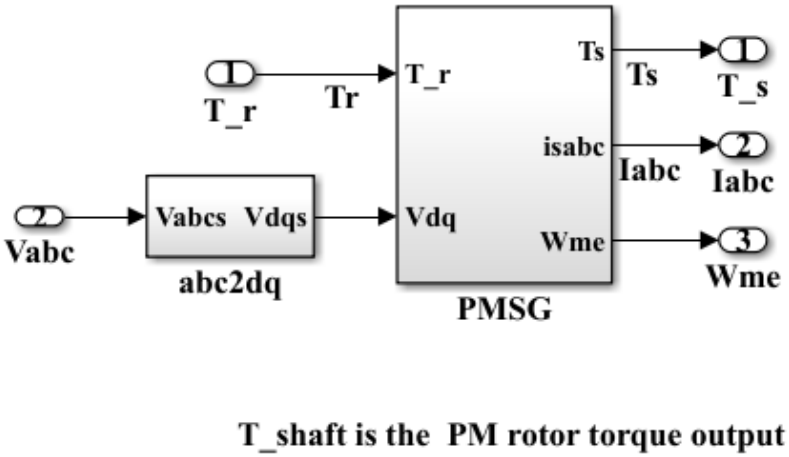

Figure 3-12: High level hierarchy of the model implemented for the SSG in Simulink.

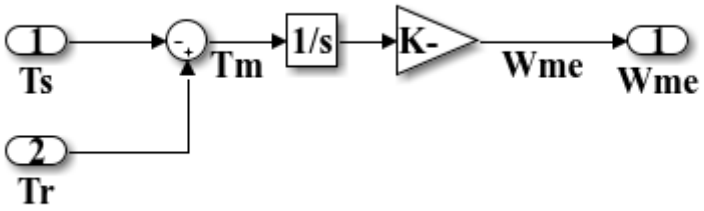

Figure 3-13: Model implemented in Simulink for the PM-rotor.

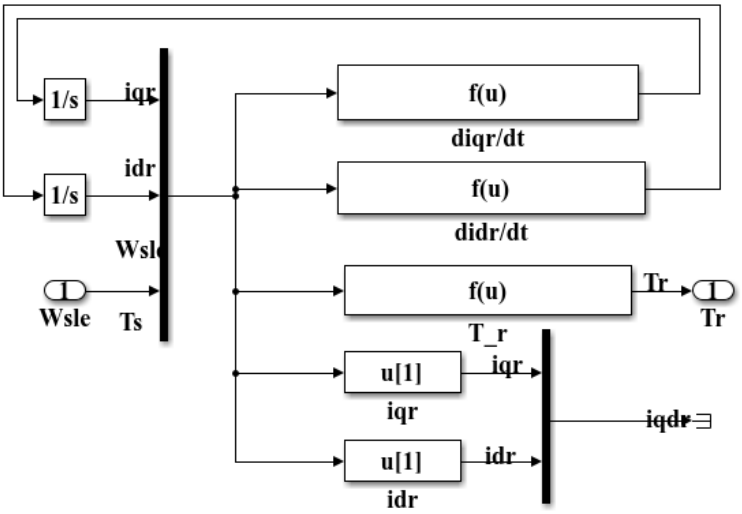

Figure 3-14: Model implemented in Simulink for the PMIG

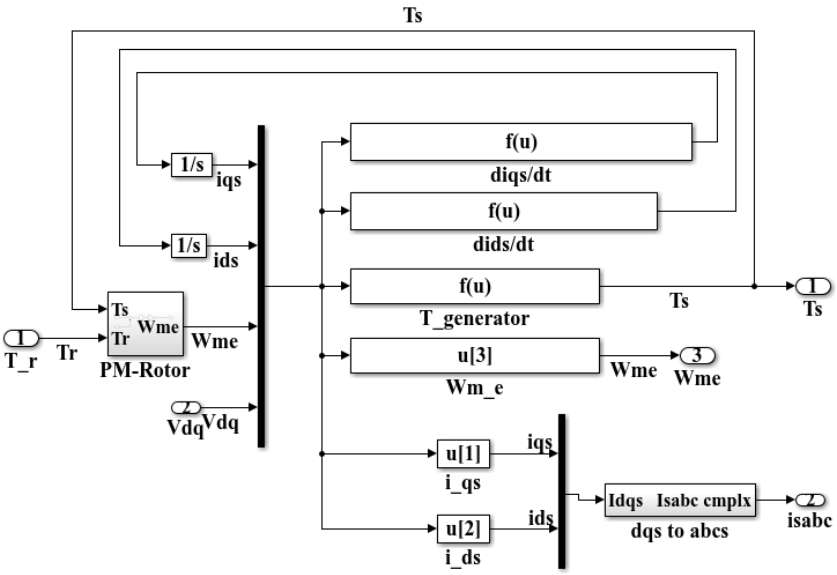

Figure 3-15: Model implemented in Simulink for the PMSG.

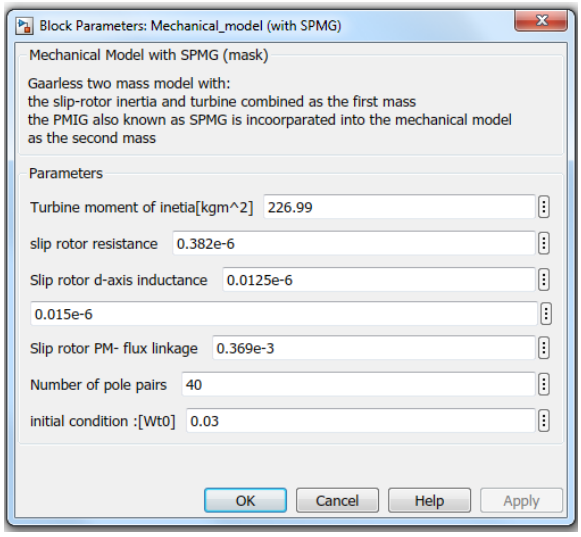

Figure 3-16: Simulink tab showing the parameter set for the PMIG model.

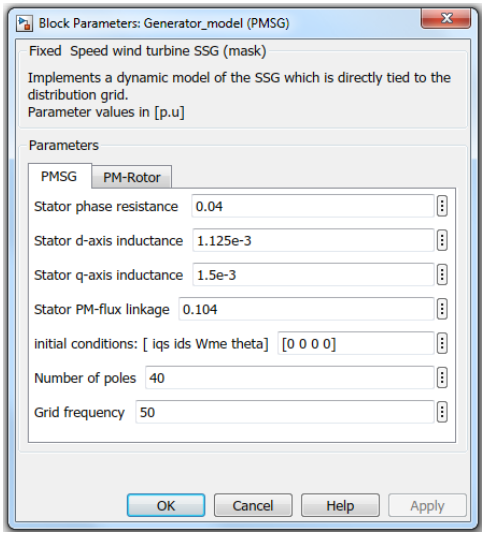

Figure 3-17: Simulink tab showing the parameter set for the PMSG model.

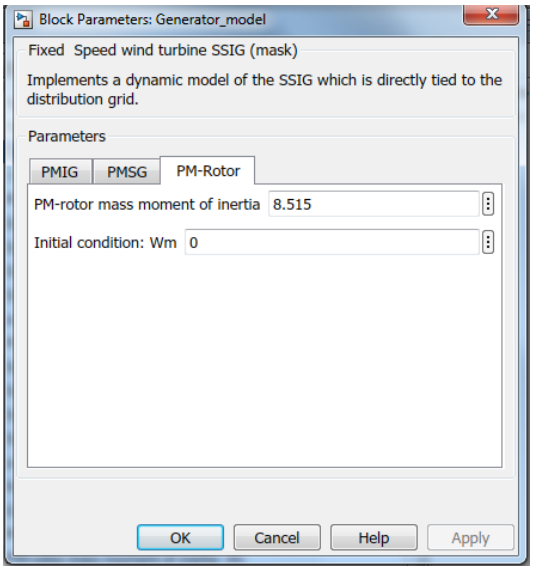

Figure 3-18: Simulink tab for the parameter set of the PM rotor model.

3.2.5 Grid model

The Thevenin equivalent circuit diagram combining the grid and transformers [68], the grid model is shown in Figure 3-19 with the R-L equivalent impedance which is an approximate representation of the transformer and distribution cables.

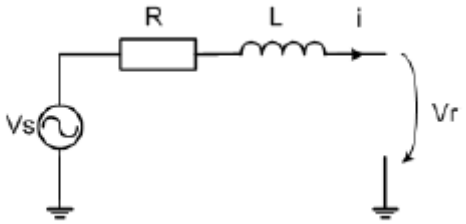

Figure 3-19: Thevenin equivalent circuit of the grid network [68]

The voltage equation per phase is given by the following expression [68]:

$$v_s = Ri + L\frac{di}{dt} + v_r \tag{3.26}$$

The Simulink implementation of the dynamic equation is outlined in Figure 3-20:

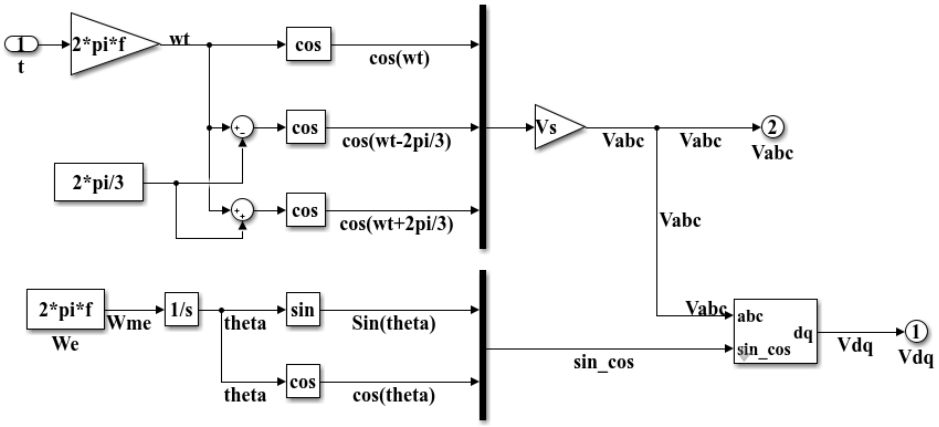

Figure 3-20: Simulink representation of the Thevenin equivalent grid network

3.3 Model implementations in DigSILENT

3.3.1 Overview

The main goal of this section investigation is to explore the modelling, implementation and performance evaluation of dynamic models of a grid-connected SSG in the DigSILENT platform.

DigSILENT is a proprietary licenced simulator, even though it is powerful in solving complex power systems, it does not necessarily present a practical platform for building new generator models. Since the SSG is a new generator topology, no generic model is available in DigSILENT.

This section explores the modelling of the novel directly grid-connected SSG topology in DigSILENT. The work is motivated by the fact that, unlike in the Simulink environment, most local rural networks have not already been implemented in DigSILENT by the local utility. Future case studies of grid-connected SSG performance can therefore be carried out much faster using DigSILENT, providing that that the dynamic SSG model can be successfully implemented in DigSILENT.

Figure 3-21 presents a hierarchical overview of the modelling scheme implemented for the grid-connected SSG wind generator system in DigSILENT. DigSILENT provides built-in models for all the electrical components for the wind turbine system, but the mechanical part of the system is developed by means of the associated dynamic simulation language (DSL).

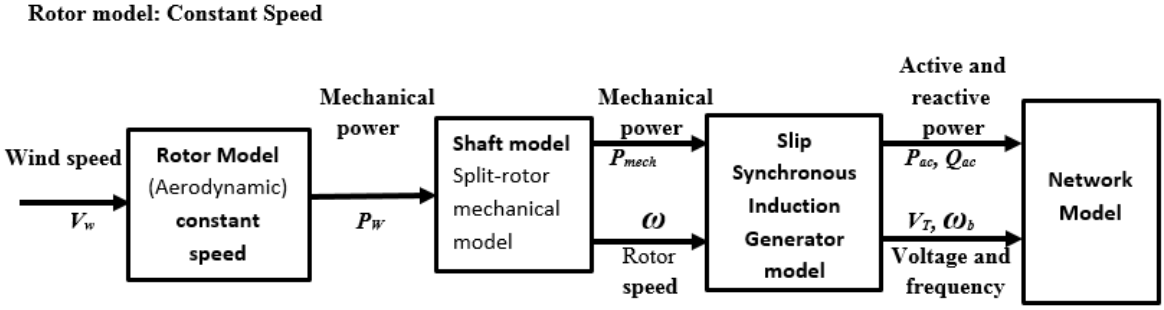

Figure 3-21: Hierarchical overview of the grid-connected SSG model implementation in DigSILENT [73].

The DigSILENT platform contains built-in generic machines or generator models (ElmSym, ElmAsm, ElmAsmsc etc), which are implemented without any controls by default. When these generic models are implemented for dynamic simulations without any modification it results in constant turbine power and excitation voltage for the duration of the simulation. Without implementation of control systems, all types of disturbances tend to translate into unstable frequency and voltage excursions [61].

DIgSILENT uses an object-oriented hierarchical approach with emphases reuse by making a distinction between library (type) and grid (element) objects. This ideology is reflected in modelling dynamic models. The type objects are contained in the library, that is the the composite frames and block model definitions, which are referenced by element objects located in the grid, that is the composite models and common models [61].

The grid elements inherit the properties of the type objects, for example a common model inherits the block structure of its linked model definition. The DSL structures, depending on the type of modelling, are shown in Figure 3-22 and Figure 3-23.

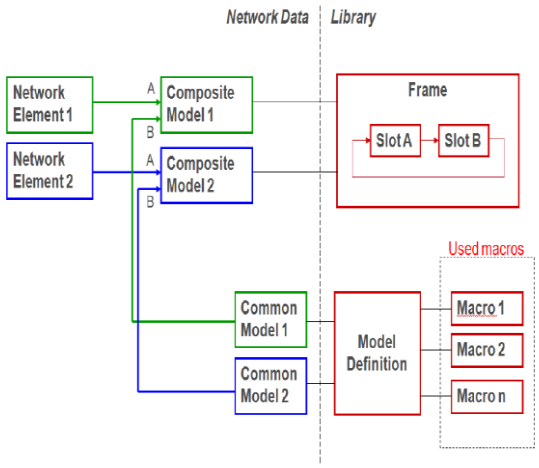

Figure 3-22: DigSILENT DSL structure [61].

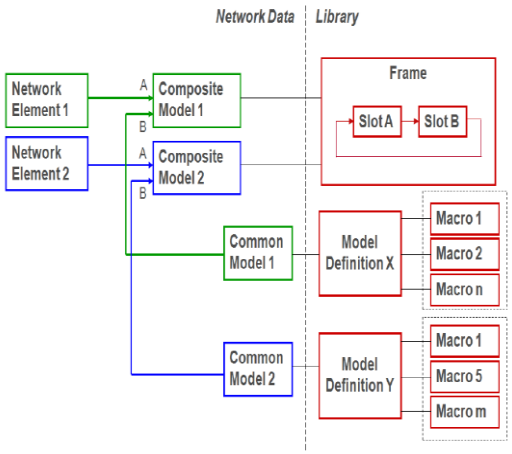

Figure 3-23: DigSILENT DSL structure. [61]

Despite having a comprehensive library of built-in generic models for the electrical components, user defined models can also be modelled for the wind speed, aerodynamic system, mechanical system and control system using the Dynamic Simulation Language (DSL), which allows the dynamic modelling of linear and non-linear systems. The investigation revealed, however, that the novel topology SSG machine cannot be easily modelled, since DigSILENT contain proprietary black box models for machines and has no platform to define new machines using their dynamic models. The SSG will have to be implemented using synchronous generator generic model.

For DSL models, in contrast with the built-in electrical models where model initialisation is based on the load flow calculations, initialisation is user defined. With DSL models it is possible, in principle at least, to evaluate the performance of the grid connected wind turbine, both during normal and during the transient dynamic studies. To initialise the wind turbine system, even though the mechanical components and the electrical power system components are formally separate systems, the wind turbine system is treated as a unified system at initialisation.

3.3.2 Mechanical model

The mechanical model has a direct influence on the grid fluctuations, so this is where most of the emphasis will be based. The drive train is directly connected to the grid, thus neglecting other parts of

the wind turbine structure, for instance the tower and the flap bending modes [35]. The SSG dynamic behaviour can modelled through a user defined DSL dynamic model that implements the built-in generator models. Since the SSG is a combination of a PMIG and PMSG coupled back to back, with the PMSG directly tied to the grid and the PMIG coupled directly to the turbine system, the SSG in DIgSILENT is modelled as a PMSG tied to the grid with the PMIG implemented as part of the mechanical system. The SSG is modelled as shown in Figure 3-24, with the wind speed denoted by V_w, and the grid frequency denoted by f_1 are the model inputs.

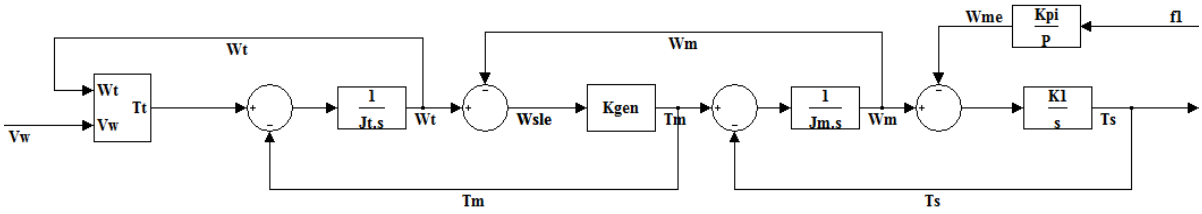

Figure 3-24: Model implementation of the mechanical model in DSL.

When modelling the SSG to the be implemented as a grid connected PMSG, the turbine is assumed as disconnected from the PM-rotor and the SG will only be dependent on the inertia of the common free rotating PM-rotor. The wind turbine system will have a combined inertia from the turbine and that of the IG unit. The torque relationships are now given as [19]:

$$T_t - T_m = J_{tr}\frac{dw_t}{dt} \tag{3.27}$$

and:

$$T_m - T_s = J_m\frac{dw_m}{dt} \tag{3.28}$$

The turbine wind speed is defined as follows [74]:

$$w_t = \int \frac{T_t - T_m}{J_{tr}}dt \tag{3.29}$$

$$w_m = \int \frac{T_m - T_s}{J_m}dt \tag{3.30}$$

where J_{tr} denotes the sum of the inertias of the turbine blades, turbine hub and the induction rotor. This is given by the following relationship:

$$J_{tr} = J_t + J_r \tag{3.31}$$

Assuming that the grid frequency varies slowly, the speed of the PM rotor, w_{me} can be also be approximated to follow the synchronous speed of the rotating MMF of the stator field. This can be represented by the following equation [74]:

$$w_{me} = \frac{4\pi f_1}{p} \tag{3.32}$$

where p denotes the number of poles of the generator. The slip is represented by the following equation [19]:

$$w_{sle} = w_t - w_{me} \tag{3.33}$$

At small slip speeds the torque of the IG is directly proportional to the slip. From the linear relationship the machine torque and slip, this implies that the IG torque can be obtained from the following equation:

$$T_s \approx K_{gen} w_{sle} \tag{3.34}$$

An expression can be derived for K_{gen} using the approach outlined in [74]. The per-phase induced voltage of the IG referred to the grid is given by following equation:

$$E_s = E_2 = \sqrt{2}\pi f_1 N_2 \phi_{PM} \tag{3.35}$$

where N_2 denotes the effective number of turn's per-phase in series of the IG. This gives the following voltage-frequency ratio for the rotor:

$$E_s/_{f_1} = \sqrt{2} N_2 \phi_{PM} \tag{3.36}$$

The IG torqueT_m is defined as follows:

$$T_m = \frac{3I_2^2 \, R_2/_s}{w_{me}} \tag{3.37}$$

Where

$$s = \frac{f_1}{f_2} \tag{3.38}$$

The generated torque is given by the equation

$$T_m = \frac{3I_2^2 R_2 p}{4\pi f_2} \tag{3.39}$$

The rotor current,I_2 is calculated from the per-phase equivalent circuit of the PMSG by the following equation:

$$I_2^2 = \frac{E_2}{\sqrt{\left(R_2/_s\right)^2 + X_2^2}} \tag{3.40}$$

For small slip speeds:

$$\lim_{R_2/_s \to X_2} (I_2) \approx \left(\frac{E_2 f_2}{f_1 R_2}\right)^2 \tag{3.41}$$

and

$$T_m = \left(\frac{3N_2^2 p f_3}{4\pi R_2}\right)\Phi_{PM}^2 \tag{3.42}$$

where

$$f_2 = \frac{p}{4\pi} w_{sle} \tag{3.43}$$

It follows that

$$T_m \approx \left(\frac{3p^2 N_2^2}{8R_2}\right)\Phi_2^2 w_{sle} = K_{gen} w_{sle} \tag{3.44}$$

with

$$K_{gen} = \left(\frac{3p^2 N_2^2}{8R_2}\right)\Phi_2^2 \tag{3.45}$$

where Φ_2 denotes the flux per pole of the PMIG unit. From the block diagram shown in Figure 3-24, a steady state transfer function for the SSG is derived, resulting in a third transfer function given by following equation [19]:

$$\frac{K_1 K_{gen}}{J_t J_m s^3 + K_{gen} J_m s^2 + K_1 J_t s + K_{gen} K_1} \tag{3.46}$$

If the closed loop poles of the transfer function in expression (3.46) are situated in the left half of the s-plane the system will be stable. It can therefore be concluded that a stable directly grid connected system is possible if the PMIG part of the SSG is incorporated within the design, since from studies [20, 21] the PMSG directly tied to the grid is not stable as shown in Appendix C.

The masses used in the model correspond to large turbine rotor inertia, J_t representing the blades and the hub, and a small inertia contributed by the slip rotor, J_r. The inertia of the generator, J_{gen}, is implemented in DIgSILENT as a part of the generator model, while the remaining parts of the mechanical model components are modelled in DSL as described in Appendix F.

The SSG wind turbine is comprised of two virtual distinct machines, namely the PMIG coupled directly to the turbine and the PMSG which is tied directly to the grid network. The PM-rotor moment of inertia is compounded to that of the generator system. Hence the mechanical contribution of the overall generator system is from the turbine and PMIG combined. The DSL shaft model element ElmDsl is related to the block/frame definition designated as 'Mechanical model', shown in Figure 3-25.

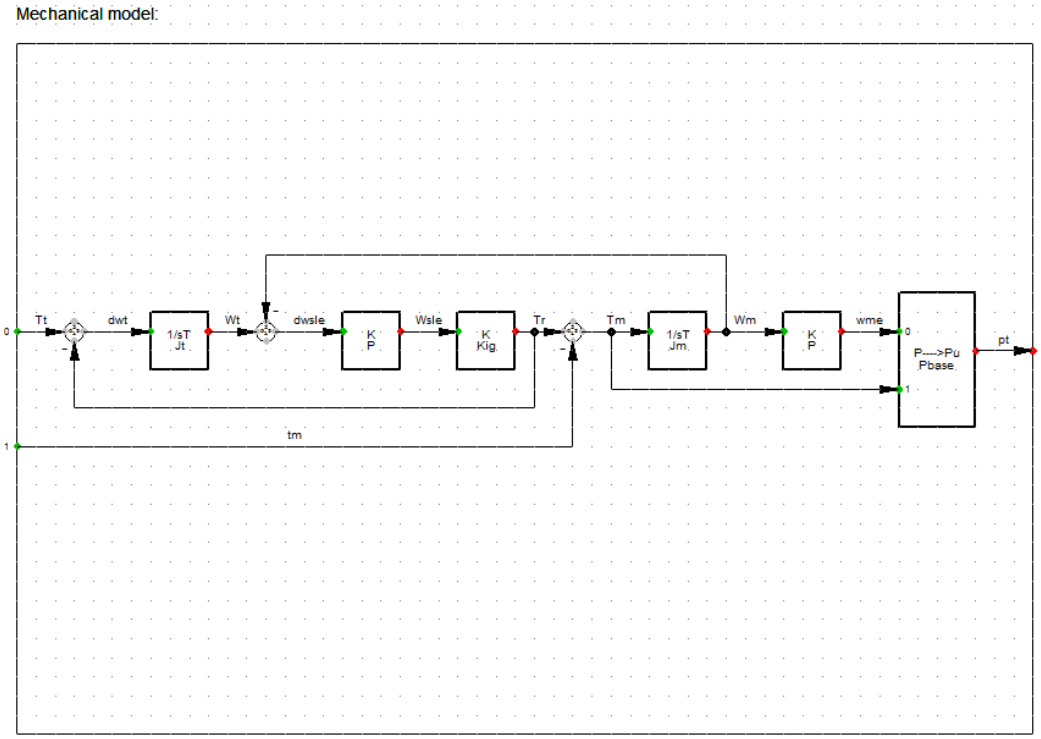

Figure 3-25: DSL mechanical model implementation.

The mechanical model frame contains the input and out signals shown in Table 3-4, as well parameters for the common models shown in Table 3-5. The common model definition for the parameters of the mechanical model is shown in Figure 3-26.

Table 3-4: Input and output parameters for the mechanical model.

Variable	Description	Unit	Variable	Description	Unit
Tt	Torque generated by turbine	Nm	pt	Turbine mechanical power	Watt
Wt	Turbine angular velocity	Rad/s			
Vw	Wind speed	m/s			

Table 3-5: Model parameters for the mechanical model.

Parameter	Description	Unit	Parameter	Description	Unit
Jt	Inertia of turbine and IG	Kgm^2	Kig	Generator constant (IG)	
P	Number of pole pairs	M	Pbase	Base power	MW
Jm	Inertia of PM-rotor	Kgm^2			

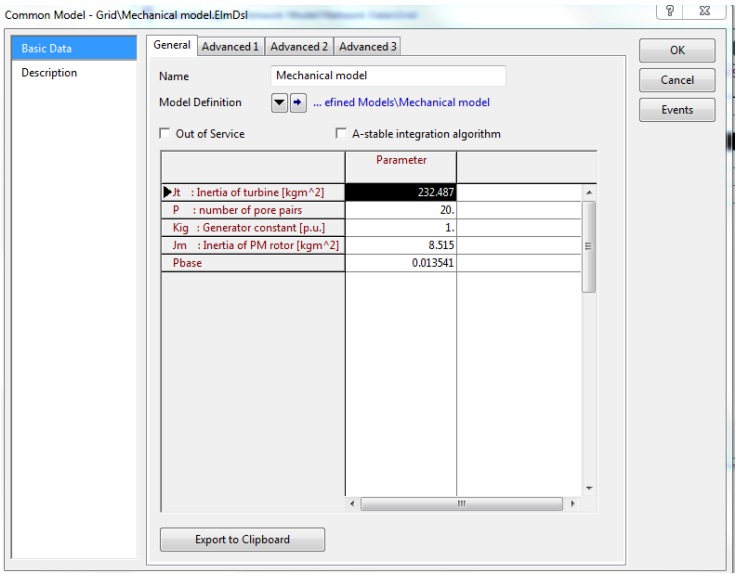

Figure 3-26: Common model parameters tab in DigSILENT.

The initial conditions of the block definition of the Mechanical model (Mechanical model. BlkDef) is obtained with the following code:

```
!Initialisation of mechanical model

inc(Tm)=0
inc(dwt)=0
inc(wt)=dwsle+wm
inc(Tt)=dwt+Tr
inc(dwsle)=wsle/P
inc(wsle)=Tr/Kig
inc(Tr)=Tm+tm
inc(wm)=wme/P
inc(wme)=pt/Tm

inc(x)= wt
inc(x1)= wm

inc0(pt)=0.95
inc0(tm)=1

!defination of parameter for the mechanical model
vardef(P)= ;': number of pore pairs'
vardef(Jm)='kgm^2';': Inertia of PM rotor'
vardef(Jt)='kgm^2';': Inertia of turbine'
vardef(Kig)='p.u.';': Generator constant'

!defination of signals for the mechanical model
vardef(Wm)=;'rad/sec';': PM-rotor angular velocity'
vardef(pt)='p.u.';': Generator mechanical power input'
vardef(wm)='rad/sec';': PM-rotor angular velocity'
vardef(Tm)='Nm';': resultant torque acting on the PM-rotor'
vardef(tm)='Nm';': Generator mechanical torque'
vardef(Tr)='Nm';': torque generated by IG'
vardef(wt)=;': turbine angular velocity'
vardef(wsle)='rad/sec';': electrical slip speed'
vardef(wme)='rad/sec';': electrical synchronous speed'
vardef(Tt)=;': torque generated by the turbine'
```

3.3.3 Wind model

The wind model is modelled as a DSL user defined model in DigSILENT. It gives a wind characteristic output, or equivalent wind speed, V_w, which acts as the input to the aerodynamic model. The average wind speed, U_0 is computed from the rotational turbulence, the tower shadow and the variations in the wind speed over the rotor disk. The model is based on the model developed by RISØ presented in section 3.2.1.

Figure 3-27 shows the structure of the wind model, which is based on two sub-models. The first is the hub wind model modelling the fixed-point wind speed at hub height of the wind turbine. For the scenario where a whole wind farm is modelled, the park scale coherence is factored in.

The second sub-model is the rotor wind model, covering the effects of the rotational turbulence and the influences caused by the tower shadow. The wind speed, V_w represents the wind speed that is extracted by the wind turbine rotor for each simulation time step, based on two inputs, that is the average wind speed and the rotor position. The average wind speed input for the purposes of this investigation is an 'ElmFile' ASCII file implemented in Power Factory. This profile can be defined by

the user and may represent real data obtained by measurements of the wind speed. The V_w values are defined as the averages of the instantaneous wind speed over a time interval, t_p around 10 to 20 min.

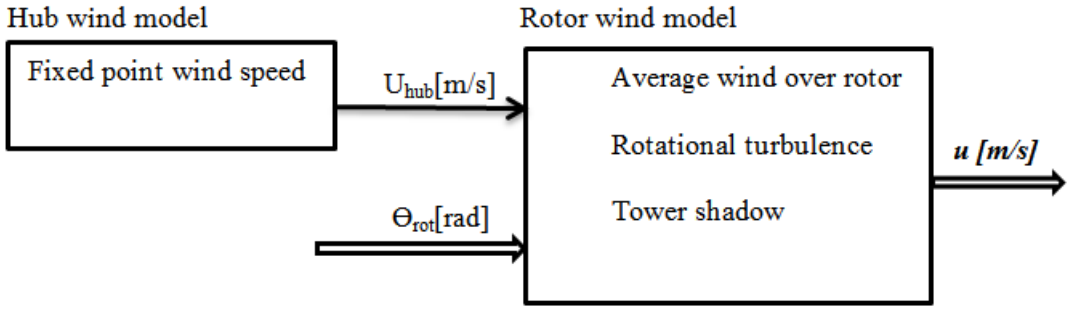

Figure 3-27: Wind model implemented in DigSILENT.

The second input is the rotor position, θ_{rot}, derived from the mechanical system. This has a notifiable impact on the fluctuations of the power with three times the rotational frequency, thus the rotational turbulence is modelled as a 3p fluctuation with variable amplitude. The hub model gives the fixed-point wind speed at the hub height of the wind turbine having as inputs one white noise generator and the average wind speed. The variations caused by the rotational turbulence and tower shadow in the wind speed held over the rotor disk are included in the Kaimal filter and the admittance third harmonic filter.

The wind model parameters as implemented in the DSL model include the blade radius, blade length, average wind speed, turbulence intensity and sample time. The turbulence intensity consists of the wind speed fluctuations which might be considered in the range of seconds or minutes and has a strong bearing on the aerodynamic loads and power quality. The wind turbulence at a certain point can be described by the Kaimal filter [64].

3.3.3.1 Initialization of the wind model

The two sub-models of the wind speed model contain a cascade of second order filters of the following form [75]:

$$y = K\frac{s^2T_4^2 + sT_3 + 1}{s^2T_2^2 + sT_1 + 1}u \tag{3.47}$$

where y and u denote the output and input respectively, while K, T_1 , T_2 , T_3 and T_4 denote the estimated parameters. The second order transfer function can be expressed in the following canonical state space form:

$$\begin{bmatrix}\dot{x}_1\\ \dot{x}_2\end{bmatrix} = \begin{bmatrix}0 & 1\\ -\frac{1}{T_2} & -\frac{T_1}{T_2}\end{bmatrix}\begin{bmatrix}x_1\\ x_2\end{bmatrix} + \begin{bmatrix}0\\ \frac{1}{T_2}\end{bmatrix}u$$

$$y = K\left[\left(1-\frac{T_4}{T_2}\right) \quad \left(T_3-\frac{T_4}{T_2}\right)\right]\begin{bmatrix}x_1\\ x_2\end{bmatrix} + \frac{T_4}{T_2}u \tag{3.48}$$

Assuming the output y is known, the initialization of the input u and the states (x_1, x_2) is given by the following:

$$\dot{x}_1 = 0 \Rightarrow x_2^{initial} = 0 \tag{3.49}$$

$$\dot{x}_2 = 0 \Rightarrow x_1^{initial} = u \tag{3.50}$$

$$u^{initial} = y/K \tag{3.51}$$

3.3.4 Aerodynamic model

The aerodynamic model structure is implemented as shown in Appendix F. The inputs are the pitch angle (since this is a fixed speed generator the pitch angle is equal to zero), the wind speed from the wind model and the speed of the rotor fed back from the mechanical model. This block is modelled by using the following:

- A look-up table of the power coefficient, C_p, which is a function of the pitch angle and tip speed ratio.
- A DSL model definition for the aerodynamic torque that describes a non-linear formulation of the aerodynamic torque of the main shaft, as defined in [73]

DigSILENT built-in model 'ElmChar2' is used to import the C_p characteristic look-up table. The torque of the rotor is calculated in the aerodynamic torque DSL block using equation (3.7). The model is initialised by making the initializing of the wind speed, pitch angle and WT rotor speed, and a common model is then defined to set up the model definition for simulation. The implementation of the aerodynamic model in DigSILENT is outlined in Appendix F.

3.3.5 Generator model

3.3.5.1 Overview

DIgSILENT machine models are black boxes with predefined inputs and outputs. The wind turbine system uses a multipole Permanent Magnet Synchronous Generator (PMSG) that is directly tied to the grid. This machine is implemented in DIgSILENT Power Factory as a built-in model. The built-in 'ElmSym, TypSym' is used to model the SG. This model has the turbine power, Pt, as input and the electrical torque as output. This section describes the implementation of a dynamic model for the PMSG with stall control in DigSILENT.

3.3.5.2 Synchronous generator models

The following section gives an overview over the features of the permanent magnet synchronous generators. Figure 3-28 shows the stator and rotor topologies for three common SGs, namely the salient pole SG, round rotor SG and permanent magnet SG.

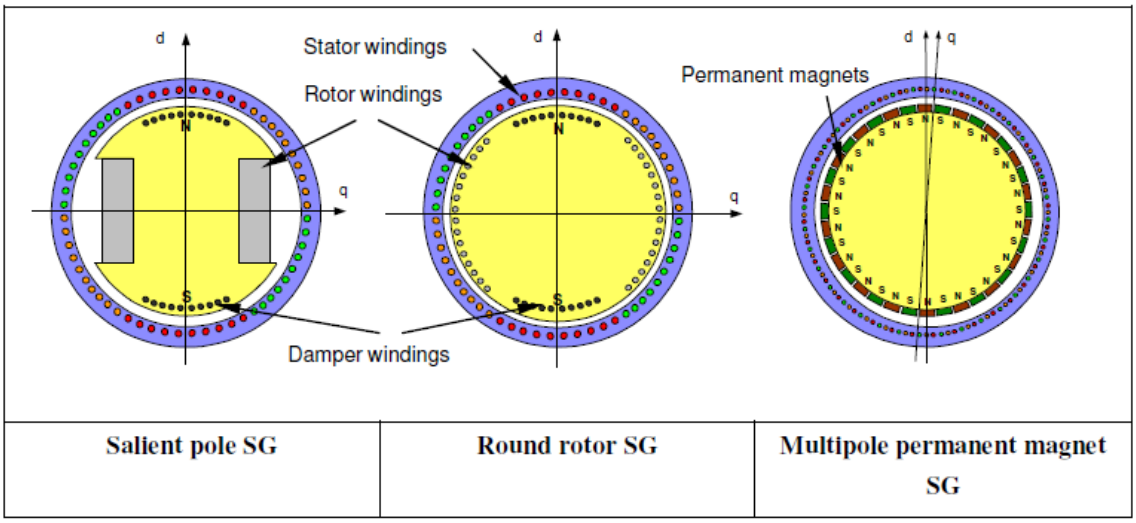

Figure 3-28: Cross sectional view of the different synchronous generator types [31].

The rotor windings of the salient pole SG are designed as a concentrated coil around the pole shoe. This results in different reactance's in the d- and q-axis, such that $X_d > X_q$. The rotor windings of the round rotor SG are evenly distributed around the rotor perimeter, which results in equal reactance's in d- and q-axis, that is $X_d = X_q$. The permanent magnet SG is self-excited with the magnetic rotor field

provided by the permanent magnets. The operating principle and the dynamic equations describing a synchronous generator is covered extensively in [76]. It is beyond the scope of this thesis to cover the extensive outline of the synchronous generators but to give an overview as to understand the most important features of the permanent magnet synchronous generators (PMSG) for wind turbine applications.

3.3.5.3 Steady state generator model

A DC excited synchronous generator single phase equivalent circuit is shown in Figure 3-29, where the phasor diagram of the SG is plotted for an arbitrary operational point. The rotor field is provided by the excitation current I_f, which in turn induces the voltage E in the stator windings. The total magnetic field is represented with the main inductance X_h.

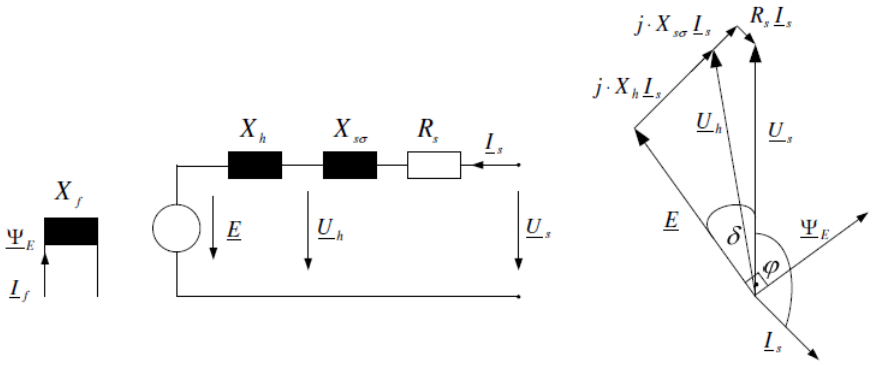

Figure 3-29: Equivalent circuit and phasor diagrams for the classical synchronous machine [31]

This equivalent circuit can further be simplified, assuming the stator windings resistance R_s and the leakage reactance $X_{\sigma s}$ are negligible, which yield a simplified equivalent circuit which is shown in Figure 3-30, representing the permanent magnet synchronous generator and subsequently implying that the voltage induced by the permanent magnet is one represented by E.

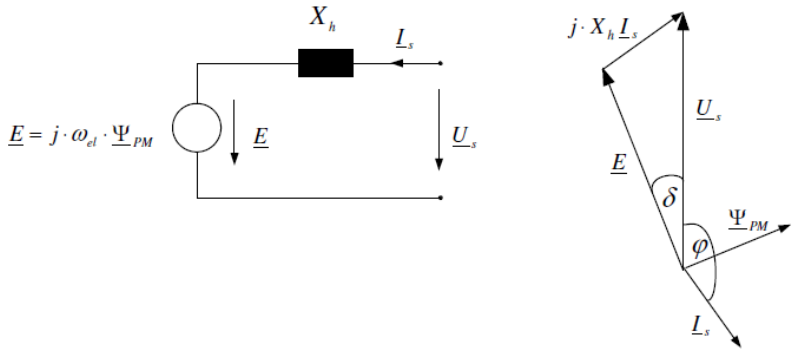

Figure 3-30: Equivalent circuit diagram and phasor diagram for the synchronous machine [31].

Where E denotes the induced electromotive force , U_s denotes the stator voltage, U_h denotes the voltage, representing the main field, I_s denotes the stator current, X_f denotes the field winding reactance, X_h denotes the main reactance, $X_{\sigma s}$ denotes the stator leakage reactance, R_s is the stator reactance, Ψ_{PM} denotes the permanent magnet flux, δ denote the load angle Ψ_E is the DC excited flux, φ denote the power factor, I_f is the excitation current and ω_{gen} denote the generator rotational speed.

The frequency and magnitude of the induced voltage E are all dependent on the rotor speed of the generator ω_{gen}, represented by the equation as follows:

$$\omega_{gen} = p\,\Omega_{gen} \tag{3.52}$$

The stator current I_s is driven by the vector difference between the two voltages, E and U_s which in turn are caused by the load angle. From this relation of the machine torque, the voltages E and $U_s$and the load angle δ, the active power of the generator, P_{gen} can be derived as follows:

$$P_{gen} = m\mathcal{R}\left\{\underline{U_s}\,\underline{I_s^*}\right\} = m.\mathcal{R}\left\{\underline{U_s}\,\frac{U_s - E\,(\cos\delta - j\sin\delta)}{-jX_h}\right\}$$

$$= -m.\frac{U_s E}{X_h}\sin\delta \tag{3.53}$$

$$T_e = \frac{P_e}{\Omega_{gen}} = \frac{-m}{\Omega_{gen}}\frac{U_s E}{X_h}\sin\delta \tag{3.54}$$

The reactive power of the generator is determined by:

$$Q_{gen} = m\Im\left\{\underline{U_s}\ \underline{I_s^*}\right\} = m.\Im\left\{\underline{U_s}\ \frac{U_s - E\ (\cos\delta - j\sin\delta)}{-jX_h}\right\}$$

$$= m\frac{U_s^2 - U_s E\cos\delta}{X_h} \tag{3.55}$$

Where m denotes the number of phases, P_{gen} denote the Generator active power, T_e is the Electromagnetic torque, Q_{gen} denotes the Generator reactive power, *p is the* number of pole pairs and Ω_{gen} denotes the Mechanical generator speed.

Under the load conditions, the stator current I_s and the stator reactanceX_h causes a magnetic field, which is superposed to the field of the rotor. Which depicts that, the voltage U_s represents the voltage induced by the total magnetic field [77]. The voltage dip over the machine's reactance X_h and is contributing factor in producing a phase delay between the electromotive force E and the stator voltage U_s, which are equal only under no-load conditions.

3.3.5.4 Dynamic model of the PMSG

The synchronous machine models for the power system analysis are usually based on the assumption that the magnetic flux distribution in the rotor is sinusoidal. With this assumption in mind, it can be shown that the flux can be described by a vector and thus the internal voltage E induced in the stator by the permanent magnets can be expressed as follows:

$$E = jw_{gen}\underline{\psi}_{PM} = j2\pi f\underline{\psi}_{PM} \tag{3.56}$$

where w_{gen} denotes the electrical generator rotational speed, $\underline{\psi}_{PM}$ denotes the flux provided by the permanent magnets of the rotor and f denotes the electrical frequency. The excitation voltage E is proportional to the electrical speed of the generator.

Since the major difference between a PMSG and convectional synchronous generator is the issue of how the generators field is excited, hence the equations of a PMSG can be derived from the equations of a DC excited SG, by using the assumption that a PMSG does not have damper windings [76]. The voltage equations of the stator, expressed in the Rotor-oriented dq-Reference Frame (RRF), i.e. the reference frame where the d-axis is aligned with the vector of the permanent magnet flux, can be expressed as follows:

$$U_{sd} = R_s i_{sd} - W_{gen}\Psi_{sq} + \dot{\psi}_{sd} \tag{3.57}$$

and

$$U_{sq} = R_s i_{sq} + W_{gen}\Psi_{sd} + \dot{\psi}_{sq} \tag{3.58}$$

where U_{sd} and U_{sq} denote the d-axis and q-axis stator voltages respectively, i_{sd} and i_{sq} denote the d-axis and q-axis are stator currents respectively and ψ_{sd} and ψ_{sq} denote the d-axis and q-axis are stator flux linkages respectively. The stator flux linkages in RRF are given by the following equations:

$$\Psi_{sd} = L_d i_{sd} + \Psi_{PM} \tag{3.59}$$

and

$$\Psi_{sq} = L_q i_{sq} \tag{3.60}$$

where L_d and L_q denote the d-axis and q-axis inductances respectively. As the stator transients can typically be neglected in stability studies [31] the stator voltage equations can be simplified in RRF to yield the following:

$$U_{sd} = R_s i_{sd} - W_{gen}\Psi_{sq} \tag{3.61}$$

and

$$U_{sq} = R_s i_{sq} + W_{gen}\Psi_{sd}. \tag{3.62}$$

The electrical torque of the generator in RRF can be expressed as follows:

$$T_e = \frac{3}{2} p.Im\left[\underline{\psi_s}^{*}\,\underline{i_s}\right] = \frac{3}{2} p\left[\Psi_{sd} i_{sq} - \Psi_{sq}\,\underline{i_{sd}}\right] \tag{3.63}$$

Expressing further the stator flux components, the electrical torque in RRF can be calculated by the following equation:

$$T_e = \frac{3}{2} p.Im\left[(L_d - L_q) i_{sd} i_{sq} - \Psi_{PM}\,\underline{i_{sq}}\right] \tag{3.64}$$

When the PMSG is taken as a round-rotor machine where$L_d = L_q$, which is a reasonable approximation for this type of generator, the electrical torque of the generator is determine only by the permanent magnet flux and the q-component of the stator current in RRF it can be expressed as follows:

$$T_e = \frac{3}{2} p\Psi_{PM} i_{sq} \tag{3.65}$$

The active and reactive power of the synchronous generator are given by the following equations:

$$P_e = \frac{3}{2}\left[U_{sd} i_{sd} + 6U_{sq}\,\underline{i_{sq}}\right] \tag{3.66}$$

and

$$Q_e = \frac{3}{2}\left[U_{sd} i_{sd} - U_{sq} \underline{i_{sq}} \right]. \tag{3.67}$$

Multipole permanent magnet synchronous generators are low speed applications and are typically connected to the grid through a frequency converter system [31]. In such an arrangement the generator has no damper windings on the rotor. Moreover, due to the permanent excitation, a PMSG has no field windings in which transient currents could be induced or damped. It is known from literature that, for the direct coupled PMSG, there is no need for damping since the generator system is stable [31]. Given that the PMSG has neither a damper winding nor a field winding, there is no transient or sub-transient reactance, as is the case for wound rotor SGs. It follows that:

$$X_d = X'_d = X''_d \tag{3.68}$$

and

$$X_q = X'_q = X''_q \tag{3.69}$$

where X_d and X_q denotes the d-axis and q-axis of the synchronous reactance respectively, X'_d and X'_q denotes the d-axis and q-axis of the transient reactance respectively and X''_d and X''_q denotes the d-axis and q-axis of the sub-transient reactance respectively.

The PMSG is conducive for low speed applications with slow dynamic [78] which trivialises the need for damper windings. For the SSG used in this research instead of damping from the grid connection the mechanical drive train is where it uses the buffer from instability from the wind fluctuations.

Chapter 4: Comparison of Simulink and DIgSILENT model performances

4.1 Overview

The different developed models in Simulink are validated by comparing their outputs to that of their corresponding DigSILENT DSL block models. The different models are simulated separately in sections 4.2 to 4.5.

4.2 Wind model

The wind turbine system utilised in this thesis is a fixed speed, stall controlled wind turbine system, in a s tall control the blade pitch angle fixed at 0°. The wind speeds for the equivalent model was approximated using the power spectral density method with parameters given in Appendix D.

4.2.1 Wind model implemented in DigSILENT

The wind speed range for the wind model implemented in DSL model is defined by the user as a vector, which has the average wind speed ranging from 6 to 25 m/s. This vector is given as a text file as specified in the measurement file 'ElmFile' block. Figure 4-1 shows the wind speed of the simulated results obtained with the DSL wind model. The result shows that the simulated wind speed varies with the input average wind speed and follows the ramp variations of the input.

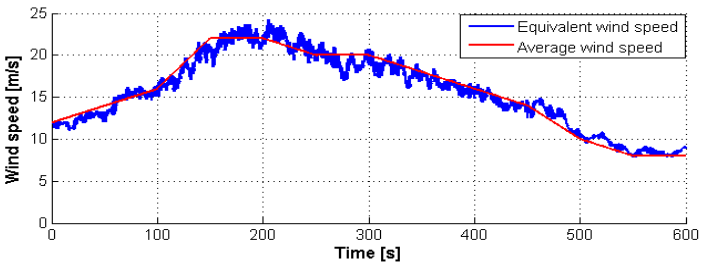

Figure 4-1: Simulated wind speed with the wind speed model implemented in DSL.

The Figure 4-2 shows the simulated wind speed obtained when the wind model implemented in DSL using the power spectral density approach while Figure 4-3 shows the corresponding power spectrum. The results show that the 3p turbulent component occurs at a frequency corresponding to 3 times the rotor speed.

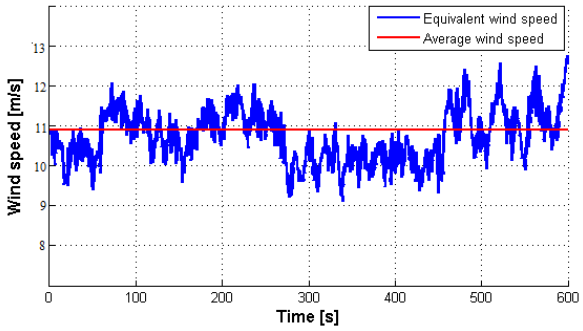

Figure 4-2: Simulated wind speed obtained with the wind model implemented in DSL using the power spectral density method.

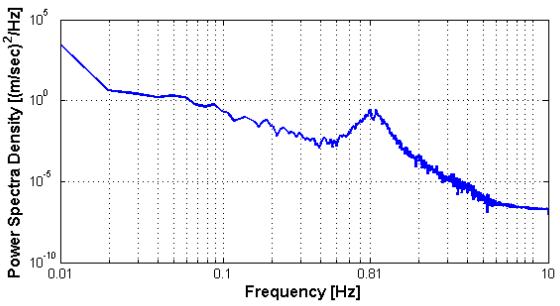

Figure 4-3: Power spectral density of the simulated wind speed obtained with the wind model implemented in DSL using the power spectral density method.

4.2.2 Wind model implemented in Matlab/Simulink

Figure 4-4 shows the wind speed simulated with the wind model implemented in the Matlab/Simulink platform, while Figure 4-5 shows the corresponding power spectral density. The wind speed time series has a duration of 3600s sampled with a sample time step of 0.05s. The wind speed is simulated for an average wind speed of 11m/s, a turbulence intensity of 10% and a length scale of 300m. The power spectrum densities obtained with DSL and Matlab/Simulink show good correlation.

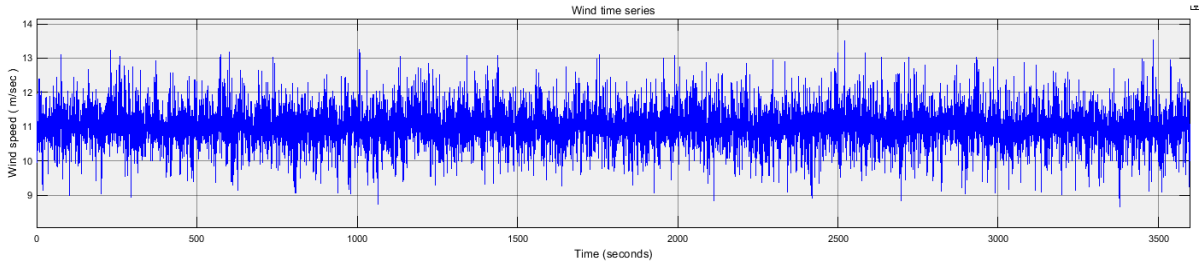

Figure 4-4: Wind speed simulated with the wind model implemented in Simulink.

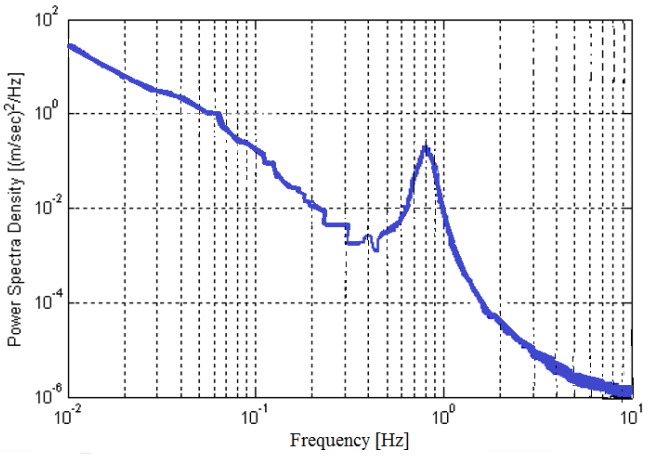

Figure 4-5: Power spectral density of the wind speed simulated with the wind model implemented in Simulink.

4.3 Aerodynamic model

The wind turbine is directly connected to the Slip Synchronous Generator (SSG), hence the aerodynamic model acts as a mechanical interface between the wind model and the electrical model. The aerodynamic output gives the torque of the rotor shaft and represents a measure of the efficiency of the wind turbine, with the efficient coefficient given by the power coefficient. The wind turbine system is implemented as a stall control system, hence for this simulation the blade pitch, hub speed and air density inputs are kept constant at 0°, 1.5 m/s and 1.225 kg/m3 respectively as summarized in Appendix A. The wind speed used in the simulation starts at 0 m/s and increases linearly to 30 m/s.

4.3.1 Aerodynamic model implemented in DigSILENT

Since the efficiency of the turbine is propositional to the power coefficient, the focus of the simulations is on the power coefficient characteristic. The power coefficient is specific for each wind turbine and is usually provided by the manufacturer. A user-defined look-up table, as is shown in Table 4-1, is used in the aerodynamic model implemented in DSL.

Table 4-1: Look-up table used for the power coefficient for the aerodynamic model implemented in DSL.

			Tip speed Ratio								
			0	0	0	0	0	0	0	0	0
	0	0	2	4	6	8	10	12	14	16	18
	-2	0	0.020646	0.220554	0.430586	0.418283	0.337117	0.188621	-0.01654	-0.19222	-0.29522
	0	0	0.031752	0.250196	0.423153	0.442292	0.388375	0.288069	0.139299	-0.06163	-0.26486
	2	0	0.042798	0.263936	0.397648	0.425513	0.396374	0.314009	0.187204	0.00907	-0.21213
Theta	4	0	0.053148	0.265855	0.351786	0.359091	0.316631	0.221977	0.066389	-0.15554	-0.44937
	6	0	0.06228	0.251562	0.290057	0.254107	0.150043	-0.03521	-0.30766	-0.68121	-1.1707
	8	0	0.070101	0.224873	0.21527	0.114197	-0.09358	-0.41428	-0.86877	-1.48032	-2.27932
	10	0	0.076925	0.189478	0.128736	-0.06086	-0.39121	-0.88548	-1.58671	-2.53121	-3.44714
	12	0	0.082284	0.150154	0.02778	-0.25954	-0.73251	-1.43841	-2.42643	-3.74104	-5.09058
	14	0	0.085084	0.107394	-0.08322	-0.47532	-1.11028	-2.05095	-3.3565	-5.08869	-6.88374
	16	0	0.084277	0.061098	-0.20123	-0.70574	-1.51995	-2.74802	-4.47183	-6.7689	-9.19911
	18	0	0.080492	0.01135	-0.32348	-0.95776	-1.99878	-3.54482	-5.69814	-8.55745	-11.6908
	20	0	0.074983	-0.04093	-0.45348	-1.2302	-2.49194	-4.36221	-6.9601	-10.4116	-14.1903
	22	0	0.069542	-0.09463	-0.58775	-1.50557	-3.00176	-5.24741	-8.37712	-12.5487	-16.8565
	24	0	0.062217	-0.14954	-0.72034	-1.78648	-3.54125	-6.14993	-9.80761	-14.6895	-19.4832
	26	0	0.051784	-0.20499	-0.84946	-2.06132	-4.05547	-7.05209	-11.2764	-16.9317	-22.239
	28	0	0.038935	-0.25878	-0.96713	-2.32405	-4.59585	-8.01641	-12.8171	-19.2253	-24.9839
	30	0	0.025236	-0.30642	-1.08194	-2.60528	-5.1552	-8.98296	-14.3454	-21.4975	-27.6806

Figure 4-6 shows the power coefficient simulated with the model implemented in DSL as a function of tip speed ratio for different pitch angles. Since the aerodynamic power is direct proportional to the power coefficient, the maximum aerodynamic power of the turbine is reached when C_P has it's maxima. The maximum C_P value is obtained for a pitch angle of 0^0 with a tip speed ratio corresponding to the rated wind speed.

The power coefficient characteristics show that C_P decreases for higher pitch angles. This reflects the behaviour of the turbine efficiency. The results are in accordance with the Betz law, which states that the turbine cannot convert more than 16/27 (59.26%) of the kinetic wind energy into mechanical energy. Therefore, the maximum limit imposed for C_P is 16/27, although. In practice, this is generally lower.

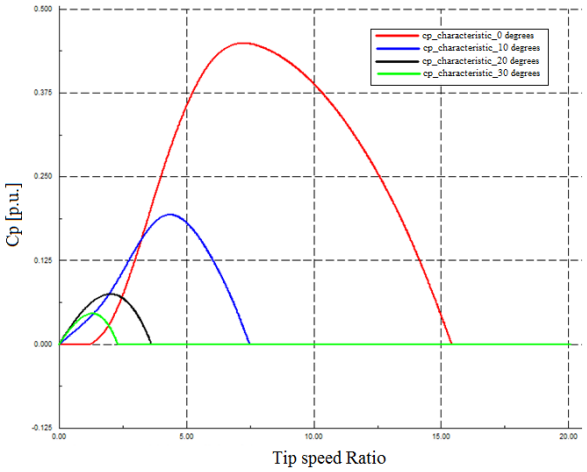

Figure 4-6: Simulated power coefficient as a function of tip speed ratio for different pitch angles.

The aerodynamic torque of the wind turbine is simulated within the operating range of the generator given in the Appendix A. Figure 4-7 shows the aerodynamic torque versus rotor speed characteristic simulated with the model implemented in DSL for different wind speeds and zero pitch angle. The DSL model requires careful initialising and proper initial conditions must be specified for the wind model and aerodynamic model.

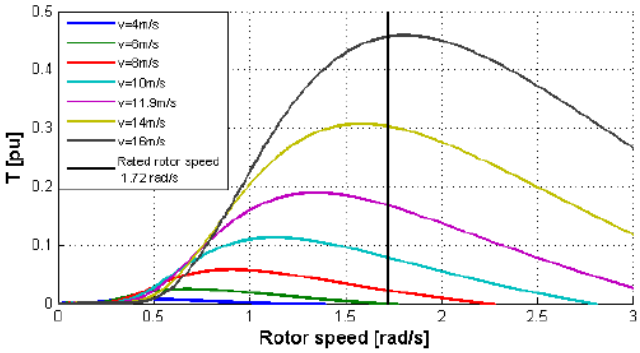

Figure 4-7: Aerodynamic torque versus rotor speed characteristic simulated with the model implemented in DSL for different wind speeds and zero pitch angle.

4.3.2 Aerodynamic model implemented in Matlab/Simulink

As in the case of the model implemented in DSL, a user-defined look-up table is used for the power coefficient in the aerodynamic model implemented in Matlab/Simulink. Figure 4-8 shows the torque

and power versus rotational speed characteristics simulated with the aerodynamic model implemented in Matlab/Simulink. The power curves show that the power maintains a constant value for higher rotational speeds. The invariable nature of the power at high rotational speeds makes the turbine suitable for fixed speed operation, although some advantage can be gained by employing variable speed and Maximum Power Point Tracking (MPPT) principles. The fixed operating point selected or the SSG when synchronised with the grid is 150 rpm.

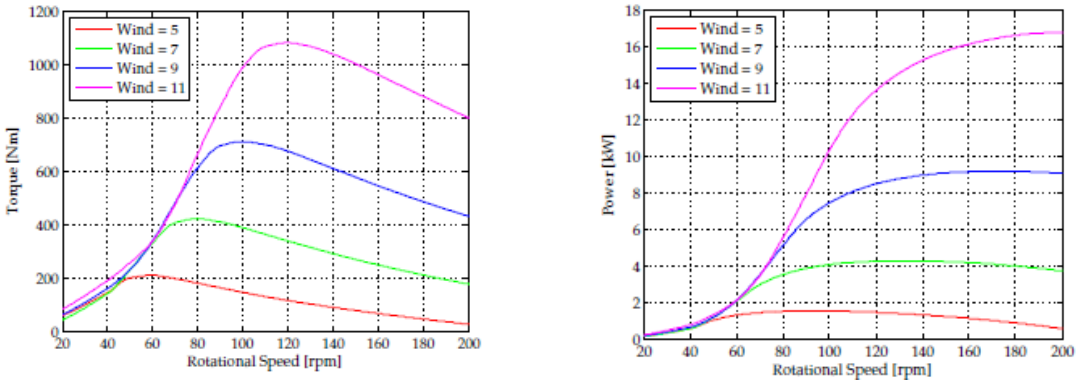

(a) Torque versus rotational speed characteristic simulated with the aerodynamic model implemented in Simulink

(b) Power versus rotational speed characteristic simulated with the aerodynamic model implemented in Simulink

Figure 4-8: Wind turbine characteristics at different wind speeds.

4.4 Mechanical model

The drive train is responsible for delivering the mechanical power to the generator model and acts as an interface between the mechanical system and electrical system. The mechanical model has a significant influence on the interaction of the wind turbine with the grid. The drive train is represented as a two mass model, which combines the moments of inertias of the wind turbine, PMIG and PMSG. It is assumed that the moment of inertia of the rotor shaft is negligible. Since it is a gearless machine, the PMIG has considerable influence on the system, acting as an external damping alternative for the PMSG.

4.4.1 Mechanical model implemented in Matlab/Simulink

4.4.1.1 Dynamic behaviour of the PMSG without damping system

The PMSG when it is coupled to the grid network through a full scale converter has no relative damping. Which is due to the following:

- The lack of damper windings for the PMSG wind turbine system. On a scenario that the PMSG happens to be connected to a frequency converter, which is the usually is the provider of variable stator frequency which is in accordance to the actual rotor speed, there is never any relative motion between stator and rotor field. Without this relative motion between stator and rotor, a damper winding would not have any impact, since there is no voltage that will be induced in the damper winding.
- The small pole pitch of the multipole generator would cause the damper winding to provide insufficient damping
- Since the PMSG uses permanent magnets it has no field windings, which is incapable of providing sufficient damping either. The system has inadequate damping even if the shaft of the generator is damped. When the system experiences fluctuations, for instance from load changes contributed by wind gust, the PMSG will be involved in exciting oscillations, which are amplified in the system and hence requiring an external damping of the wind turbine system.

Variations of load due to wind gusts or grid faults can excite oscillations in the mechanical part of the wind turbine, which might be insufficiently damped. For this reason of instability, it is essential to represent the mechanical system of the PMSG WTS by means of a two mass model, but when a representation by means of a one mass model is implemented it would diminish such oscillations. Due to the nature of the high number of poles in the generator and it`s large diameter, it raises generator inertia compared to most of the convectional 2 or 4 pole generators. The effective shaft stiffness of a generator is assumed to be reduced by increasing number of poles, sin a manner as follows:

$$K_{shaft,eff} = \frac{K_{shaft}\Omega_{gen}}{S\,p} \tag{4.1}$$

where $K_{shaft,eff}$ denotes the effective shaft stiffness, K_{shaft} is the shaft stiffness in (Nm/rad), S denotes the rated MVA-base of the generator and p is the number of pole pairs.

From the equation it is clear that any mechanical torsion of the system results in amplified dynamic changes of the electrical rotor angle for a multipole generator. A torsional twist of the shaft connected to a multipole generator has thus a stronger impact on the electrical systems, hence the two mass model makes it ideal to represent a detailed model of the shaft system.

4.4.1.2 Dynamic behaviour of the PMSG with the external damping system

For a convectional PMSG to be damped from its drive train oscillations an external damping system must be utilised. Some of the ways in which damping can be implemented are to damp the generator as a result of a compliant mounting of the generator [79] which can be provided from the electrical system. For large synchronous generators the damping for speed and rotor angle oscillations is provided by as a result of controlling the generator excitation. For wind applications a similar method is present in [36] where wind turbines with DC excited synchronous generator and a diode rectifier uses the excitation voltage to control and buffer transiently the power flow in the DC-link capacitor.

However, the PMSG has a fixed excitation electrical damping is only achievable by utilising a frequency converter. Since the DC-link capacitor serves as a buffer between generator and the grid the Dc-link voltage can be used for damping. The general working principles of such damping and investigation is covered in detail in [76]

The novel SS-PMG or SSG generator topology, in contrast to the PMSG, has damping provision along with other beneficial characteristics integrated into the generator itself as a result of its construction design. As expressed in [33, 21] utilising a radial flux SS-PMG, which has a slip rotor capable of being implemented as a short-circuited wound rotor or as a cage rotor connected to another half coupled with the grid to form a grid-connected PMSG. This grid side of the machine is driven indirectly by the torque from the wind turbine, which is transmitted through the first PMIG stage. The advantage of this back to back connection is that it introduces damping and allows for some rotational speed difference between the turbine and the PM-rotor.

The SS_PMG comprises of two masses namely the turbine and slip rotor combined with the PM-rotor and the grid-connected stator. Even if the connection between the PM-rotor and stator is very lightly damped, it is possible to avoid oscillations in this connection by making it substantially stiffer than the connection between the slip-rotor and the PM-rotor. If the slip-rotor to PM connection is less stiff, then any disturbances will cause an oscillation to develop between these masses. Any such oscillations will be quickly dealt with since the slip-rotor to PM-rotor connection is sufficiently damped. As a result, the SS-PMG will be able to remain connected to the grid in a stable manner, despite torque disturbances from wind gusts and tower shadow effects. Figure 4-9 shows the Simulink implementation for the system, showing the effect of wind speed fluctuation given as a result of the turbine torque fluctuation from stand still till rated torque in per unit system.

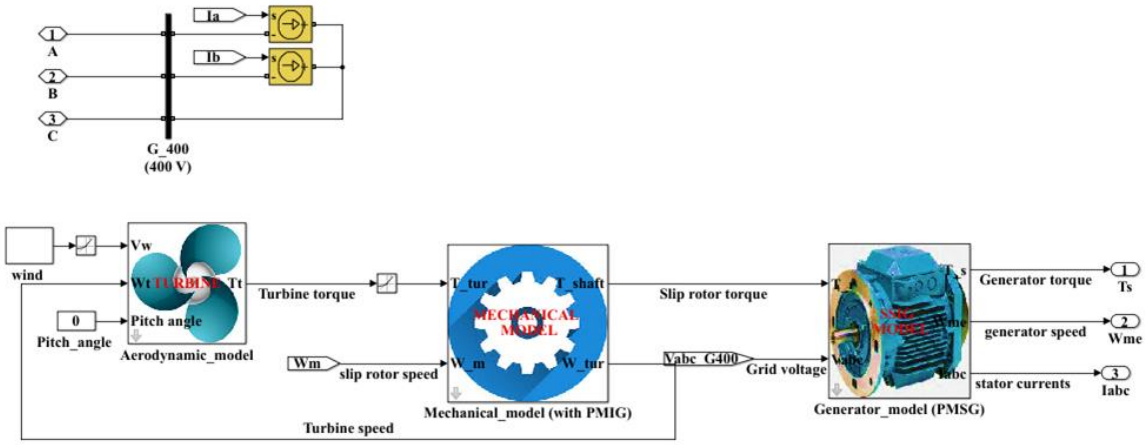

Figure 4-9: Simulink implementation of the complete wind energy system.

Figure 4-10 shows the simulation results of wind speed, generator speed, stator currents and torque production for the cases of when a mechanical drive train is integrated with the PMIG which provides external damping of the system, after a wind speed step change which is represented by a change in turbine torque from standstill to rated torque in per unit after 1 sec. The simulation results illustrate the impact of the damping system, the oscillations of the drive train are supressed effectively when the PMIG is implemented.

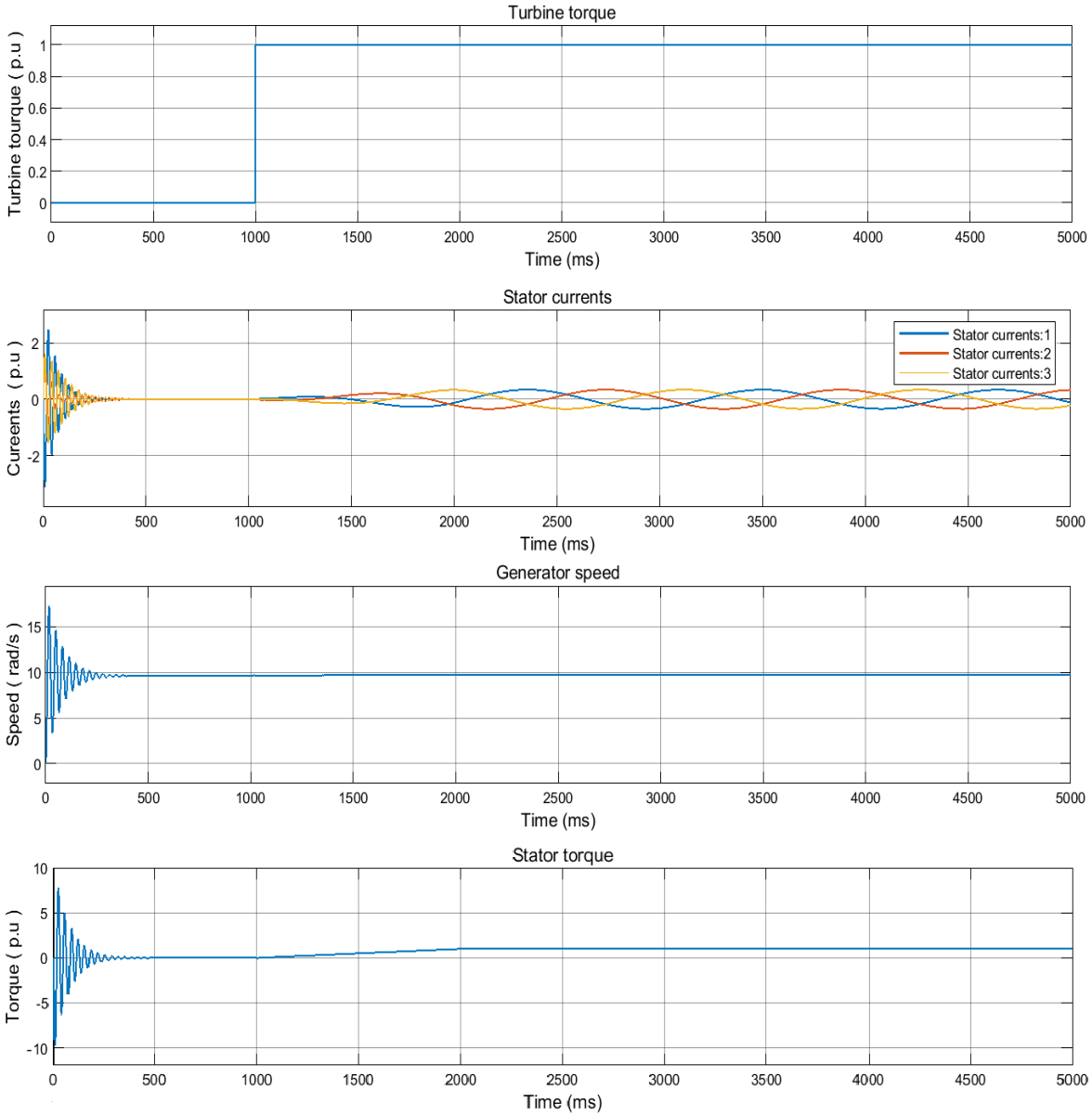

Figure 4-10: Simulation results of wind speed, generator speed, stator currents and torque production for the cases of when a mechanical drive train is integrated with the PMIG.

The simulations in Figure 4-10 illustrate the impact of the damping system. When the wind speed changes no oscillations of any nature are experienced showing a suppressed effectively when the PMIG is treated as part of the drive train.

4.4.2 Mechanical model implemented in DigSILENT

The shows how the drive train shaft speed and the turbine mechanical power varies over time for fixed wind speed respectively. As the turbine shaft angular velocity increases it corresponds to a fluctuating output of mechanical power which implies need for an external damping system which is provided by the PMIG, The PMIG attached to the SSG is represented by a generator constant with a characteristic that shows a linear relationship between slip and torque.

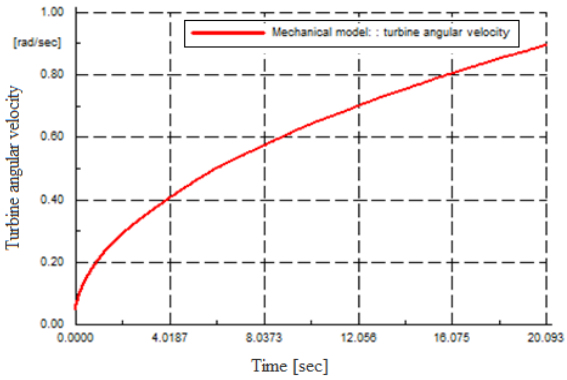

Figure 4-11: Simulation results of the turbine shaft speed in DigSILENT for constant mean wind speed.

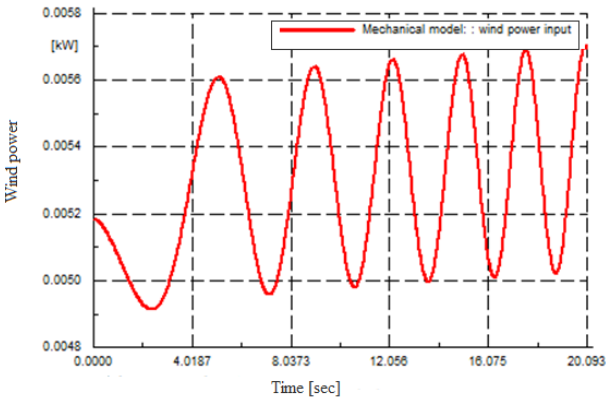

Figure 4-12: Simulation results the mechanical power in DigSILENT.

4.5 Generator model

This section gives an overview of the generator characteristics when modelled in both the Matlab/Simulink and DigSILENT platforms. This will be a review of the generator dynamic response under steady state conditions. When operating under steady state conditions, for the stall-controlled generator it consists of the parameters given in the Figure 4-13 as follows:

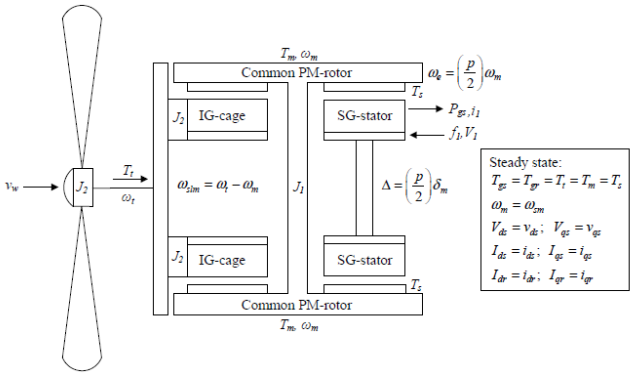

Figure 4-13: Overview of the mechanical and electrical interaction of the turbine and the generator [80]

4.5.1 Steady State dynamic response of SSG in DigSILENT

The SSG steady state response of the speed and power of the generator from standstill is shown in Figure 4-14 for operating speed range given in the Appendix A, the generator power fluctuates slightly for constant speed operations as shown in the simulations. The generator is able to achieve constant speed operations for fluctuation in wind speed.

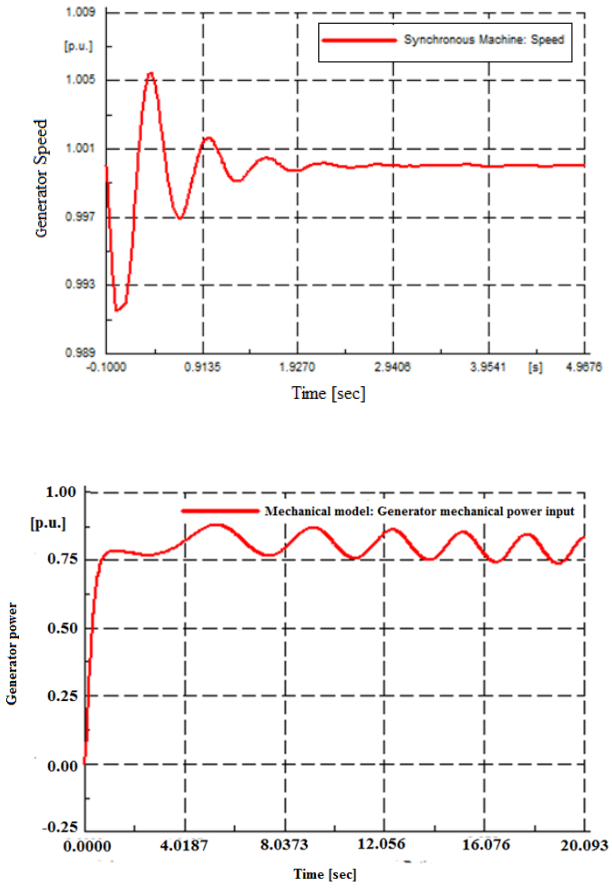

Figure 4-14: Generator speed and power response for steady state conditions in DigSILENT

4.5.2 Steady state dynamic response of SSG in Matlab/Simulink

The SSG steady state response of the generator power with input mechanical torque is shown in Figure 4-5. For wind speeds within the operating range of the wind turbine system the generator produces a steady state power output which does not fluctuate with increase in wind turbine speed.

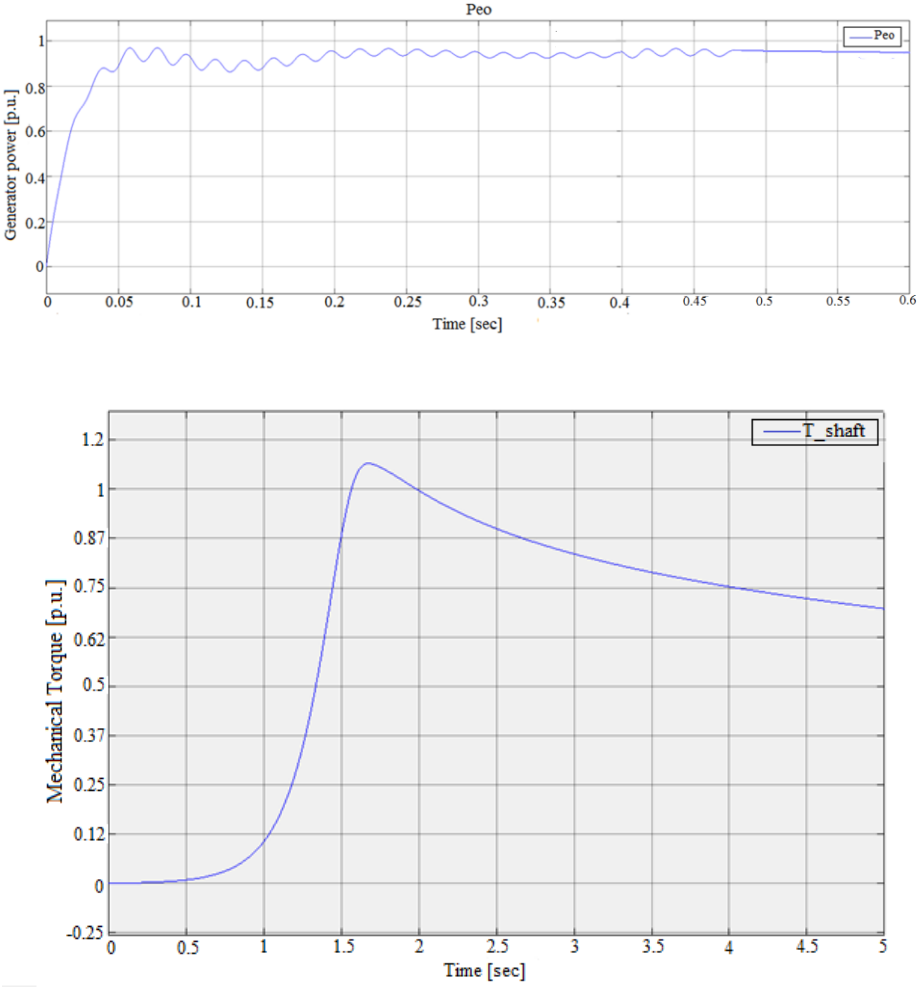

Figure 4-15: Generator power response for steady state conditions in Simulink from mechanical torque input.

4.6 Comparison of the wind Matlab/Simulink and DigSILENT simulation results

As shown from sections 4.2 to 4.5 the simulation for the Simulink and DigSILENT platforms are similar for the wind model and the aerodynamic model. Their responses differ for the mechanical and generator response due to difference in the models used for the simulation procedure. The Simulink model uses the unaltered dynamic equations since it is possible to model the generator equations from its equations. In the DigSILENT platform the difference arises from the limitation which arises from modelling the SSG as the platform is a proprietary software only using generic in-build models.

Chapter 5: Modelling Results and Performance Evaluation

5.1 Introduction

As the multipole PMSG wind turbine system is directly connected to the grid it can be presumed that this wind turbine concept has a relatively weak grid support capability compared to any other wind turbine concepts. The generator and turbine are more subjected to the grid fault impact than turbines with converter system which decouples generator and turbine from the grid. In order to approve the assumptions above the dynamic behaviour of PMSG wind turbines under grid faults is analysed in this chapter.

This chapter is a detailed investigation of the grid fault impact on both the electrical and mechanical system and this chapter is going to cover the following:

- A detailed overlook of the case study objectives
- A review of the methodology taken to evaluate the various case studies analysed.
- The steady state analysis of the SSG in Matlab/Simulink platform
- The steady state analysis of the DSL user defined model in DigSILENT platform
- The dynamic study of the SSG in Matlab/Simulink model
- The dynamic response analysis of the user defined SSG in DigSILENT platform
- Grid integration of the SSG in weak distribution network.

5.2 Case study objectives Steady State dynamic response of SSG

The section is going to cover the following case study objectives:

- Outline a benchmark description of the SSG wind system representing the grid connection of imbedded systems to remote weak grid networks.
- Analyse and compare the steady state and dynamic responses of the SSG in Matlab/Simulink and DIgSILENT platforms.

5.3 Case study methodology

5.3.1 Introduction

The case study methodology is covered in a summary table which contains the different scenarios investigated for the different models shown in the proceeding sections.

5.3.2 Case study scenarios

All the possible steady state and dynamic system response are summarised on the table below the thesis is focusing on two study cases simulation for the single and three phase grid faults:

	Steady state	Dynamic Platform		Response	
Case		Single-phase fault	3-phase fault	Matlab	DIgSILENT
A1	✓			✓	
A2		✓		✓	
A3			✓	✓	
B1	✓				✓
B2		✓			✓
B3			✓		✓

5.4 Group A case study

5.4.1 Introduction

To evaluate the dynamic behaviour of the SSG turbine system when exposed to specified fault conditions at the Point of Common Coupling (PCC), which is typically medium or a high voltage level, the equivalent single line diagram used to represent the electrical network is shown in Figure 5-1 with the parameters provided in Appendix A. The single line diagram is a representation of a weak distribution network, which is highly resistive and mostly characterised by long radial lines.

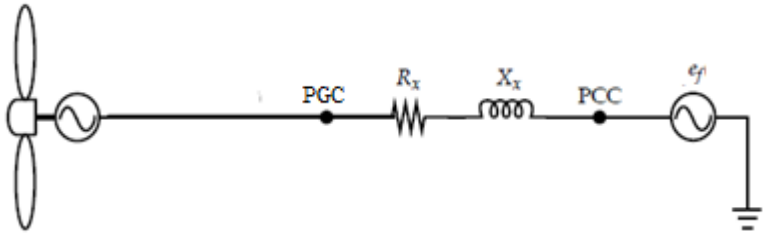

Figure 5-1: Per phase single line diagram representing the WEC and electrical network during faults.

The assumptions made for the dynamic analysis of the SSG are that the mechanical time constant of the system is assumed to be much longer than the electrical time constant, for the PMSG unit the synchronous reactance is assumed to the dominant part of the impedance and the per phase resistance

is neglected. The IG unit part is assumed to operate in the linear torque slip region at very small values. A more resistive representation is proposed which is a close depiction of the weak grids in which the SS-PMG is to be installed usually for remote distribution networks.

5.4.2 Model A3

5.4.2.1 Introduction

For this case scenario a three phase balanced fault is experienced at, the medium voltage grid connection terminal of the wind turbine generator, which is at the point of common coupling (PCC) and the resultant fault impedance is represented with the short circuit $R_f + jX_f$.

5.4.2.2 Three phase fault dynamic response of SSG

The simulations for this study case assume the generator is in its stead state running at rated conditions and has already been synchronised, with the synchronization techniques covered in [81, 33]. The fault is applied for duration of 100ms applied at time of 0.1 seconds which will mark the beginning of the fault the resulting signals are plotted for time duration of about 0.4s.

For the duration of the whole simulation, it is assumed that the turbine is operating at rated conditions. The wind is kept constant at 11 m/s at its average wind speed

The three phase fault is conducted without any voltage control capabilities. As shown in Figure 5-2 the three phase fault causes a huge voltage sag on the grid voltage, which results a corresponding increase in the grid current for to about three times it`s nominal value in all phases. simulation as wind speed changes are little compared to the time frame of the fault.

As illustrated in Figure 5-2 the three phase fault causes a voltage drop down to 0 % of the rated voltage, resulting in a drop of the active power, too. The d-axis current PMSG, controlling the active power, tries to compensate for the droop in active power.

Immediately voltage drops, there is a relative increase in reactive power but since the permanent magnet produces a fixed excitation the reactive power cannot fully recover to furnish the grid from the voltage drop. There is a very substantial decrease in the real power output of the grid network.

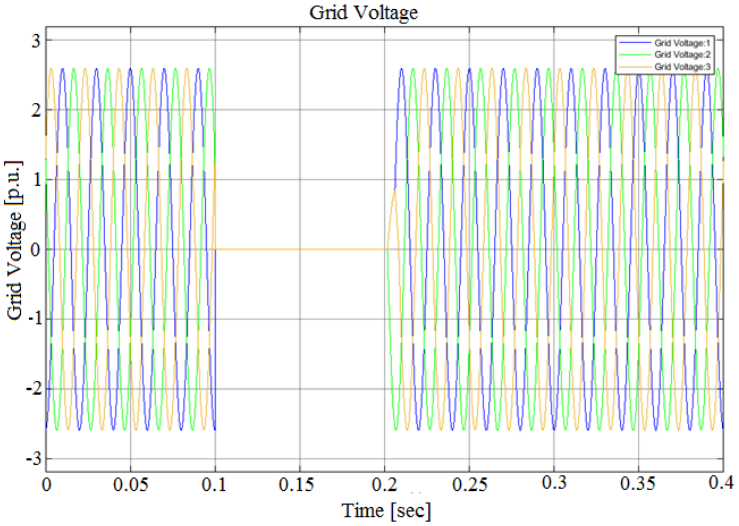

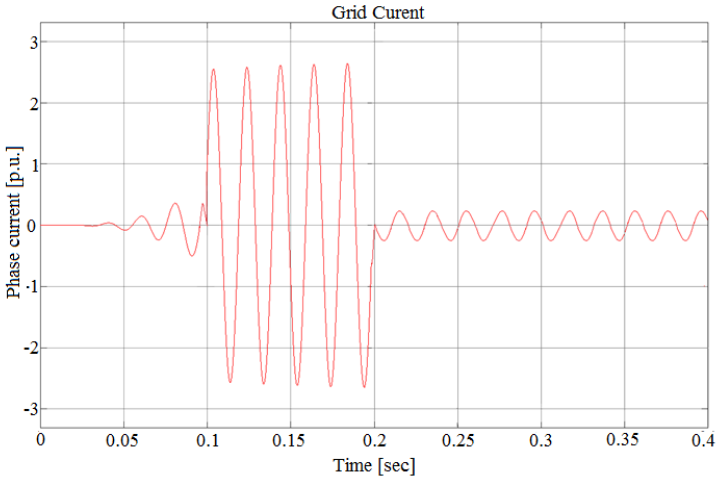

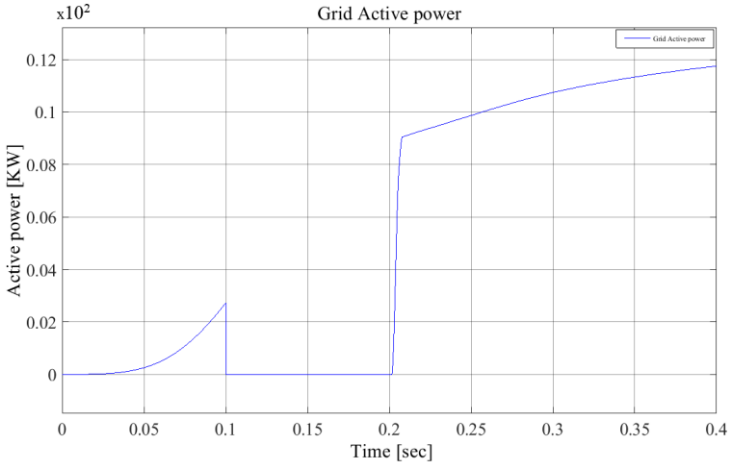

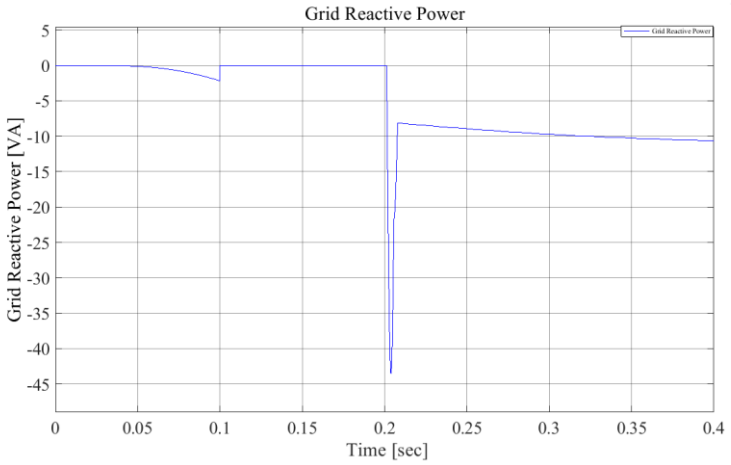

Figure 5-2 : Simulation of results at the PCC: grid voltage, phase current, active and reactive power production duration of 100ms for 3-phase fault in Simulink

5.4.3 Model A2

5.4.3.1 Introduction

For the single phase fault for the Wind Turbine (WT) system for the SSG, Figure 5-3 gives the voltage, active and reactive power production of the wind turbine system at the point of common coupling (PCC). The unbalanced fault occurs at time 0.1 s for duration of 100ms, during this period, the turbine is assumed to be operating at rated conditions with wind speed kept constant at 11 m/s since wind speed hardly changes within the duration of the fault.

5.4.4 Single phase dynamic response of SSG

The simulation results for this test are shown in Figure 5-3. The voltage drops to approximately 60% of its rated value for the respective phase associated with the fault whilst both other phases remain unaffected. During the fault the reactive power of the grid is seen to be fluctuating but the active power is mildly affected from the voltage drop.

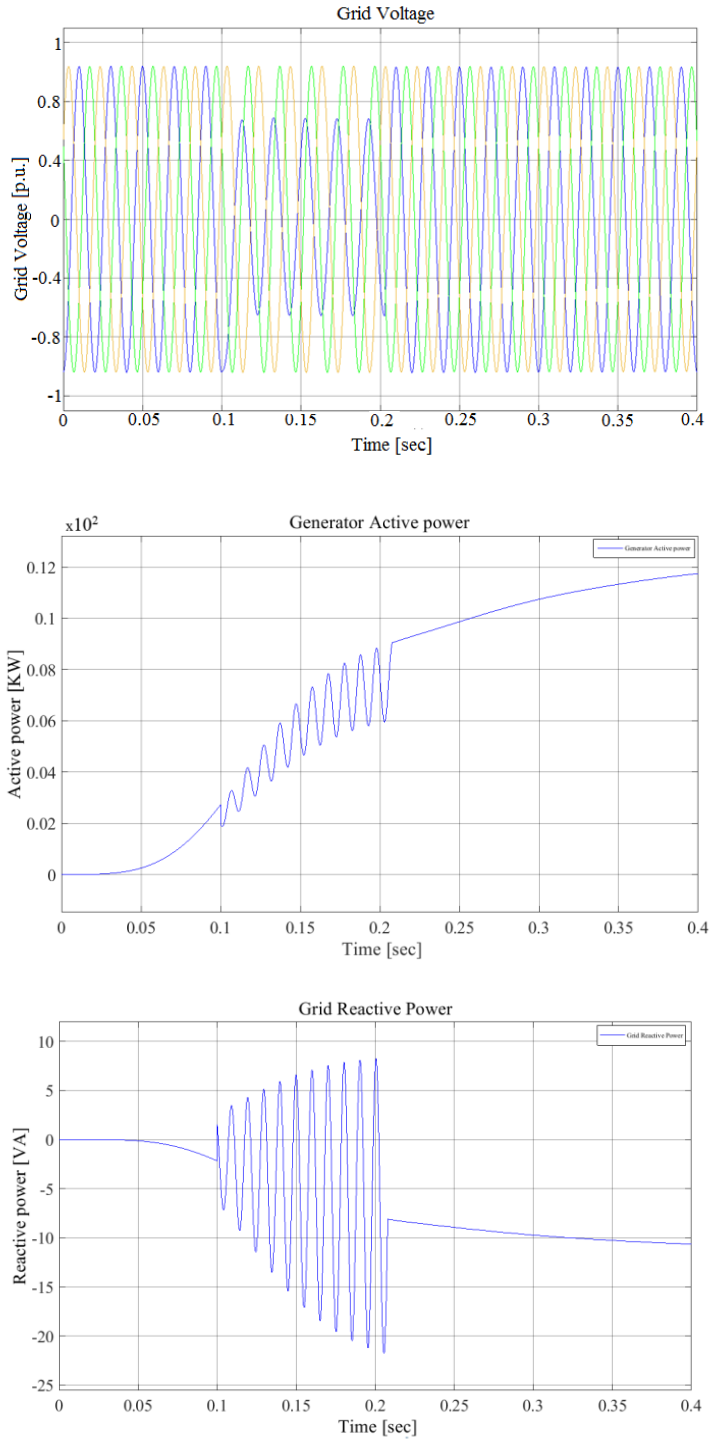

Figure 5-3:Simulation of results at the PCC: grid voltage, active and reactive power production duration of 100ms for single phase fault in Simulink

5.5 Group B case study

5.5.1 Benchmark model for SSG wind system in DigSILENT

To evaluate the dynamic behaviour of the embedded PMSG wind turbine system under grid faults a couple of selected simulation case studies are conducted. For the dynamic analysis for the wind turbine system the weak network is represented as shown in Figure 5-4.

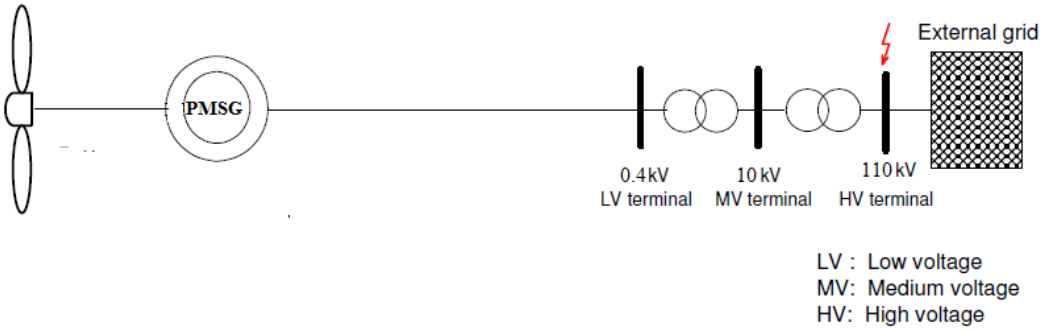

Figure 5-4 PMSG wind turbine system subjected to grid faults at HV terminal

5.5.2 Multipole PMSG wind turbines grid support capability

As the multipole PMSG wind turbine is directly tied to the grid, without the use of any form of electronic converter which decouples the generator from the grid it can be assumed that this wind turbine has poor grid support capability when comparing to any other wind turbine concept. In order to approve the presupposition, the dynamic behaviour of PMSG wind turbine under grid faults is analysed in the following, the grid fault impact on the mechanical and electrical systems is investigated during simulations. Based on the investigations a control strategy to enhance the grid fault ride-through and grid support capability of the PMSG wind turbine.

The grid is modelled by means of a Thevenin equivalent circuit shown in Figure 5-5 and is characterised by a short circuit power S_k which is approximately 10 times the rated wind turbine power P_{rated} and an X/R ratio of 0.1. The short circuit happens at the high voltage grid connection the point of common coupling and is represented with the short circuit impedance $R_f + jX_f$.

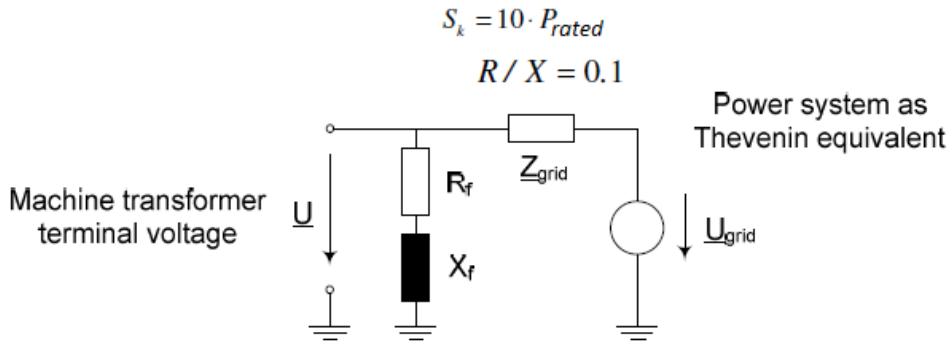

Figure 5-5 Single phase Thevenin equivalent circuit of the grid during a short circuit.

5.5.3 Model B3

5.5.3.1 Introduction

The three phase short-circuit happens at the high voltage grid connection terminal of the turbine and is represented with the short circuit $R_f + jX_f$. the weak networks are highly resistive and usually in most instances are characterised by long radial lines, to investigate the effect of faults along at different locations from the PCC it's simulated by simulating the system by varying the grid impedance Z_{grid} .

5.5.3.2 Grid fault impact on the grid network

In Figure 5-6 the voltage as well as active and reactive power production of the wind turbine system at medium voltage terminal. The wind turbine system experiences a balanced symmetrical three-phase fault occurring at the point of common coupling (PCC) at its medium voltage terminal. The fault occurs at time 0s and lasts for a duration of 100ms, the resulting signals are plotted for a time duration of about 5s after the fault incident.

When the fault occurs, it is assumed that the turbine is operating at rated conditions. The prevailing wind speed at this condition is kept constant at 11m/s for the whole duration of the simulation as wind speed changes are little compared to the time frame of the fault.

In this case no form of additional control for fault ride through and voltage support was implemented. The machine is only depending on the stall control of its turbine which is only effective for strong

wind conditions. As illustrated in Figure 5-6 the three phase fault causes a voltage drop down to 20 % of the rated voltage, which results a drop of the active power, too. The d-axis current PMSG, controlling the active power, tries to compensate for the droop in active power. However, due to the reduced voltage level, the power cannot be controlled to its reference value during the fault.

Meanwhile, the q-axes current from the PMSG continues to control the reactive power to its reference, which is close to zero covering only the reactive power demand of the transformers. The reactive power from the synchronous machine will remain constant since the magnetisation current of permanent magnets cannot be controlled even at the fault inception.

When the voltage drop occurs, it causes a drop of the active power of the generator delivered to the grid, while on the other hand the wind turbine should continue its power generation sustaining the required reactive power needed by the voltage drop.

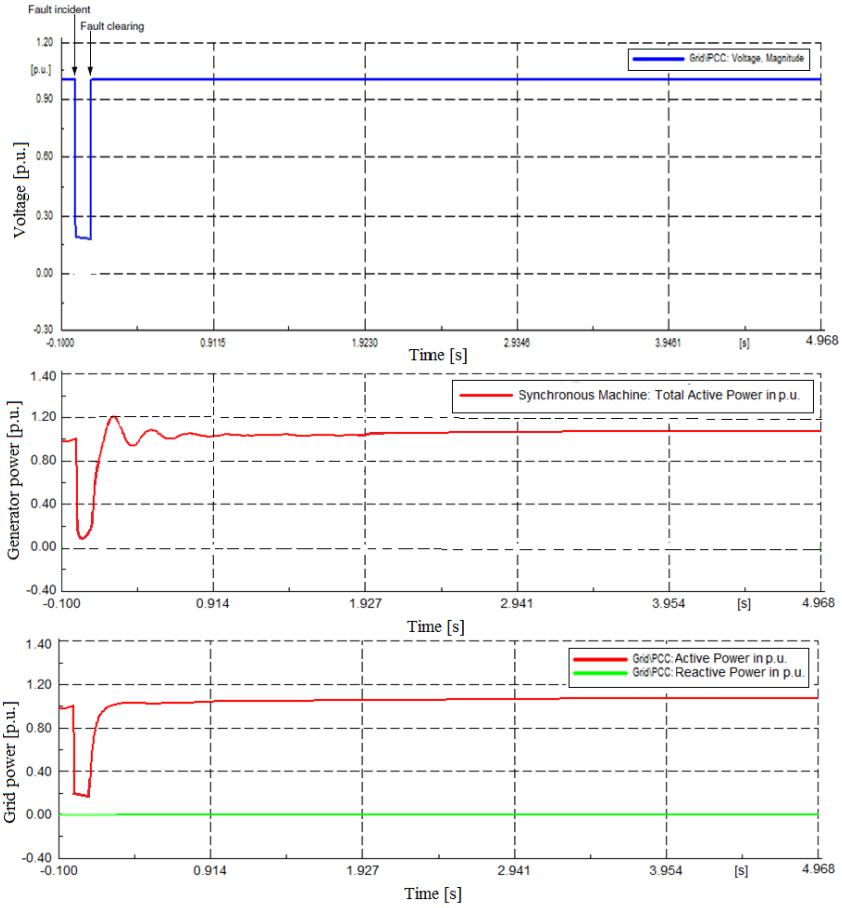

Figure 5-6: Simulation of results at the PCC: grid voltage, active and reactive power production duration of 100ms for 3-phase fault.

.

5.5.3.3 Grid fault impact on the mechanical system

As stated, in the previous subsection 5.5.2, the power instability caused by the grid fault is transferred through the generator to the wind turbine system. Thus, the mechanical system of the wind turbine system is subjected to fault as well. The same three phase grid fault we considering how the mechanical aspects is influenced.

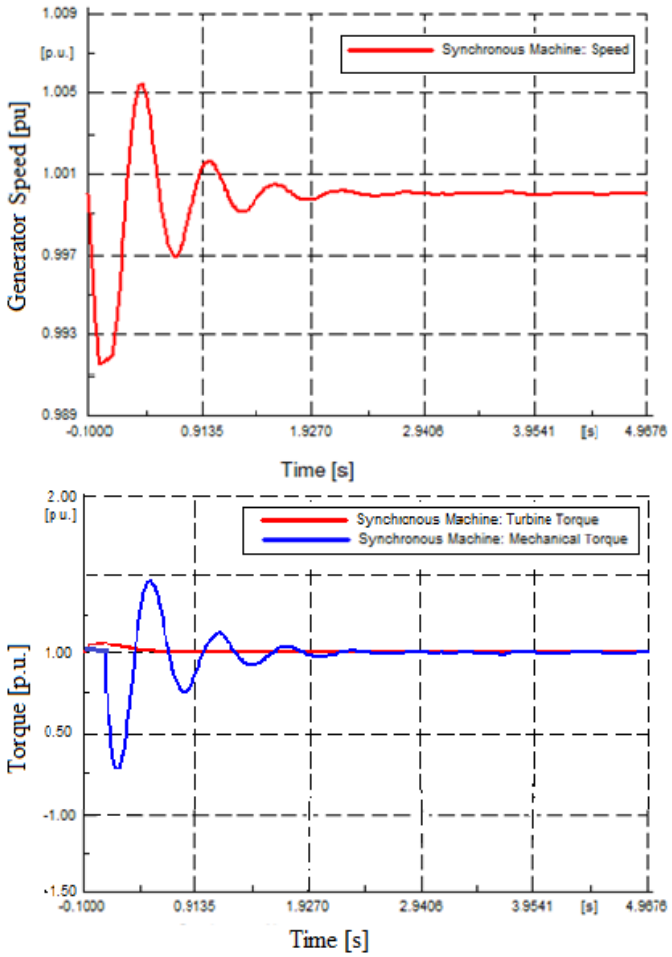

Figure 5-7 Simulation of results of PMSG: turbine mechanical torque production and generator speed for duration of fault.

The mechanical system has larger time constants than the electrical system the fault has longer noticeable impact in the mechanical system. Representative mechanical signals such as, turbine mechanical power and the speed are plotted in Figure 5-7.

The power imbalances between the turbine and the generator power results in the turbine to start to accelerate and the generator oscillations occur. The oscillations of the generator are visible in the shown signal. The oscillations are damped by means of the damping SPMG which acts as an interface between the turbine and PMSG.

5.5.4 Model B2

5.5.4.1 Introduction

The single phase short-circuit occurs in phase A at the point of common coupling grid of the turbine and is represented with the short circuit $R_f + jX_f$. It is one of the types of the unbalanced transients, in this scenario the phase experiencing the earth fault will have a voltage sag from the fault current passing through it.

There will be no flow of current in the other two phases and the unbalanced fault current is a sum of the symmetrical components of the system. The single-phase equivalent circuit will be given by the positive, negative and zero sequence impedance networks connected in series.

5.5.4.2 Grid fault impact on the grid network

In Figure 5-6 gives the voltage, active and reactive power production of the wind turbine system at medium voltage terminal which is the point of common coupling. The unbalanced fault occurs at time 0s for a duration of 100ms, during this period, the turbine is assumed to be operating at rated conditions with wind speed kept constant at 11m/s since wind speed hardly changes within the duration of the fault.

As in all other cases no form of additional control for fault ride through and voltage support was implemented. As illustrated in Figure 5-8 the single phase fault causes a voltage drop down to 20% of the rated voltage, resulting in a drop of the active power, too. From the reactive power response, the magnetic current tries to compensate for the droop in active power. However, due to the severe reduction in the voltage level, the power cannot be controlled to its reference value during the fault.

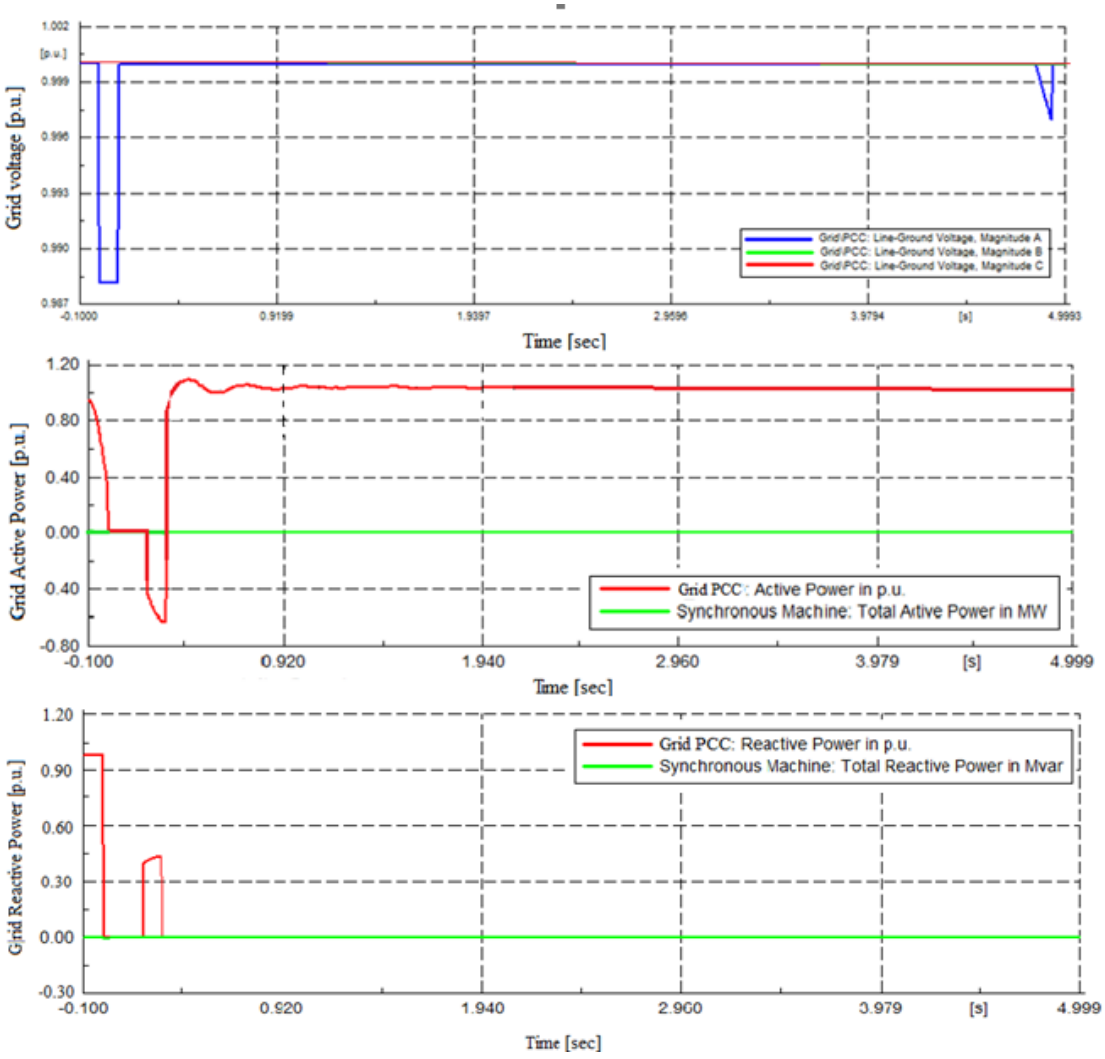

Figure 5-8: Simulation of results at the PCC: grid voltage, active and reactive power production duration of 100ms for single phase fault

5.5.5 Grid ride through capability

The SSG will act as two sided virtual machines with a PMIG connected to the turbine and a PMSG connected to the grid [81, 33]. If a drop-in supply voltage occur the synchronous machine should immediately attempt to support the terminal voltage by providing capacitive reactive power to the grid. When there is a sudden dip in the voltage the reactive currents induced by the PM machine could be very large, which is usually pose a potential grid instability problem.

The SG as proposed in [80] makes use of a non-overlapped single layer winding which has a large inductance. The high synchronous impedance due to the high inductance could act as a buffer during low voltage conditions and it limits the current flow from the machine during this condition.

From the simulation of the grid faults in section above it shows the limitation in the direct driven generator when directly coupled to the grid network. The system reactive power is limited to stabilise the grid voltage and grid compensation must be supplied from an external source for the supply of reactive power.

Chapter 6: Conclusion and recommendations

A new novel SSG wind turbine generator is studied on how it interacts with weak distribution grid network during normal and abnormal operating conditions. Indore to be able to analyse the generator dynamic behaviour it`s model needs to be developed from its dynamic equations. The SSG is model is developed using the Matlab/Simulink and DigSILENT. The choice of using these two platforms are explored from the literature review. The embedded wind turbine network is then applied to the single and three phase faults, with the former being the most common fault occurring in power networks and the later though it is rare in occurrence, implementing the three phase fault will give an indication of maximum fault levels which switching devices, switch gear and the whole power system network must tolerate.

6.1 Conclusion

The first part of the thesis involves modelling the SSG in Matlab/Simulink and DigSILENT. After the models where developed they are used for transient stability analysis mainly focusing on the single and three phase faults. From the response of the network to the abnormal conditions it will be an indicating measure on the stability of the system, and a measure for performing Low Voltage Ride Through capability, in order to maintain uninterrupted supply during fault conditions.

This project looks on the impact of the dynamic model of a fixed speed, stall controlled SSG in Matlab/Simulink and DigSILENT when directly tied to weak grids. From the benchmark network defining typical weak grids, the thesis aimed to cover the following:

- The development and implementation of a dynamic model of the SSG in Matlab/Simulink.
- Analysing the effects of changing wind conditions on the behaviour of the SSG.
- The development and implementation of a dynamic model of the SSG in DigSILENT
- Comparing simulated dynamic model responses obtained with Matlab/Simulink to those obtained with DigSILENT.
- Conducting a case study of the SSG connected in a weak network with the view to investigate the effects on grid stability.

6.1.1 SSG wind turbine modelling

The Matlab/Simulink platform is conducive for modelling the appropriate SSG wind turbine system from its dynamic equations. For the DigSILENT platform, it is limited in its design platform to model

the SSG from its dynamic equations. The SSG was then converted to be able to be represented as a synchronous generator with fixed excitation which is a representation of PMSG. The other part of the SSG which is the PMIG was incorporated into the mechanical model to form a two mass model with the turbine mass inertia. The PMIG was implemented to convey a linear relationship between slip and torque for slip values with a generator constant, K_{gen}.

The power system network used was defined from benchmark model to represent an embedded wind turbine generator connected to a weak network feed from a radial feeder. The models consist of the mechanical and electrical components, with the wind model, aerodynamic and mechanical drive train forming part of the mechanical components and the SSG and grid network forming part of the electrical components.

The network was represented as a Thevenin equivalent circuit of the whole network with the transformer and line parameters treated as an aggregated single impedance. It is also possible to model a practical actual network from the Matlab/Simulink platform but emphasis on this thesis was on how the generator will be able to interact with typical weak network.

6.1.2 SSG steady-state and stability analysis

Finally, the Matlab/Simulink and DigSILENT models where simulated for their steady state and dynamic behaviour. During faults the SSG wind turbine system is analysed to see if it`s stable and if it`s possible for the generator to be able to achieve Low Voltage Ride Through (LVRT) when exposed to faults.

The fault chosen in this thesis are the single fault which makes the majority of the faults in power system and the 3-phase fault though it is rare it is a measure of the maximum fault level which the whole system can be able to tolerate.

6.2 Recommended further study

The thesis extensively studies the modelling of a new concept SSG in DigSILENT for transient studies, this software package is important for such studies. The proprietary nature of the platforms makes it difficult to design the SSG. Recommendation is made to change the assumption of the slip rotor permanent induction generator (PMIG). It was assumed that generator constant defining the PMIG has a characteristic that shows a linear relationship between slip and torque, since this forms part of the mechanical drive train assumed to efficiently damp the wind turbine transients from wind fluctuations more work should be put to find the appropriate characteristic of the generator.

The SSG from both Matlab/Simulink and DigSILENT shows that the direct grid integration of the generator to the distribution grid, though it is possible is not a safe guard for the generator when transient disturbances occur. To achieve LVRT recommendation is made to use compensating techniques to increase the reactive compensation capabilities of the system.

Bibliography

[1] "Constitution of the rupublic of South Africa," Government, Pretoria, 1996.

[2] "State of renewable energy in south africa," Department of energy, Pretoria, 2015.

[3] "White Paper on energy Policy of the Republic of South Africa," Department of Minerals and Energy, Pretoria, 1998.

[4] "White paper on Rewable Energy," Department of Minerals and Energy, Pretoria, 2003.

[5] " National Climate Change Response Policy White Paper," Department of Environmental Affairs , Pretoria, 2011.

[6] "Kyoto Protocol to tthe United Nations Framework Convention on Climate Change," United Nations, Kyoto, 1998.

[7] "The Wind Energy Industry Localisation Roadmap in support of Large-scale Roll-Out in South Africa," Department of Trade and Industry, Pretoria, 2015.

[8] "South Africa's Long Term mitigation scenarios and climate change policy responce," Department of Environmental Affairs and Tourism, Bonn, 2009.

[9] "Independent Power Producers Procurement Programme (IPPPP) An Overview," Department of Energy, Pretoria, 2015.

[10] "REIPPPP focus on wind Quarter 1 | 2015/16," Department of Energy, Pretoria, 2015 .

[11] D. de Jongh , D. Ghoorah and A. Makina , "South African renewable energy investment barriers:An investor perspective," *Journal of Energy in Southern Africa,* vol. Vol 25, no. No 2, pp. 15-27, May 2014.

[12] "Renewable Energy Technologies:Cost Analysis Series," International Renewable Energy Agency, 2012.

[13] G. Stefan and J.-D. Pitteloud, "2015 Small Wind World Report Summary," World Wind Energy Association, Bonn Germany, 2015.

[14] "US Energy Information Administration:South Africa," 29 April 2015. [Online]. Available: http://www.eia.gov/beta/international/analysis_includes/countries_long/South_Africa/south_africa. [Accessed 3 February 2016].

[15] E. H. Camm, M. R. Behnke, O. Bolado, M. Bollen, M. Bradt, C. Brooks, W. Dilling, M. Edds, W. J. Hejdak, D. Houseman, S. Klein, F. Li, J. Li, P. Maibach, T. Nicolai, J. Patiño, S. V. Pasupulati, N. Samaan, S. Saylors, T. Siebert, T. Smith, M. Starke and R. Walling, "Characteristics of Wind Turbine Generators for Wind Power Plants," *IET,* vol. 6, no. 1, pp. 1-8, 2009.

[16] J.-D. Pitteloud and S. Gsenger, "Small wind report 2016 Summary," World Wind Energy Association (WWEA), Bonn,Germany, 2017.

[17] . L. Fried, , . L. Qiao, S. Sawyer and S. Shukla, "Global wind reoport:Annual Market Update 2014," Global Wind Energy Council, Brussels, Belgium, 2015.

[18] H. Polinder, F. . F. A. van der Pijl, . G.-J. de Vilder and P. . J. Tavner, "Comparison of Direct-Drive and Geared Generator Concepts for Wind Turbines," *IEEE transactions on energy conversion,* vol. 21, no. 3, pp. 725-733, 2006.

[19] J. H. J. Potgieter and M. J. Kamper, "Design of new concept permanent magnet induction wind generator," in *IEEE/ECCE,* Atlanta, Sept 2010.

[20] J. . H. J. Potgieter and M. J. Kamper, "Design of new concept gearless direct-grid connected slip-synchronous permanent magnet wind generator," *IEEE transactions on industry applications,* vol. 48, no. 3, p. 913–922, 2012.

[21] J. H. J. Potgieter and M. J. Kamper, "Modelling and Stability Analysis of a Direct-Drive-Direct-Grid Slip-Synchronous Permanent Magnet Wind Generator," *IEEE,* Aug 2013.

[22] N. G. Mortensen, E. Mabille and A. Otto, "Interim (5 km) High-Resolution Wind Resource Map for South Africa," WASA, October 2017.

[23] S. Anderson, "Comparing Offshore and Onshore Wind," The Economics of Oil and Energy, 2013.

[24] T. Al-Shemmeri, "Wind Turbines," Ventus Publishing Aps, 2012.

[25] M. Ragheb, "Control of wind turbines," 2009.

[26] National Insruments, "Wind Turbine Control Methods," Dec 22, 2008. [Online]. Available:

http://www.ni.com/white-paper/8189/en/. [Accessed 10 December 2018].

[27] A. Hansen and . L. Hansen, "Wind turbine concepts market penetration over ten years (1995 to 2004)," *Wind Energy*, vol. 10, no. 1, pp. 81-97, 2007.

[28] T. Ackermann, Wind Power in Power Systems, Chichester: John Wiley and Sons Ltd, January, 2005.

[29] D. P. Kadam and B. E. Kushare , "Overview of different wind generator systems and their comparisons," *IJESAT*, vol. 2, no. 4, p. 1076 – 1081, 2012.

[30] F. Blaabjerg and Z. Chen, Power electronics for modern wind turbines, 1st ed., USA: Morgan & Claypool,, 2006.

[31] G. Michalke, T. Hartkopf and A. D. Hansen, "Variable Speed Wind Turbines - Modelling, Control, and Impact on Power Systems," Wind Energy Department Risø National Laboratory, Darmstadt, 2008.

[32] J. H. Potgieter, "Evaluation and Application of a Slip-Synchronous Permanent Magnet Wind Generator," Center for Renewable and Susstainable Energy Studies.

[33] U. Hoffmann and M. J. Kamper, "Direct Grid Connection and Low Voltage Ride-Through for Slip Synchronous Magnet Wind Turbine Generator," University of Stellenbosch , Stellenbosch, March 2012.

[34] A. T. Spies and M. J. Kamper, "An investigation into the grid compliance of the slip synchronous permanent wind generator," Stellenbosch, March 2013.

[35] A. D. Hansen, P. Sorensen, F. Blaabjerg and J. Becho, "Dynamic modelling of wind farm grid interaction," *Wind ngineering*, vol. 26, no. 4, p. 191–208, 2002.

[36] C. Jauch, P. Sørensen, I. Norheim and C. Rasmussen, "Simulation of the impact of wind power on the transient fault behavior of the Nordic power system," 2007.

[37] L. A. Fajardo, F. Lov, J. A. Medina, A. D. Hansen and F. Blaabjerg, "Induction generator model in phase coordinates for fault ride-through capability studies of wind turbines," Aalborg, Denmark, 2007.

[38] "Grid connection code for renewable power plants (RPPs) connected to the electricity transmission

system (TS) or the distribution system (DS) in South Africa," National Energy Regulato rof South Africa (NERSA), Pretoria, 2012.

[39] T. Mchunu and T. Khoza, "Grid connection code for renewable power plants South Africa," AMEU Technical Convention, 2013.

[40] C. Sourkounis and P. Tourou, "Grid Code Requirements for Wind Power Integration in Europe," Limassol, Cyprus., 2013.

[41] I. Erlich, W. Winter and A. Dittrich, "Advanced grid requirements for the integration of wind turbines into the German transmission system," Montreal, Canada, June 2006.

[42] R. Rene., "Application of double fed induction generator wind systems to weak networks," Curtin University, 2014.

[43] W. L. Kling and . J. G. Slootweg, "Wind Turbines as Power Plants," IEEE/Cigré Workshop on Wind Power and the Impacts on Power Systems, Oslo, Norway, June 2002.

[44] Wind Plant Collector System Design Working Group, "Wind Power Plant Collector System Design Considerations,," Calgary, Canada, 2009.

[45] Australian Energy Market Operator, "Wind turbine plant capabilities report 2013 Wind Integration Studies," Australian Energy Market Operator (AEMO), 2013.

[46] W. Qiao and R. G. Harley, "Grid Connection Requirements and Solutions for DFIG Wind Turbines," Atlanta, GA USA, 2008.

[47] Ferc united states of america federal energy regulatory commission, "Interconnection for Wind Energy," Federal Energy Regulatory Commission, June 2, 2005).

[48] Wind Plant Collector SystemDesign Working Group,, "Reactive Power Compensation for Wind Power Plants," Calgary, 2009..

[49] W. P. C. S. D. W. Group, "Wind Power Plant Collector System Design Considerations," IEEE Power and Energy Society General Meeting, Calgary, Canada, 2009.

[50] . J. Martinez, P. C. Kjar, P. Rodriguez and R. Teodorescu, "Short Circuit Signatures from Different Wind Turbine Generator Types," Phoenix, 2011..

[51] R. A. Walling and M. L. Reichard, “Short Circuit Behavior of Wind Turbine Generators,” Texas, 2009.

[52] M. Z. Kamh and R. Iravani, “Three-Phase Steady-State Model of Type-3 Wind Generation Unit-Part I: Mathematical Models,” *IEEE Transactions on Sustainable Energy,*, vol. 2, pp. 477-486, 2011..

[53] J. Morreu and S. W. H. de Haan, “Short-Circuit Current of Wind Turbines With Doubly Fed Induction Generator,” *IEEE Transactions on Energy Conversion,* vol. 22, pp. 174-180, 2007..

[54] J. Mourreu and . S. W. de Haan, “Ridethrough of Wind Turbines with Doubly-Fed Induction Generator During a Voltage Dip,” *IEEE Transactions on Energy Conversion,* vol. 20, no. 2, 2005.

[55] P. Piwko,, N. Miller, J. Sanchez-Gasca, X. Yuan, R. Dai and J. Lyons, “Integrating Large Wind Farms into Weak Power Grids with Long Transmission Lines”.

[56] H. Bindner , “Power Control for Wind Turbines in Weak Grids:Cocepts Devellopment,” Riso NAtional Laboratory, Roskilde, MArch 1999.

[57] P. D. Ladakakos, M. G. Ioannides and M. I. Koulouva, “Assessment of wind turbines impact on the power quality of autonomous weak grids,” International Conference on Harmonics and Quality of Power, Athens,Greece, 1998.

[58] J. O. G. Tande and K. Uhlen, “Wind Turbines In Weak Grids-Constraints and solutions,” SINTEF Energy Research, Norway.

[59] H. Holttinen, “State of the art of design and operation of power systems with large amounts of wind power –A summary of IEA Wind collaboration”,,” in *European Wind Energy Conference EWEC,*, Mila, Italy, 2007.

[60] A. Morales, X. Robe, M. Sala, P. Prats, C. Aguerri and E. Torres, “Advanced grid requirements for the integration of wind farms into the Spanish transmission system,” in *The Institution of Engineering and Technology,* 2008.

[61] DIgSILENT PowerFactory 15 User Manual, Gomaringen: DIgSILENT GmbH, May 2014.

[62] Simulink R2009b User's Guide, Natick: The MathWorks, Inc., 2009.

[63] 2013. [Online]. Available: http://www.mathworks.com/.

[64] C. Gavriluta, S. Spataru, I. Mosincat, C. Citro, I. Candela and . P. Rodriguez, "Complete methodology on generating realistic wind speed profiles based on measurements," in *International Conference on Renewable Energies and Power Quality*, Santiago de Compostela (Spain),, 2012.

[65] . L. Van der Hoven, "Power Spectrum of Horizontal Wind Speed in the Frequency Range from 0.0007 to 900 Cycles per Hour," *Journal of Atmospheric Sciences*, vol. 14, no. 2, pp. 160-164, 1957..

[66] . D. Fernando, H. De Battista and R. . J. Mantz, "Wind Turbine Control Systems. Principles, Modelling and Gain Scheduling Design," Springer, London,, 2007..

[67] W. Lagrander, "Models for variable speed wind turbine. Master's thesis," CREST Loughborough University UK,, Leicestershire, 1996.

[68] F. Lov, A. D. Hansen, P. Sorensen and F. Blaabjerg, "Wind Turbine Blockset in Matlab/Simulink General Overview and Description of the Models," Aaborg University, 2004, 2004.

[69] D. Garcia and J. Luis, "Modeling and control of Squirrel Cage Induction Generator with Full Power Converter applied to windmills," University of Oulu, Oulu, 2009.

[70] S. Heier, "Grid Integration of Wind Energy Conversion Systems," John Wiley and Sons,, 1998.

[71] F. M. Gonzalez-Longatt, "Example: Constant Speed Wind Turbine in DigSILENT PowerFactory," DigSILENT, Manchester, 2010.

[72] P. Bouwer, J. ,. H. J. Potgieter and M. J. Kamper, "Modelling and Dynamic Performance of a Direct-Direct-Drive Direct-Grid Slip Permanent Magnet Wind Generator," IEEE International Electric Machines and Drives Conference (IEMDC), 2011.

[73] A. D. Hansen, . F. Iov and P. Sørensen, "Dynamic wind turbine models in power system simulation tool DIgSILENT," Roskilde, Denmark, August 2007.

[74] R. Vermaak, J. H. Potgieter and M. J. Kamper, "Grid-connected VSC-HVDC wind farm system and control using permanent magnet induction generators," Tapei, Taiwan, Nov. 2009.

[75] A. D. Hansen, P. Sørensen, F. Iov and F. Blaabjerg, "Initialisation of Grid-Connected Wind Turbine Models in Power-System Simulations," *Wind Engineering*, vol. 27, no. 1, pp. 21-38, 2003.

[76] P. Kundur, Power System Stability and Control, New York: McGraw Hill, 1994.

[77] A. Grauers and S. Landström , “The Rectifiers Influence on the Size of Direct-driven Generators,” in *European Wind Energy Conference*, Nice, 1999.

[78] V. Akhmatov , A. H. Nielsen , J. K. Pedersen and O. Nymann , “Variable-speed wind turbines with multipole synchronous permanent magnet generators Part I. Modelling in dynamic simulation tools,” *Wind Engineering*, vol. 27, no. 6, pp. 531-548, 2003.

[79] A. J. G. Westlake , . J. R. Bumby and E. Spooner , “Damping the power-angle oscillations of a permanent-magnet synchronous generator with particular reference to wind turbine applications,” *EE Proceedings, Electr. Power Appl*, vol. 143, no. 3, pp. 193-201, 1996.

[80] J. H. J. Potgieter and M. J. Kamper, “Design and Analysis of Gearless Direct-Grid Permanent Magnet Induction Wind Generator MSC dissertation,” University of Stellenbosch, Stellenbosch, 2011.

[81] U. Hoffmann and M. J. Kamper, “Low Voltage Ride-Through Compensation for a Slip-Permanent Magnet Wind Turbine Generator,” Cape Town, July, 2011.

Appendix A **SSG parameters**

The SSG is a new concept generator not much is found of its manufacturing parameters, the values of the wind turbine system for this thesis where obtained from literature [81, 20, 21, 34] and are given in Table A-1 as follows:

Table A-1: SSG parameters.

Parameter	Symbol	Value
Turbine Parameters		
Air Density	p	1.225kg.m^{-3}
Operational wind speed range		4-12m/s
Survival wind speed range		0-25m/s
Nominal hub height	h_t	10m
Terrain roughness constant	K_e	0.189
Blades		3
Rotor radius	R	3.6m
Mass moment of inertia	J_t	226.99Kg.m^2
SSG Mechanical Parameters		
Rotational speed range		0-200rpm
Rated rotational speed	ω_r	150rpm
Rated input torque	T_r	1000Nm
Slip-rotor mass moment of inertia	J_r	5.497Kg.m^2
Slip-rotor static friction constant	B_{r0}	3.779Nm
Slip-rotor viscous friction coefficient	B_r	0.11998Nm/rads^{-1}
PM-rotor mass moment of inertia	J_m	8.515Kg.m^2
PM-rotor static friction constant	B_{m0}	11.338Nm
PM-rotor viscous friction coefficient	B_m	0.3599Nm/rads^{-1}

SSG Electrical Parameters			
			per-unit
Phases		3	-
Poles (slip-rotor and PM-rotor)	p	40	-
Rated line voltage	V_n	400V	base
Rated phase current	I_r	23A	base
Rated power	S_r	15.93kVA	base
Rated frequency	f_n	50Hz	-
Stator phase resistance	R_s	0.4Ω	0.04
Stator d-axis inductance	L_{ds}	11.25mH	1.12e-3
Stator q-axis inductance	L_{qs}	15.0mH	1.5e-3
Stator PM-flux linkage	λ_{ms}	1.0396Wb.t	0.104
Slip-rotor phase resistance	R_r	3.84μΩ	0.382e-6
Slip-rotor d-axis inductance	L_{dr}	0.125μH	0.0125e-6
Slip-rotor q-axis inductance	L_{qr}	0.15μH	0.015e-6
Slip-rotor PM-flux linkage	λ_{mr}	3.693mWb.t	0.369e-3
Electrical Network Parameters			
LV line voltage		400V	base
MV line voltage		10 kV	base
HV line voltage		110kV	base
Network source phase voltage	V_s	230V	-
Network phase resistance	R_g	0.15Ω	0.015
Network phase reactance	X_g	0.15Ω	0.015
Transformer phase resistance	R_t	0.129Ω	0.013

Transformer phase reactance	X_t	0.26Ω	0.026

Appendix B **Per unit system of the wind turbine model**

All the electrical and the mechanical parameters of the wind turbine model are in the Per Unit system, with the following base values:

1) The rated electric power of the wind turbine,S_r ,in Watts
2) The rated terminal voltage of the wind turbine, V_n, in Volts phase-phase RMS
3) The rated electric frequency at the wind turbine terminal,f_n, in Hz
4) The base impedance of the wind turbine generator

For power, voltage, current and impedance, the per-unit quantity may be obtained by dividing the respective base of the quantity.

$$S_{pu} = \frac{S}{S_{base}} \qquad V_{pu} = \frac{V}{V_{base}} \qquad I_{pu} = \frac{I}{I_{base}} \qquad Z_{pu} = \frac{Z}{Z_{base}}$$

Calculation for three-phase systems

In the three phase systems the line voltage and the total power rather than the single-phase quantities, if $VA_{3\emptyset base}$ and V_{LLbase} are the three-phase base power and line-to-line voltage respectively.

Base current : $I_{base} = \frac{VA_{base}}{V_{base}} = \frac{3VA_{base}}{3V_{base}} = \frac{VA_{3\emptyset base}}{\sqrt{3}V_{LLbase}}$

Base impedance; $Z_{base} = \frac{V^2{}_{base}}{VA_{base}} = \frac{V^2{}_{LLbase}}{VA_{3\emptyset base}}$

In terms of $MVA_{3\emptyset base}$ and KV_{LLbase}

Base current : $I_{base} = \frac{MVA_{base}}{\sqrt{3}KV_{LLbase}}$

Base impedance; $Z_{base} = \frac{KV^2{}_{LLbase}}{MVA_{3\emptyset base}}$

Thus in three phase, the calculations of per unit quantities becomes;

$$S_{pu} = \frac{S_{actual}(MVA)}{MVA_{3\emptyset base}}$$

$$V_{pu} = \frac{V_{actual}(KVA)}{KV_{LLbase}}$$

$$I_{pu} = I_{actual}(KA)\frac{\sqrt{3}KV_{LLbase}}{MVA_{3\emptyset base}}$$

$$Z_{pu} = Z_{actual}(\Omega)\frac{MVA_{3\emptyset base}}{\sqrt{3}KV_{LLbase}}$$

P and Q have the same base as S , so that

$$P_{pu} = \frac{P_{actual}(MVA)}{MVA_{3\emptyset base}}, \quad Q_{pu} = \frac{Q_{actual}(MVA)}{MVA_{3\emptyset base}}$$

Similarly, R AND X have the same base as Z, so that

$$R_{pu} = R_{actual}(\Omega)\frac{MVA_{3\emptyset base}}{\sqrt{3}KV_{LLbase}}, \quad X_{pu} = X_{actual}(\Omega)\frac{MVA_{3\emptyset base}}{\sqrt{3}KV_{LLbase}}$$

The power factor remains unchanged in per unit.

For the SSG:

S_{base} =15.93 kVA, $V_{LLbase} = 400\ V$

$$I_{base} = \frac{VA_{3\emptyset base}}{\sqrt{3}V_{LLbase}} \frac{15.93}{\sqrt{3}*400} = 22.9929\ A \approx 23\ A$$

$$Z_{base} = \frac{KV^2_{LLbase}}{MVA_{3\emptyset base}} = \frac{400^2}{15930} = 10.04\ \Omega$$

Appendix C Directly grid-connected PMSG

The effects of directly coupling a PMSG to the grid and turbine are investigated using the per-phase equivalent circuit shown in the Figure C-1.

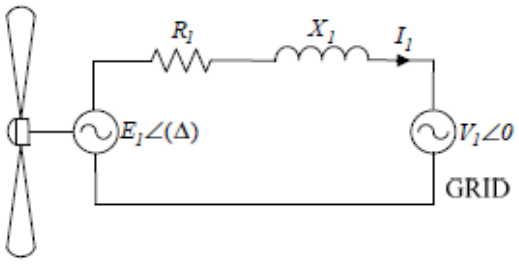

Figure C-1: Per-phase equivalent circuit of PMSG [80].

When the PMSG is couple directly to the grid network and operating at steady state where the turbine torque produced will be equal to the IG torque generated: $T_m = T_t$. To model the mechanical model of the PMSG the turbine motion is given by the equation [80] as follows:

$$T_t - T_s = J_1 \frac{dw_t}{dt} \tag{C.1}$$

Where T_t denote the turbine torque and T_s denote the electrical generator torque response. With the IG mass inertia seen as contributing to the drive train, the inertia $J_1$is the combined turbine and the PM rotor inertia and the inertia of the turbine is assumed to be considerably greater than that of the PM rotor. The turbine torque of the wind turbine system is as a function of both the wind speed and turbine speed is given by the following equation:

$$T_t = f(V_w, w_t) \tag{C.2}$$

Where w_t denotes the rotational speed of the turbine and V_w denotes the wind speed.

Assuming the per-phase resistance is negligible the developed power of the PMSG can be given the following approximation:

$$P_{gs} \approx \frac{E_1 V_1}{X_1} \sin\beta \tag{C.3}$$

With the power and torque directly equivalent the developed generator torque response is given by:

$$T_s \approx K_1 \sin\beta \tag{C.4}$$

For very small values of the power angle, $\beta \sin\beta \approx \beta$ and it is assumed that

$$E_1 \approx V_1 = \sqrt{2}\,\pi f_1 N_1 \varphi_1 \tag{C.5}$$

and it is known that

$$X_1 = 2\pi V f_1 L_1$$

The machine constant K_1 can be approximated as follows:

$$K_1 \approx \left(\frac{3p^2 N_s^2}{4L_1}\right)\varphi_1^2 \tag{C.6}$$

Where φ_1 denotes the SG flux per pole and L_1 denote the per-phase winding inductance, and also the power angle δ_m dynamics are described by the following:

$$w_t - w_{sm} = \frac{d\delta_m}{dt} \tag{C.7}$$

Where:

$$w_{sm} = \frac{4\pi f_1}{p} \tag{C.8}$$

$$\beta = \left(\frac{p}{2}\right)\delta_m \tag{C.9}$$

Where p denotes the number of poles of the generator, hence from the above machine and turbine relationships, the basic dynamic block diagram shown in figure is derived. From the block diagram in Figure C-2 it is possible to derive a steady state transfer function given as follows:

$$\frac{T_s(s)}{T_t(s)} = \frac{\frac{K_1}{J_1 s^2}}{1 + \frac{K_1}{J_1 s^2}} \tag{C.10}$$

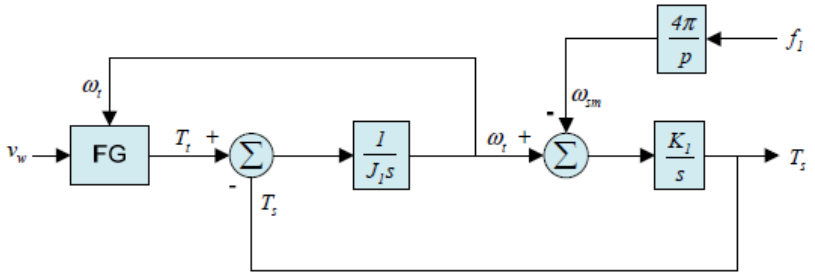

Figure C-2: Per-phase equivalent modelling of a PMSG coupled directly to both the turbine and grid.

The standard form of the second order system is given by the following:

$$H(s) = \frac{w_n^2}{s^2 + 2\xi w_n s + w_n^2} \tag{C.11}$$

Where ξ denotes the damping coefficient for the generator and w_n denote the undamped natural frequency, then this translates the transfer function given to be given as follows:

$$\frac{T_s(s)}{T_t(s)} = \frac{\frac{K_1}{J_1}}{1 + 0s\frac{K_1}{J_1}} \tag{C.12}$$

For convectional synchronous machines they need damper windings for stable connection to the grid network. In this case there are no additional damper windings available and the damping coefficient is negligible. This can be seen in figure with

$$0 = 2\,\xi w_n \tag{C13}$$

and

$$w_n{}^2 = {K_1}/{J_1}$$

Taking into consideration the damping effect produced due to the copper losses, wind and friction losses and the core and eddy current losses of the machine, this have little or no effect to the stability of the machine. Hence from the transfer function given in this shows the PMSG directly connected to the grid network is an un-damped system, which is prone to oscillations which can be translated to the grid when the system is loaded.

Appendix D **Wind model parameters**

The parameters of the wind model are:

- Sample time step, s_t = 0.05s
- Blade radius, R=3.6m taken from the data sheet of the wind turbine appendix A
- Average wind speed, Vm output from a DSL "ElmFile" block as a *.txt* file.
- Length scale, L = 300m
- Turbine intensity, σ= 10%

For the wind model, both the hub and rotor sub-models contain a cascade of Kaimal, zero and third order filters which are covered in detail in

The Kaimal spectrum can be expressed by the following second order transfer function:

$$H_{KF}(S) = K_K \frac{S^2T_4^2 + ST_3 + 1}{S^2T_2^2 + ST_1 + 1} \tag{D.1}$$

Where K_F, T_1, T_2, T_3 and T_4 denotes the estimated parameters calculated based on the constants C and T which are function of the turbulence intensity, the length scale and the average wind speed. C denotes the estimation of the frequency bandwidth of the turbulence and is determined as follows:

$$C = \frac{L}{2\pi V_m} \tag{D.2}$$

T Denotes the estimation of the turbulence intensity and is given by the following equation:

$$T = \frac{\delta}{100}\sqrt{\frac{LV_m}{2}} \tag{D.3}$$

Where L denotes the length scale, δ is the turbine intensity and V_m is the average wind speed. The zero and the third harmonic filters use the length scale and the average wind speed expressed in a constant D, where D is expressed by the following equation:

$$D = \frac{R}{V_m} \tag{D.4}$$

Where R denotes the blade radius of the wind turbine.

The zero-order harmonic filter is described by the transfer function as follows:

$$H_{ZF}(S) = K_Z \frac{ST_3 + 1}{S^2T_2^2 + ST_1 + 1} \tag{D.5}$$

The third order harmonic filter is described by the transfer function as follows:

$$H_{TH}(S) = K_{TH} \frac{ST_3 + 1}{S^2T_2^2 + ST_1 + 1} \tag{D.6}$$

With the above constants in equation (D.1), (D.5) and (D.6) the parameters K_{TH}, $K_{Z,}$ K_K,T_1, T_2, T_3 and T_4 are given in the Table D-1 as following :

Table D-1: The parameter values for the Kaimal spectrum constants.

Parameter	First order filter	Zero order filter	3rd order filter
K_i^*	$0.9846T$	0.9904	0.0307
T_1	$3.7593C$	$7.3518D$	$1.7722D$
T_2	$1.3463C^2$	$7.6823D^2$	$0.3691D^2$
T_3	$1.3866C$	$4.8333D$	$9.0098D$
T_4	$0.01848C^2$	-	-

*where i is dependent on the type of filter chosen

Appendix E **Matlab/Simulink models**

This appendix shows the models and their respective masks created for each of the SSG wind turbine system components. The models provided are the wind, the turbine (which includes the aerodynamic and mechanical model), the DQ SSG and the grid network.

E.1 Wind model

E.1.1 Mask

The Figure E-1 shows the masked Simulink block of the wind model. The masked parameter dialog window of the block is shown in Figure E-2.

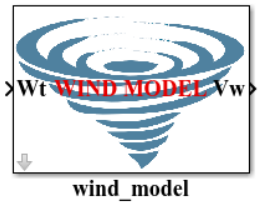

Figure E-1: Masked Simulink block of wind model representation.

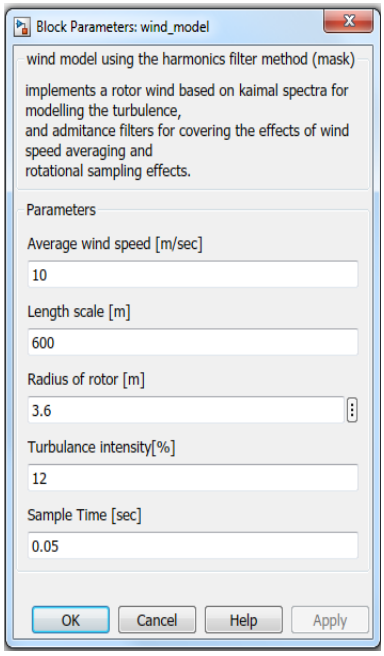

Figure E-2: Simulink wind model masked parameter dialogue window.

E.1.2 Under the mask

The unmasked parameter window of the wind model is shown in Figure E-3, it shows the relationship existing between the inputs and output of the wind model.

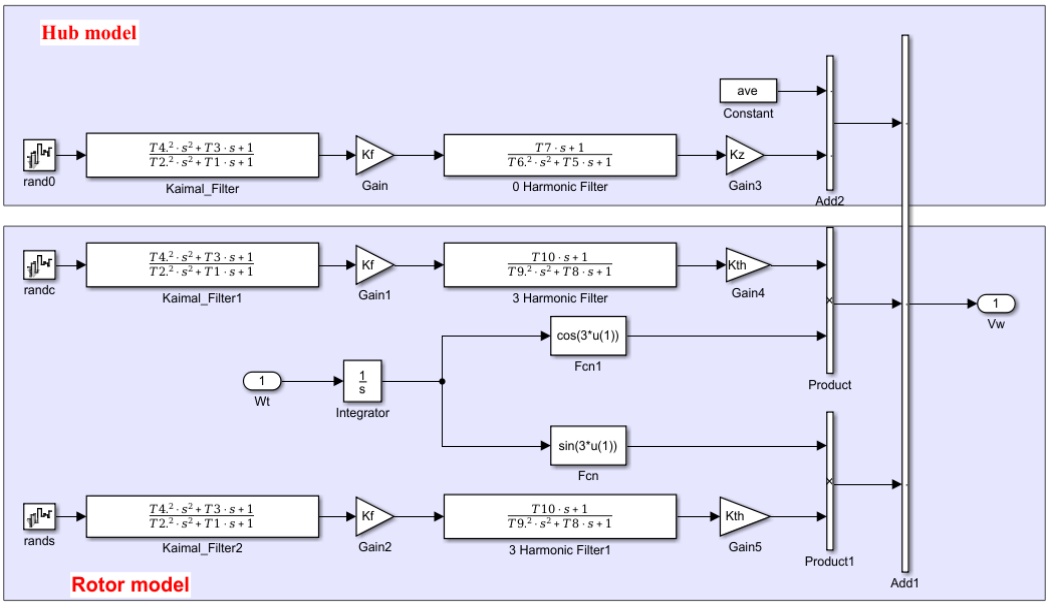

Figure E-3: Simulink wind model design.

E.1.3 Mask configuration

The mask configuration windows, utilising icon and port tab in Figure E-4 as well as the parameter and dialogue tab parameter and dialogue tab in Figure E-5, are shown below.

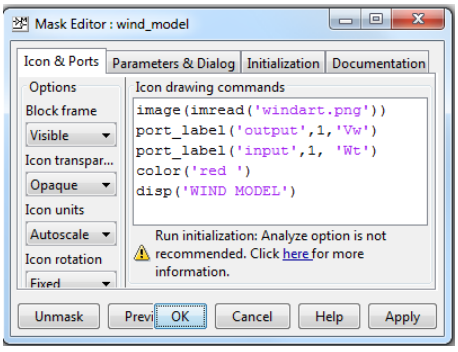

Figure E-4: Simulink wind model mask configuration window - Icon & Port.

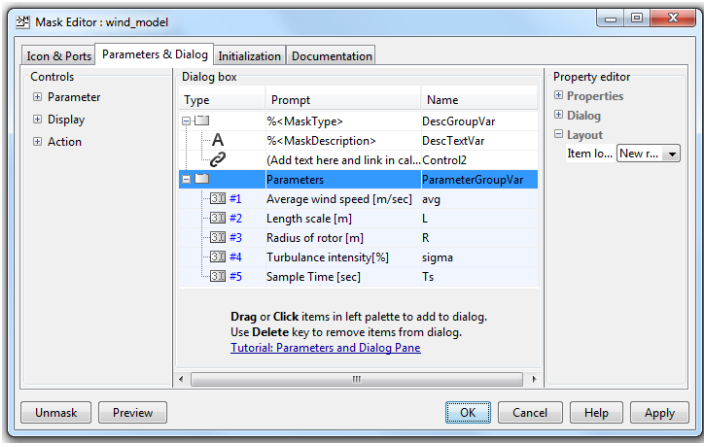

Figure E-5: Simulink wind model mask configuration window - Parameters and Dialog tab.

G 1.

E.2 Mechanical model

E.2.1 Mask

Figure E-6 shows the masked Simulink block showing all the inputs and outputs for the mechanical model block. The parameter values and their description are shown in the masked parameter dialogue window which is shown in Figure E-7.

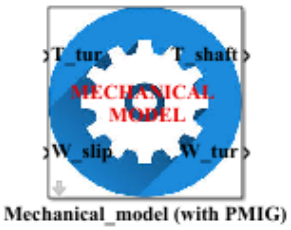

Figure E-6: Simulink masked block of mechanical representation.

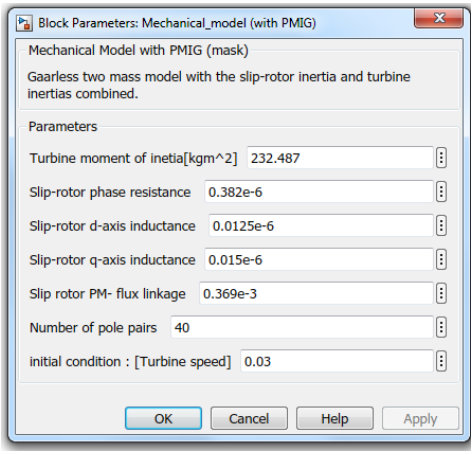

Figure E-7: Simulink mechanical model masked parameter dialogue window.

E.2.2 Under the mask

The unmasked parameter window of the wind model is shown in Figure E-8, showing the coupling of the turbine to the SSG without the use of a gearbox.

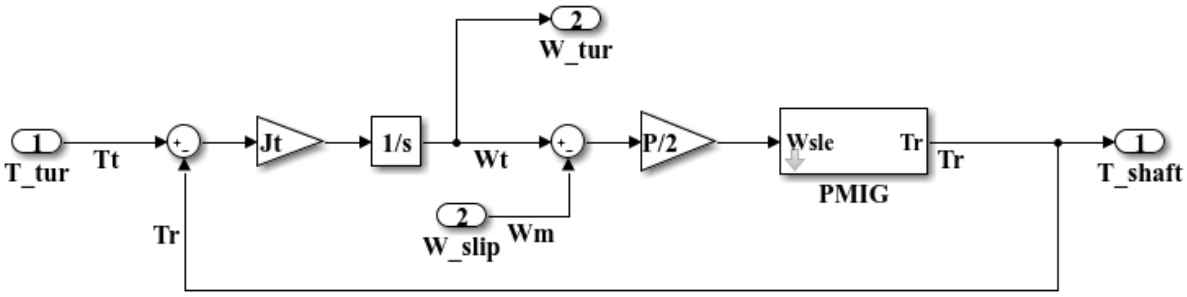

Figure E-8: Simulink mechanical model design

E.2.3 Mask configuration

The mask configuration windows, utilising an icon and port tab in Figure E-9 as well as the parameter and dialogue tab parameter and dialogue tab in Figure E-10, are shown below.

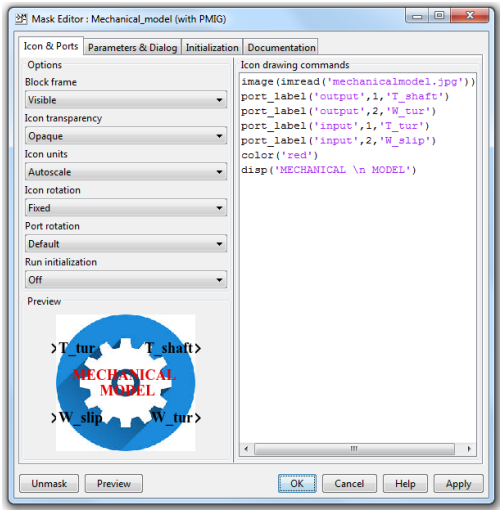

Figure E-9: Simulink mechanical model mask configuration window - Icon & Port.

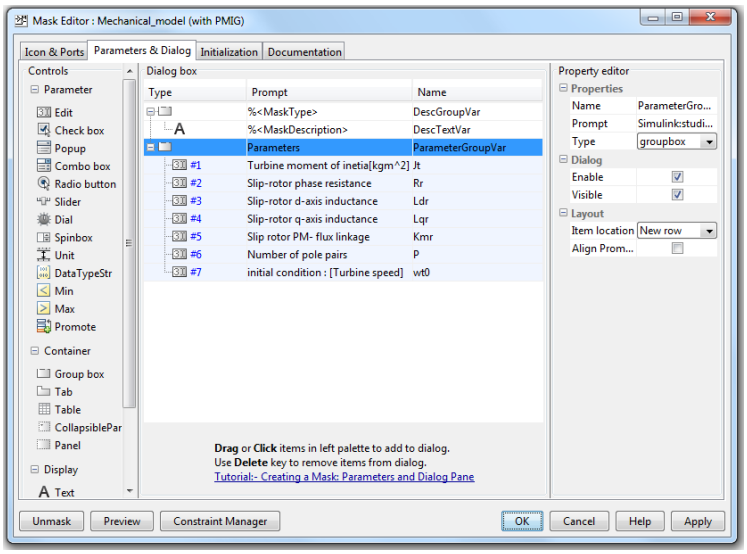

Figure E-10: Simulink mechanical model mask configuration window – parameters & Dialog.

E.3 Aerodynamic model

E.3.1 Mask

Figure E-11 shows the masked Matlab/Simulink block of the aerodynamic model, the masked parameter dialog window of the block is also shown in Figure E-12.

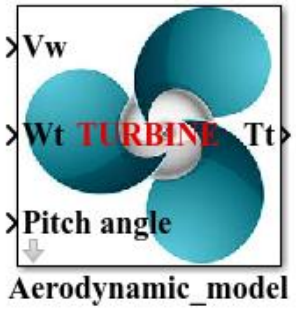

Figure E-11: Simulink masked block of aerodynamic model representation

G 2.

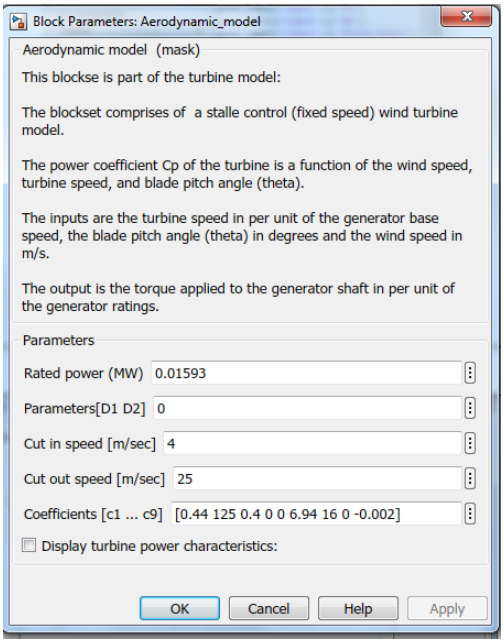

Figure E-12: Simulink aerodynamic model masked parameter dialogue window

G 3.

E.3.2 Under mask

The unmasked designed model of the wind model is shown in Figure E-13 it shows the relationship existing between the inputs and output of the wind model.

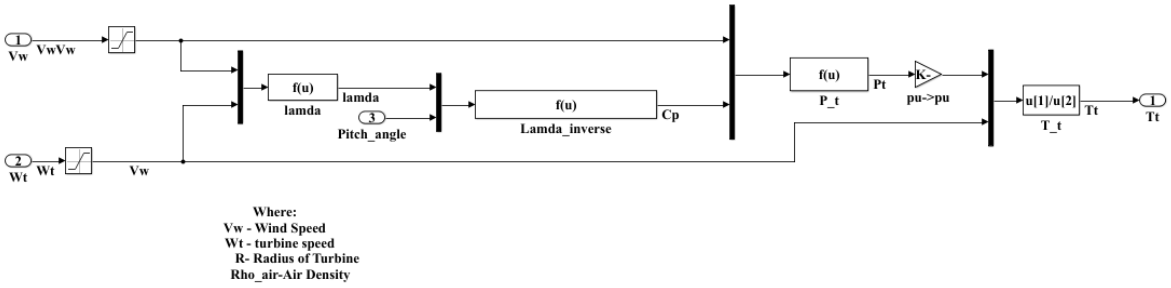

Figure E-13: Simulink aerodynamic model design.

E.3.3 Mask Configuration

The mask configuration windows for the aerodynamic model, is developed from the parameter and dialogue tab in Figure E-14 as well as the parameter and dialogue tab parameter and dialogue tab in Figure E-15, are shown below.

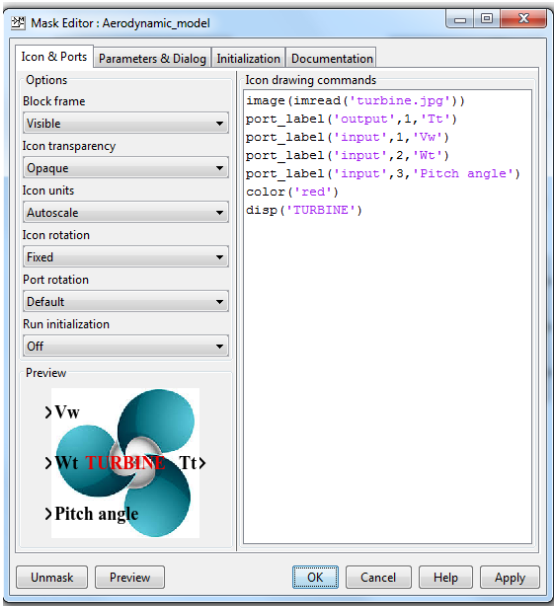

Figure E-14: Simulink aerodynamic model mask configuration window - Icon & Port.

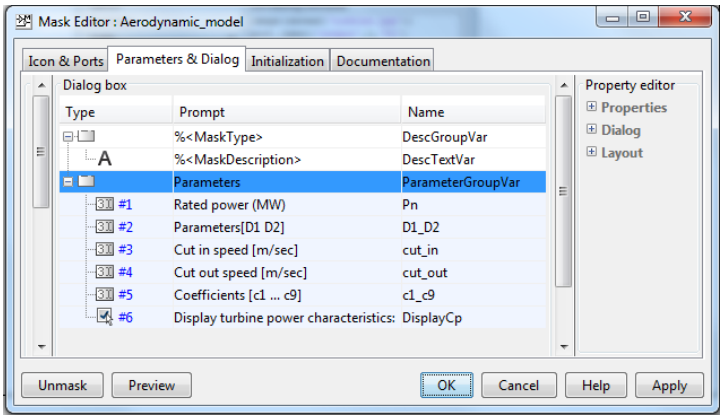

Figure E-15: Simulink aerodynamic model mask configuration window - Parameters and Dialog tab.

The initialisation of the aerodynamic model is outlined in the following algorithm:

```
% Turbine data
%c1=0.44; c2=125; c3=0.4; c4=0; c5=0; c6=6.94; c7=16.5; c8=0; c9=-0.002;
%cp_max=0.5;
c1 = 0.44;
c2 = 125;
c3 = 0.4;
c4 = 0;
c5 = 0;
c6 = 6.94;
c7 = 16;
c8 = 0;
c9=-0.002;
theta=0;
Prated=0.01593;
CpMax=0.5;
```

```
lamda_CpMax=9.9495;

c1_c9= [c1 c2 c3 c4 c5 c6 c7 c8 c9];

%   Cp = c1*(c2*(1/ (lambda + c8*theta) - c9/ (1 + theta^3) +...
%   - c3*theta -c4*theta^c5 -c6) /exp (c7*(1/ (lambda + ...
%   c8*theta) - c9/ (1 + theta^3));

      rated_omegar=1.5;
      omegar = rated_omegar;
      wind_speed_CpMax=0.5427;

      if wind_speed_CpMax < 4
         wind_speed_CpMax=4;
         disp ('Warning: Wind speed at nominal speed and at Cp max has been set to 4 m/s')
      end
      if wind_speed_CpMax > 25
         wind_speed_CpMax=25;
         disp ('Warning: Wind speed at nominal speed and at Cp max has been set to 25 m/s')
      end

      D1=lamda_CpMax/omegar*wind_speed_CpMax;
      Prated=Pn;
      P_rated_omegar_theta_zero=0.015;
```

```
        D2=P_rated_omegar_theta_zero*Prated/(wind_speed_CpMax^3*CpMax);
        D1_D2= [D1 D2];

DisplayCp=get_param(gcb,'DisplayCp');
if strcmp (DisplayCp,'on')
    vect_theta = 0:2:30;

    vect_lamda = 1:0.2:30;

    clear Cp;

    %   Ploting the power coefficient characteristic curve
    %   Cp=c1*(c2/((1/(lamda+theta) + 0.002/(theta^3+1))-c3*theta-c4-c6) *exp (-c7/....
    % (1/(lamda+theta) +0.002/(theta^3+1));
    for i=1: length (vect_theta)
     for j=1:length(vect_lamda)
            Cp(i,j) = c1*(c6 - c3*vect_theta(i) -c4*vect_theta(i)^c5 + c2*(1/(vect_lambda(j) + ...
            c8*vect_theta(i)) - c9/(1 +  vect_theta(i))^3))/exp(c7*(1/(vect_lambda(j) + ...
            c8*vect_theta(i)) - c9/(1 +  vect_theta(i))^3));
     end
    end

    figure(1);
    clf;
    hold on;
```

```
plot(vect_lambda, Cp);
axis([0, 25, 0, .6]);
title('Wind Turbine Cp Characteristic ');
ylabel('Power Coefficient');
set(gca,'ytick',[0 .1 .2 .3 .4 .5 .6]);
xlabel('Tip Speed Ratio');
grid on;

hold off

% Plotting wind turbine mechanical power output (pu) lamda and Cp
% characteristics against wind speed (m/s) for a range of theta.

wind_speed_range = [1,.2,30];
vect_wind_speed = 1:0.2:30;
R=3.6;
rho_air=1.225;

clear lamda;
clear Cp;
clear P;

for i=1:length(vect_theta)
   for j=1:length(vect_wind_speed)
```

```
        lamda(i,j) = D1*omegar/vect_wind_speed(j);
        Cp(i,j) = c1*(c6 - c3*vect_theta(i) -c4*vect_theta(i)^c5 + c2*(1/(vect_lambda(j) + ...
        c8*vect_theta(i)) - c9/(1 +  vect_theta(i))^3))/exp(c7*(1/(vect_lambda(j) + ...
        c8*vect_theta(i)) - c9/(1 +  vect_theta(i))^3));
        P(i,j) = D2/Prated*vect_wind_speed(j)^3*Cp(i,j);
    end
end



figure(2);
clf;
hold on

subplot(3,1,1);
plot(vect_wind_speed, P);
axis([0, 35, 0, 1.5]);
title('Wind Turbine Characteristics ');
ylabel('P (pu)');
set(gca,'ytick',0:.5:4);
grid on;

subplot(3,1,2);
plot(vect_wind_speed, lamda);
axis([0, 35, 0, 20]);
ylabel('Tip speed ratio');
```

```
grid on;


subplot (3,1,3)
plot (vect_wind_speed, Cp);
axis ([0, 35, 0, .6]);
xlabel ('Wind Speed (m/s)');
ylabel ('Cp');
set (gca,'ytick',[0 .1 .2 .3 .4 .5 .6]);
grid on;
hold off
set_param(gcb,'DisplayCp','off')


end
```

G 4.

E.4 Grid model

E.4.1 Mask

The masked simulink design of the grid model is shown in Figure E-16, it shows the output of the grid network. The parameters corresponding to the grid network are defined in the parameter dialogue window shown in Figure E-17 as follows

Figure E-16: Masked Simulink block of grid network model representation.

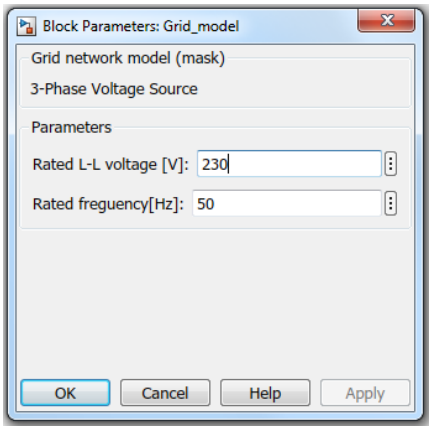

Figure E-17: Simulink grid network model masked parameter dialogue window.

E.4.2 Under mask

The Figure E-18 shows the Simulink design under the mask of the grid network model. Showing all the relationships between the inputs and outputs.

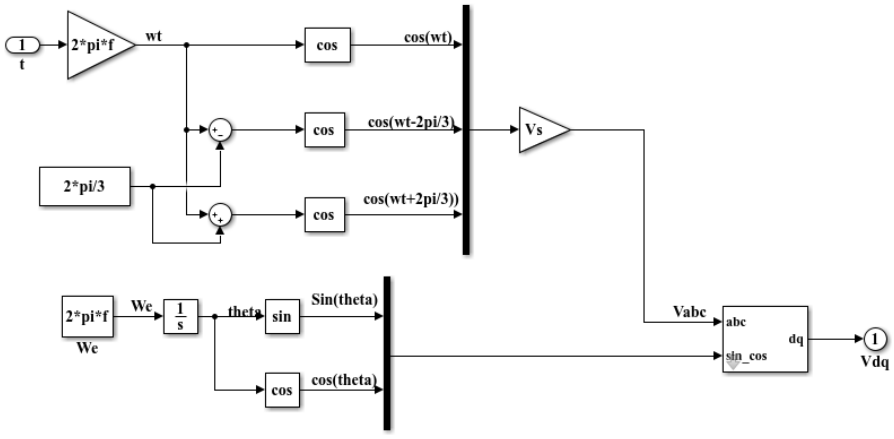

Figure E-18: Simulink grid network model design.

E.4.3 Mask configuration

The masked configuration window for the grid network model is shown from the Icon and port tab shown in Figure E-19 and the parameters and dialogue tab shown in Figure E-20 as follows:

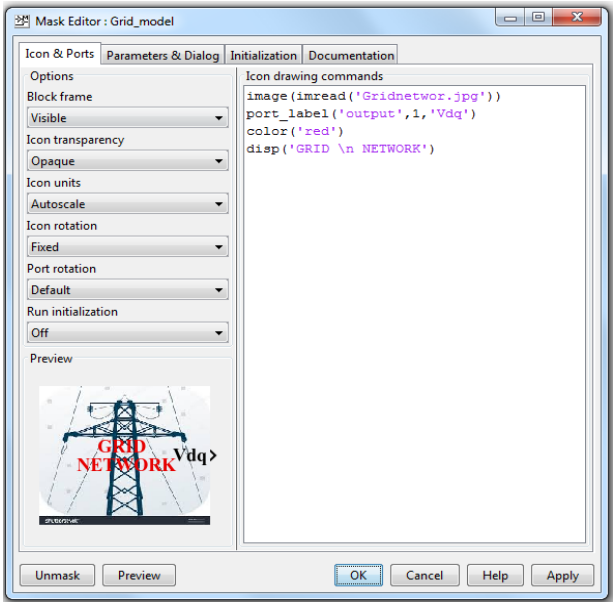

Figure E-19: Simulink grid network model mask configuration window - Icon & Port.

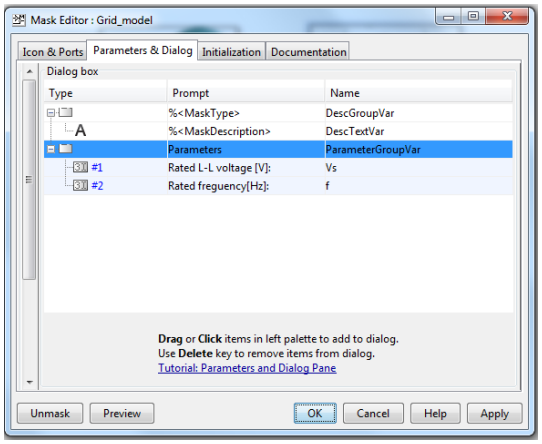

Figure E-20: Simulink grid network model mask configuration window – Parameters & Dialog

E.5 Capacitor bank

The model for capacitor bank is derived from the electrical circuit as it is shown in Figure E-21. For the SSG specifically its functionality is optional, when utilised the capacitor unit is connected in series.

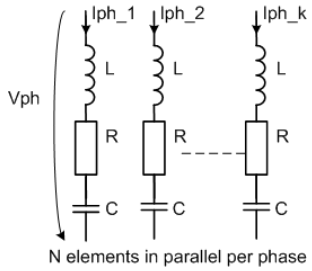

Figure E-21: Electrical equivalent circuit for the capacitor bank.

In the continuous domain (also termed the s-plane) the transfer function for one branch of the capacitor bank is given by the following:

$$H(s) = \frac{I(s)}{V(s)} = \frac{sC}{s^2LC + sRC + 1} \tag{E.1}$$

The total energy which is outlined as:

$$I_t(s) = \sum_k I_k\,(s) \tag{E.2}$$

Since the electrical parameters in each branch are equal, the transfer function for up to N parallel capacitor elements is given by the following:

$$H_t(s) = \frac{I_t(s)}{V(s)} = \frac{sNC}{s^2LC + sRC + 1} \tag{E.3}$$

Where N denotes the number of all the parallel branches.

Usually for practical purposes in order to decrease the capacitance value per phase the capacitors are connected in delta. The Simulink implementation for the model is shown in Figure E-22 and including the mask interface Figure E-23.

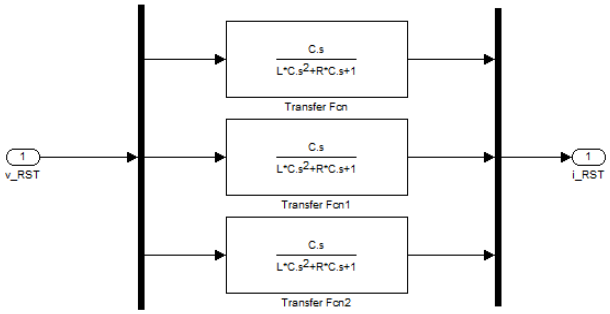

Figure E-22: Simulink design model for the capacitor bank.

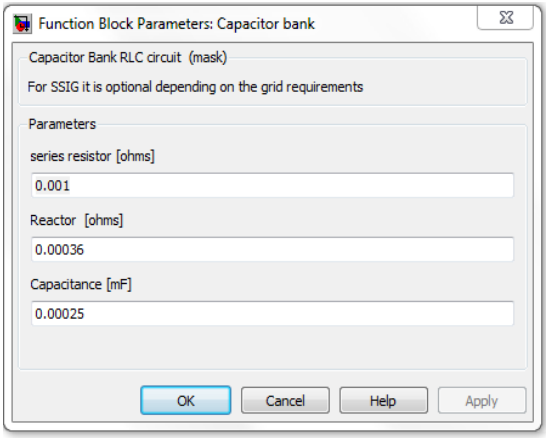

Figure E-23: Simulink capacitor bank model masked parameter dialogue window.

Appendix F DigSILENT DSL models

F.1 Wind model

The wind model in DigSILENT start with a block/frame definition called 'Wind model'. This frame as shown in the following Figure F-1 which contain inputs and outputs signals given by the Table F-1 and Table F-2 as follows:

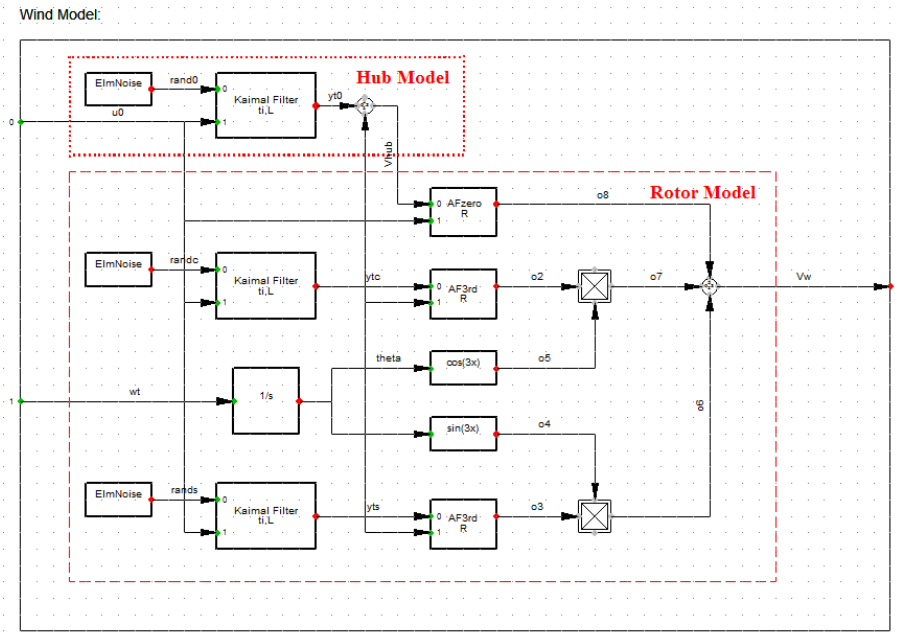

Figure F-1: DigSILENT wind model design.

Table F-1: DigSILENT inputs and outputs signals variables for the wind model design.

Variable	Description	Unit	Variable	Description	Unit
u0	Mean wind speed	m/s	Vw	Wind speed	m/s
Wt	Turbine angular velocity	Rad/s			

Table F-2: DigSILENT internal variables for wind model design.

Parameter	Description	Unit	Parameter	Description	Unit

Ti	Turbulence intensity	%	theta_int	Power coefficient	degrees
R	Blade radius	M			
L	Length scale	M			

The block definition (***ElmBlk***) shows the physical relationship between the inputs and outputs signals and is comprised of the various parameters which are defined in a common model. The common model (***ElmDsl***) are formed from the block definition and provides a specific set of parameter definitions and initialisation of each block. The common model for the wind model is shown in Figure F-2.

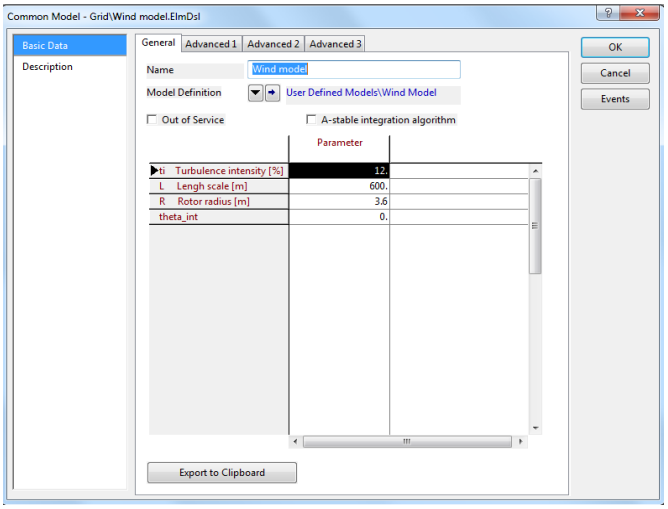

Figure F-2: DigSILENT common model for the wind model.

The common model element (***ElmDsl***) is the front-end object for all user-defined block definitions, hence in DigSILENT either the user-defined or the built-in block definitions, cannot be implemented other than through a common model.

The initial conditions of the block definition of the Wind model (***Wind model. BlkDef***) is obtained based on the following equations:

```
!calculation of Initial conditionms hub model

inc(x1)=0
inc(x2)=0
inc(x3)=0
inc(x4)=0
inc(x5)=0
inc(x6)=0
inc(x7)=0
inc(x8)=0
inc(x9)=0
inc(x10)=0
inc(x11)=0
inc(x12)=0

inc(rand0)=0
inc(randc)=0
inc(randS)=0

inc(yt0)=0
inc(ytc)=0
inc(yts)=0

inc(u0)=Vw
```

F.2 Rotor model

The Rotor model in DigSILENT starts with a Block/Frame Definition called 'Turbine', Figure F-3 shows the Aerodynamic model block with input and output as defined in Table F-3, whereas parameters and internal variables as defined in Table F-4. This frame contains the following:

Table F-3: DigSILENT inputs and outputs signals variables for the rotor model design.

Variable	Description	Unit	Variable	Description	Unit
Theta	Blade Pitch Angle	degrees	Pwind	Turbine mechanical power	Watt
Omega_tur	Turbine angular velocity	Rad/s			
Vw	Wind speed	m/s			

Table F-4: DigSILENT internal variables for the rotor model design.

Parameter	Description	Unit	Internal variable	Description	Unit
Rho_air	Air density	Kg/m^2	Cp	Power coefficient	
R	Blade radius	M	lamda		
Matrix_cp	Cp look up table values				

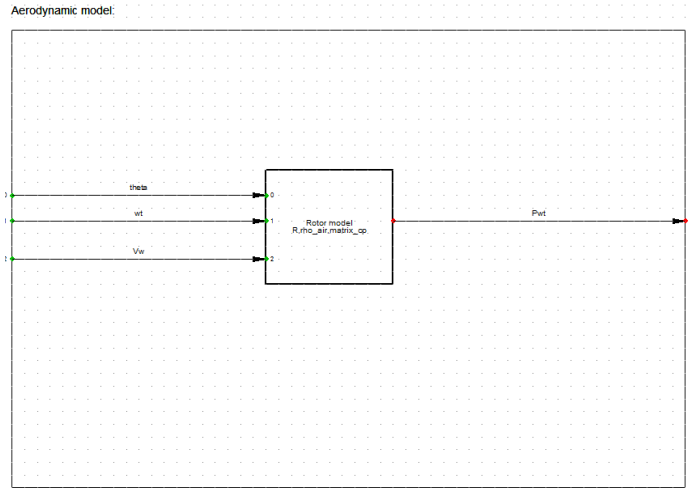

Figure F-3: DigSILENT aerodynamic model design.

The common model for the Aerodynamic model is shown in Figure F-4 as follows:

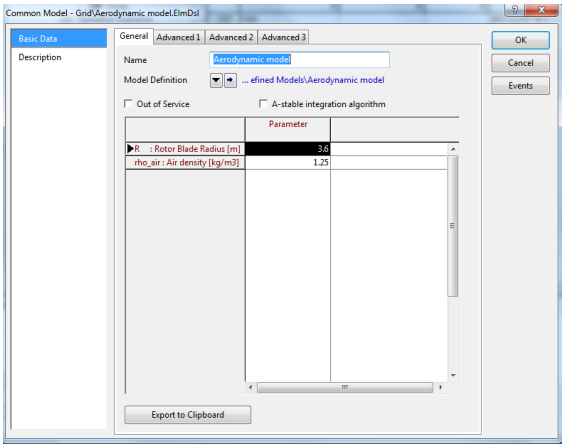

Figure F-4: DigSILENT common model for the aerodynamic model.

The Rotor model is described by macros equation described below:

```
Pwind = 0.5*rho_air*pi()*sqr(R)*Cp*pow(Vw,3)/1E3
Cp = abs(sapprox2(lamda,theta,matrix_cp))
lamda = wt*R/Vw
```

The initial conditions of the block definition of the Aerodynamic model (Aerodynamic model. BlkDef) is obtained based on the following equations:

```
!Calculation of Initial condition

inc0(theta)=0
inc(Vw)=12
inc(Cp)=0.48
inc(lamda)=wt*R/Vw
!Variable definitions

vardef(R)='m';': Rotor Blade Radius'
vardef(rho_air)='kg/m3';': Air density'
```

F.3 Plant WT

A composite models (***ElmComp***) are used to combine and interconnect the common models which will be located as shown from the data manager Figure F-6 to build up the wind turbine system, in this thesis the composite model called 'Plant WT' is made. The composite model element (ElmComp) Plant WT shown in Figure F-7 is related to the composite Frame Wind Turbine which is in shown in Figure F-5.

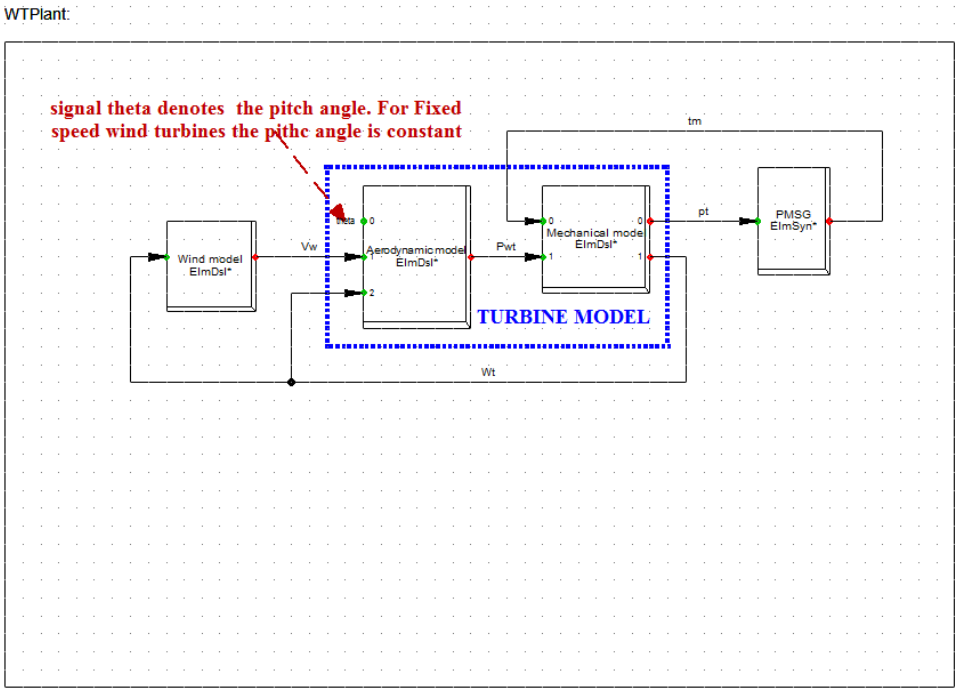

Figure F-5: DigSILENT composite frame for Wind Turbine Plant (WTP).

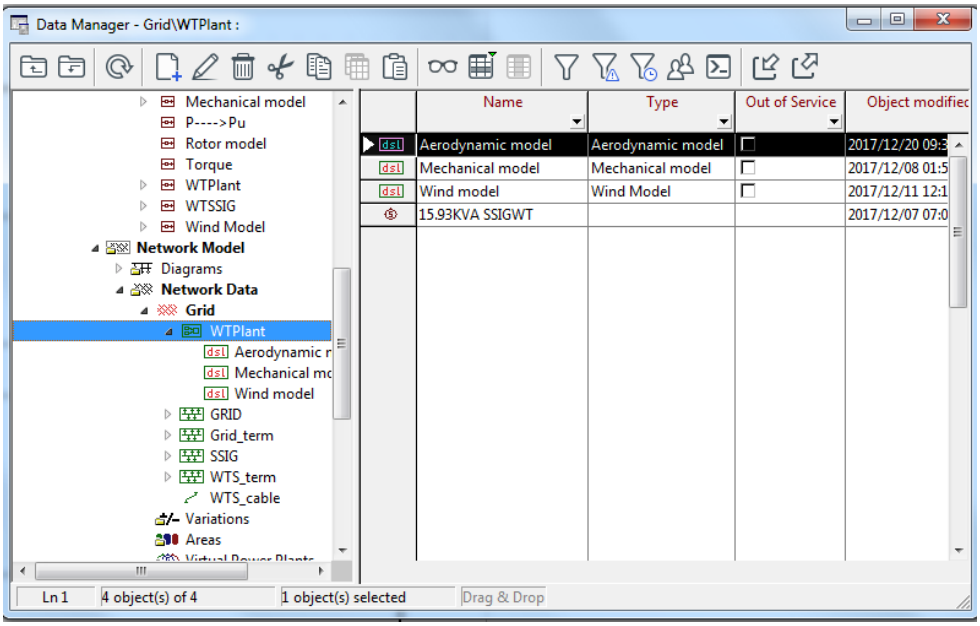

Figure F-6: DigSILENT data manager showing the Grid elements common models for the wind turbine system (WTS).

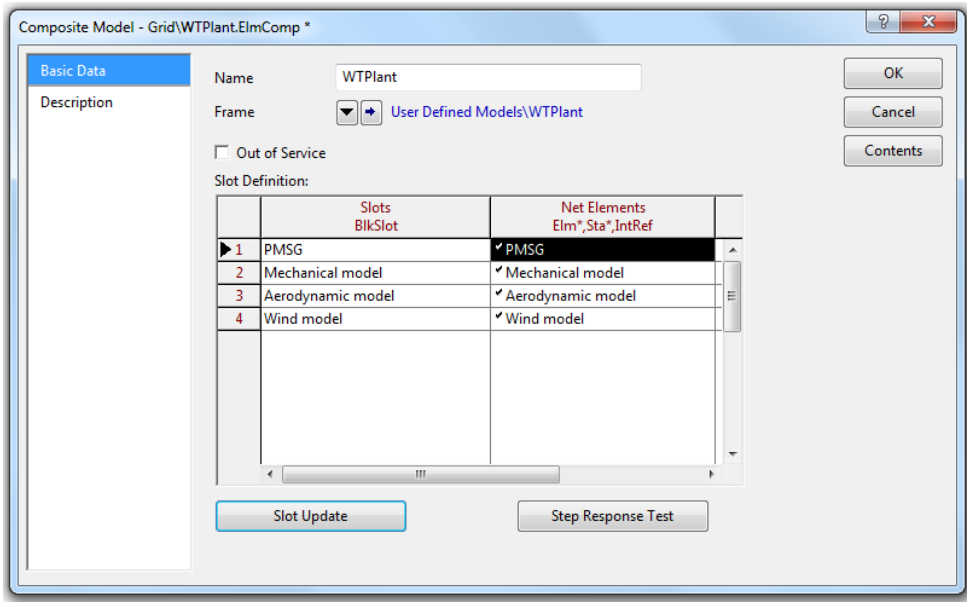

Figure F-7: DigSILENT composite model for Wind Turbine Plant (WTP).

Appendix G **Benchmark model**

G.1 Introduction

A benchmark model for small wind turbine systems interfaced to the grid is not covered in literature, in this thesis a benchmark model is defined which provide the description of a simplified simulation cases of short circuit in an embedded wind turbine system. The benchmark model is illustrated in the single line diagram shown in Figure G-1.

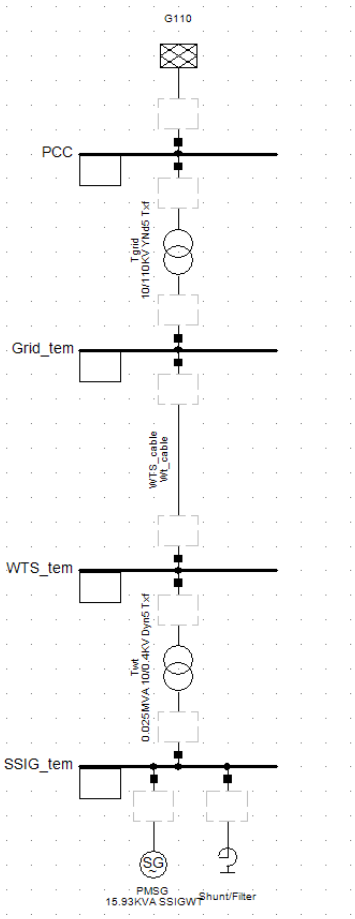

Figure G-1: single line diagram representing the SSG connected to grid.

G.2 110 kV grid

The equivalent circuit of the grid model is shown in Figure G-2. An aggregated impedance value of 0.02 + j 0.2 p.u. was derived from literature. However, a more resistive impedance is adopted with

values given in table which approximately model remote distribution networks where the SSG is deployed

The 110 kV grid G_{110} is given by external connected to the slack bus shown in Figure G-1 is modelled by a Thevenin equivalent with the data given in Table G-1. The phase of the voltage is 0 degrees.

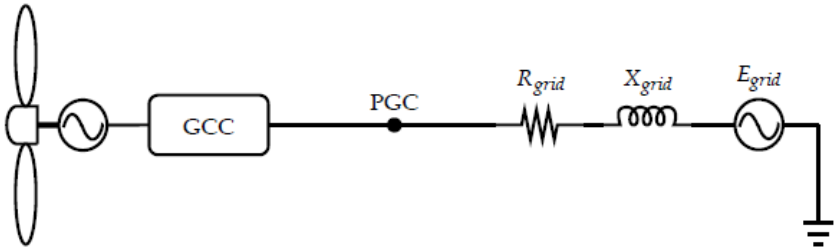

Figure G-2: Equivalent circuit of the grid model.

Table G-1: Slack bus parameters.

Parameter	Value
Uth	110 kV
Rth	0.15 Ω
Xth	0.15 Ω

G.3 110/10 kV transformer

The 10/110 kV step-up transformer Tgrid in Figure G-2 is modelled by a T-equivalent with the data given in Table G-2. All reactance's are without saturation, No-load losses are not included. The phase connection is YNd5. The transformer is directly grounded.

Table G-2: Grid transformer parameter values.

Parameter	Value
Sn	1 MVA
Up	110 kV

Us	10 kV
Rdx	0.01 p.u.
Xdx	0.06 p.u.
Xm	0.02 p.u.
Rs’	0.01 p.u.
Xs’	0.06 p.u.

G.4 10 kV collection cable

The generated power is distributed to the MV grid using a collection cable represented by in Figure G-1. The cable is modelled by a π equivalent circuit with the parameters given by the following Table G-3:

Table G-3: Collector cable parameters.

Parameter	Value
C_1	1.58 µF
R	0.07 p.u.
X	0.05 p.u.
C_2	1.58 µF

G.5 0.4/10 kV transformer

The 0.4/10 kV step-up transformer Twt in figure is modelled by a T-equivalent circuit shown in Figure G-1 with the data given in Table G-4. All reactance’s are without saturation, No-load losses are not included. The phase connection is Dyn5. The transformer is directly grounded.

Table G-4: Generator transformer parameters.

Parameter	Value
S_n	25 kVA

U_s	0.4 kV
U_p	10 kV
R_p	0.02 p.u.
X_p	0.04 p.u.
X_m	0.01 p.u.
R_s'	0.02 p.u.
X_s'	0.04 p.u.

G.6 Wind turbine generator

The synchronous generator is modelled by the data given in Table G-5.

Table G-5: SSG parameters.

Parameter	Value
S_n	15.93 kVA
U_n	400 V
N_o	10 kV
N_o	150 rpm
R_s	0.15 p.u.
X_s	0.15 p.u.
X_m	0.16 p.u.
R_r'	0.02 p.u.
X_r'	0.04 p.u.